ISSN 1854-6250

Advances in Production Engineering & Management

APEM

Volume 5 Number 1

January 2010

ADVANCES IN PRODUCTION ENGINEERING & MANAGEMENT

Identification Statement

ISSN 1854-6250 Abbreviated key title: **Adv produc engineer manag** Start Year: 2006
ISSN 1855-5531 (on-line)

Published quarterly by **Production Engineering Institute, University of Maribor**
Smetanova ulica 17, SI – 2000 Maribor, Slovenia - EU
Phone: 00386 2 2207522 Fax: 00386 2 2207990
Institute homepage: http://www.fs.uni-mb.si/en/inst/
APEM homepage: http://apem-journal.org

Place of publication: Maribor, Slovenia - EU Language of text: English

Subscription: 120 Euro per year (for Europe: included postage & handling, for other countries: add 50 Euro)
Nova kreditna banka Maribor, TRR 01100-6090102935; for APEM journal
Account Name: University of Maribor, Faculty of Mech. Eng.; VAT Nr. SI71674705

Advertising: back cover page – 150 Euro; internal page – 100 Euro (all black & white)

Postmaster: Send address changes to Publisher (see Address above)

Abstracted in INSPEC & EBSCO; Listed in Ulrich's Periodicals Directory & Cabell's Directory

HEADINGS should be typed in capitals and underlined, starting with **1. INTRODUCTION**, and should be set in **bold** (font size 12 pt) and aligned flush left. Do not add dashes, colons, etc. All headings from the Introduction to Acknowledgments are numbered sequentially using 1, 2, 3, etc. Headings must be short and clearly defined.

Subheadings appear in upper and lower case letters, and set in **bold** (font size 11 pt). Subheadings are numbered 1.1, 1.2, etc. Make no further divisions (two-level numbering at most).

Text
Use single column format and single line spacing. Use 11 points font size. Symbols for physical quantities in the text should be written in italics.
The first paragraph under each heading or subheading should be flush left and subsequent paragraphs should have a six-space indentation.

A colon is inserted before an **equation** is presented, but there is no punctuation following the equation. All equations are numbered and referred to in the text solely by a number enclosed in a round bracket (i.e. (3) reads as "equation 3").

Figures and Tables
To ensure a high-quality product, figures (and charts, diagrams, photos) must be computer-drafted or digitized with at least 300 dpi. They must be black and white with minimum shading. Figure captions appear below the figure, are centred, and are in upper and lower case letters. When referring to a figure in the body of the text, the abbreviation "Fig." is used. Each figure should have a number in Arabic numerals.
Table captions appear centred above the table in upper and lower case letters. When referring to a table in the text, "Table" with the proper number is used. Each table should have a number in roman numerals. Tables are numbered consecutively and independently of any figures. Tables should be kept to a minimum. All figures and tables must be incorporated into the text (in Portrait orientation).

Introduction
The introduction of the paper should explain the nature of the problem, previous work, purpose, and the contribution of the paper. It is assigned the number "1" and following sections are assigned numbers as needed.

Conclusion
A conclusion section must be included and should indicate clearly the advantages, limitations and possible applications of the paper. Discuss about future work.

Acknowledgements
An acknowledgement section may be presented after the conclusion, if desired.

References
This heading is not assigned a number. A reference list MUST be included using the following information as a guide. Only cited text references are included. Each reference is referred to in the text by a number enclosed in a square bracket (i.e., [3]). No reference to the author is necessary. Use 10 points font size.

*Please **cite** the papers from our journal APEM in your papers published in other journals (from JCR Database).*

References **must be numbered and ordered according to where they are first mentioned in the paper,** not alphabetically. All references must be complete and accurate. Examples follow.

Journal Papers:
Surname1, Initials; Surname2, Initials (year). Title, journal, volume, number, pages, doi (if existent)
[1] Eldabi, T.; Irani, Z.; Paul, R. J.; Love, P. E. D. (2002). Quantitative and qualitative decision-making methods in simulation modelling, Management Decision, Vol. 40, No. 1, 64-73, doi:10.1108/00251740210413370
Journal titles should not be abbreviated. Note that journal title is set in italics.

Books:
Surname1, Initials; Surname2, Initials (year). Title, publisher, place of publication
[2] Noorani, R. (2006). Rapid Prototyping: Principles and Applications, John Wiley & Sons, Hoboken
Note that the title of the book is italicized.

Chapters in Books:
Surname1, Initials; Surname2, Initials (year). Chapter title, editor(s) of book, book title, publisher, place of publication, pages
[3] Carbone, G.; Ceccarelli, M. (2005). Legged robotic systems, Kordic, V.; Lazinica, A.; Merdan, M. (Editors), Cutting Edge Robotics, ARS International Vienna, pro literatur Verlag, Mammendorf, 553-576

Proceedings Papers:
Surname1, Initials; Surname2, Initials (year). Paper title, proceedings title, pages
[4] Kittl, D.; Stopper, M. (2005). Digital manufacturing for industrial robotic workcells, Proceedings of the 16th International DAAAM Symposium, 187-188

WWW pages:
Surname, Initials or Company name. Title, from http://address, date of access
[5] SECO Tools. Product Range, from http://www.secotools.com, accessed on 29-09-2006

One complete copy of the journal is sent free of charge to the corresponding author of each contribution. No payment is made for papers.

APEM journal

Advances in Production Engineering & Management

Volume 5: Number 1: January 2010
pp. 1-69

CONTENTS

http://apem-journal.org

ISSN 1854-6250

UNIVERSITY OF MARIBOR

FACULTY OF MECHANICAL ENGINEERING
Production Engineering Institute

Advances in Production Engineering & Management

Volume 5: Number 1: January 2010
pp. 4-69

CONTENTS

http://apem-journal.org

ISSN 1854-6250
ISSN 1855-5531 (on-line)

SCOPE & TOPICS

Advances in Production Engineering & Management (APEM) is an interdisciplinary refereed academic journal. The main goal of the APEM is to present high quality research developments in all areas of production engineering and production management, as well as their applications in industry and services, to a broad audience of academics and practitioners. In order to bridge the gap between theory and practice, applications and case studies are particularly welcome. For theoretical papers, their originality and research contributions are the main factors in the evaluation process. Fields of interest include, but are not limited to:

Artificial Intelligence
Automatic Control
Cutting and Forming Processes
Decision Support Systems
Discrete Systems and Methodology
Education
Fuzzy Systems
Human Behaviour Representation
Industrial Engineering
Industrial Processes
Inventory Management
Knowledge Management
Logistics
Manufacturing Systems
Mechanical Engineering
Numerical Techniques
Operations Research
Operations Strategy
Operations Planning, Scheduling and Control
Optimisation Techniques
Production Processes
Project Management
Rapid Prototyping
Robotics and Manipulators
Quality Management
Queuing Systems
Risk and Uncertainty
Self-Organizing Systems
Simulation
Statistical Methods
Supply Chain Management
Technology, Technological Improvement
Virtual Reality
Visualisation

General approaches, formalisms, algorithms, or techniques should be illustrated with significant applications that demonstrate their applicability to real-world problems.

EDITORIAL

Welcome to the new issue of the *Advances in Production Engineering & Management* (APEM), ISSN 1854-6250. The mission of the APEM is to serve as a non-profit platform for publishing of scientific and professional articles and other useful resources (practical information, book reviews, equipment and software reviews etc.). Production engineering and production management are branches that concern the development, improvement, implementation and evaluation of integrated systems of people, knowledge, equipment, energy, material and process. They draw upon the principles and methods of engineering analysis and synthesis, as well as mathematical, physical and social sciences together with the principles and methods of engineering analysis and design to specify, predict and evaluate the results to be obtained from such systems. Whereas most engineering disciplines apply skills to very specific areas, production engineering & management can be applied in virtually every industry or in services.

We welcome contributions for the publication of research work in academic institutions, in industry, in services or in consultancy. The editors of the APEM are searching primarily for original, high-quality, theoretical and application-oriented research papers (based on theory development, practical experience, case study situations or experimental results).

Till now research papers from the field of manufacturing, machining and production management were published. We are planning to publish also special issues, dedicated to Layered technology, Internet based Manufacturing, Assessment management and more.

Editor-In-Chief

APEM journal ISSN 1854-6250 *Advances in Production Engineering & Management* 5 (2010) 1, 5 - 12 Scientific paper

WELD QUALITY PREDICTION OF SUBMERGED ARC WELDING PROCESS USING A FUNCTION REPLACING HYBRID SYSTEM

Dhas, J., E., R. and Kumanan, S.
Department of Mechanical Engineering,
Noorul Islam University, Thuckalay,
Nagercoil 629161
India
edwinrajadhas@rediffmail.com

Abstract:
Product variety, quality level and stiff competition have driven the manufacturing systems to be automated. Success of automation depends on effective and efficient decision making tools. This paper details about the development of intelligent decision making tool using a function replacing hybrid system for Submerged Arc Welding (SAW) process parameters to attain desirable weld quality. Experiments are designed according to Taguchi's principles and a multiple regression model is developed. Experimental data is supported with the data generated by regression model while developing the Neural Network model trained with Particle Swarm Optimization (NNPSO) technique. NNPSO model is found to be superior over in terms of computational speed and accuracy for the prediction of weld quality than the neural network model trained with traditional algorithm. The developed model is validated. The proposed method is flexible, competent, accurate, enhance automation, increase productivity, flexibility, safety and risky jobs is avoided by deployment of robots. Further, hardware controls are to be setup for online weld quality monitoring. Similar intelligent systems can be developed for real time monitoring and quality control of other welding process. This paper promotes manufacturers to develop unmanned factories to achieve the highest level for automation.

Key Words: Automation, Decision Making Tools, Function Replacing Hybrid System, Particle Swarm Optimization, Submerged Arc Welding, Weld Quality, Weld Bead Width

1. INTRODUCTION

To consistently produce high quality of weld, SAW requires skilled welding personnel with significant experience and a proper selection of welding parameters for a given task. Many attempts are made by researchers to establish the SAW process for a desired weld quality. Traditionally the desired welding parameters are obtained based from experience, charts or handbook values which are difficult, cumbersome and they does not ensure that the chosen welding parameters are optimal for the particular welding environment.

Later mathematical models have been developed to correlate the welding performance such as weld bead width, shape and size [1-5] with welding parameters. Multiple linear regression techniques were used to establish mathematical models for the weld bead geometry [6, 7]. Due to the inadequacy and inefficiency of the linear regression models to explain the nonlinear properties existing between the weld geometry parameters and welding parameters, intelligent systems such as ANN, fuzzy logic and expert system have been emerged. ANN is a good technique used to handle problems of nonlinearity. ANNs trained with back propagation algorithm [8-16] have been used to predict the weld bead geometry and penetration in shielded metal-arc welding process.

ANN and regression approaches were used to predict back-bead of gas metal arc [17] welding process. Data from regression analysis are used to train ANN with back propagation algorithm (NNBPA) to predict shear wave velocity from wire line log data for a carbonate reservoir [18]. In real-world applications, the back-propagation algorithm cannot guarantee an optimal solution since it may converge to a set of sub-optimal weights from which it cannot escape. Function replacing hybrid (FRH) can address this issue.

FRH is a hybrid system in which the principal function of a particular intelligent technique is replaced by another intelligent processing technique. A neural network combined with genetic algorithm is proposed [19] to determine the initial process parameters for injection moulding. GA-based neural network was used to model the explosive welding process [20], to optimize the design for a ball grid array wire bonding process [21], the electrical discharge machining process. [22], welding parameters [23] and neural networks trained by a genetic algorithm was used to predict machining forces [24].

PSO is used instead of back propagation algorithm in neural network for the prediction of tool life in turning operation [25].This paper details the design and development of a function replacing hybrid system to predict the weld parameters involved in SAW process. This hybrid system is composed of ANN trained with particle Swarm Optimization technique, which is a predictive neural network where weight updating is done using PSO algorithm. It scopes to build fast, accurate predictive networks.

2. DATA ACQUISITION

Experimentation is done on SAW is done using Taguchi method, a systematic application of design of experiments technique to improve the product quality. It uses a special design of orthogonal arrays to study the entire process parameter space with a small number of experiments. Orthogonal array is chosen based on the number of factors of interest and the number of levels of interest. An L8 orthogonal array is selected with number of factors involved is four and number of levels as two to conduct experiments in the semiautomatic SAW (SURARC of type XRCP 1200) machine. Single pass butt-welding is performed on the commercially available steel of IS 2062 grade (0.25%C, 0.20%Si, 0.75%Mn and balance Fe) (500 mm x 50 mm x 6mm) keeping the electrode positive and perpendicular to the plate. Electrode (diameter of 3.15 mm) utilized is AWS ER70S-6. The sizes of 10mm (width) samples are cut from the test piece. Then the specimens are cleaned, polished and etched. Profile projector is used to measure the weld bead width. Experimental observations for different combinations of weld parameters are shown Table I. Figure 1 shows the photographic views of weld samples. The dependency of weld quality to welding current, arc voltage, welding speed and electrode stick out is established using the multiple regression equation [26] for the SAW process.

Weld bead width,

$$\text{mm} = -34.833 + (6.667\times10^{-2} \times \text{welding current, ampere}) + (0.75\times\text{arc voltage, volts}) + (1.25\times10^{-2} \times \text{welding speed, mm/ min}) - (4.17\times10^{-2} \times \text{electrode sickout, mm}) \quad (1)$$

From the above equation, new values of weld bead width are generated to train the networks R^2 value for weld bead width is high which shows the strength on correlation of weld process parameters with weld bead width is significant.

Table I: Observed values from the test specimen.

Trial nos.	Weld bead width (mm)	Weld bead reinforcement(mm)	Depth of bead penetration (mm)	Weld bead hardness (H_RC)
1	13.0	2.0	3.0	37
2	11.0	2.0	3.5	40
3	12.5	3.0	3.5	42
4	13.5	1.5	4.0	34
5	14.5	2.0	5.0	52
6	14.0	2.5	4.5	48
7	14.5	2.0	4.0	49
8	15.0	3.0	3.5	48

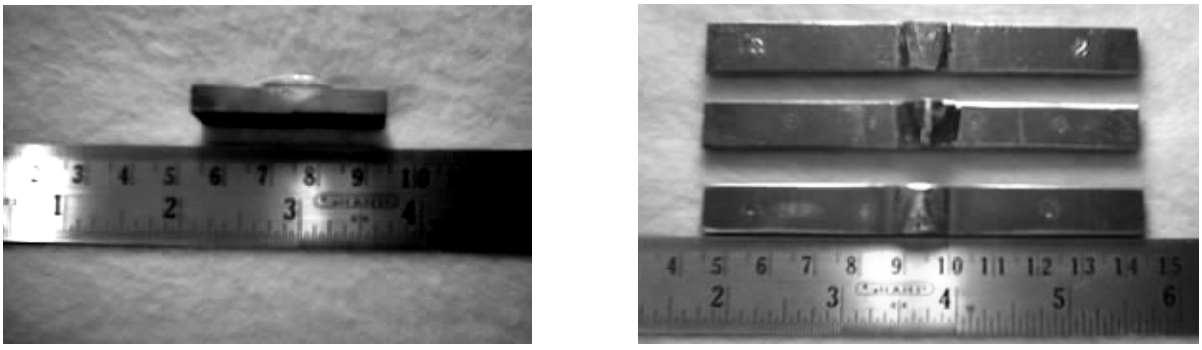

Figure 1: Photographic view of weld samples.

3. PREDICTIVE NEURAL NETWORKS

There are different algorithms to train ANN models. The most widely used method is back propagation algorithm. But is has limitations owing to the time taken to converge to a optimum solution and accuracy of result is less. This work exemplifies the use of PSO technique for weight updating in Neural Networks.

3.1 Development of NNBPA model

In submerged arc welding, the width of the weld bead is changed due to the complicated welding conditions, and accurate mapping is needed to produce the desired weld bead according to the welding parameters. Therefore, artificial neural network trained with back-propagation algorithm is used. The architecture of developed NNBPA is shown in Figure 2. It is feed forward back propagation network trained with Levenberg-Marquardt back propagation algorithm. The data set required for training the network is obtained using the experimental values together with data generated from regression analysis. The number of samples for training and testing are 51 and 5 respectively. The learning function is gradient descent algorithm with momentum weight and bias learning function. The number of hidden

layers and neurons are determined through a trial and error method, in order to accommodate the converged error. The structure of the proposed neural network is 4-12-9-1 (4 neurons in the input layer, 12 neurons in 1st hidden layer and 9 neurons in 2nd hidden layer and 1 neuron in the output layer) . With a learning rate of 0.55 and a momentum term of 0.9, the network is trained for 10000 iterations. The error between the desired and the actual outputs is less than .001 at the end of the training process. The back-propagation learning algorithm used in this neural network cannot guarantee an optimal solution since it might converge to a set of sub-optimal weights from which it cannot escape. Prediction technique using neural networks needs attention.

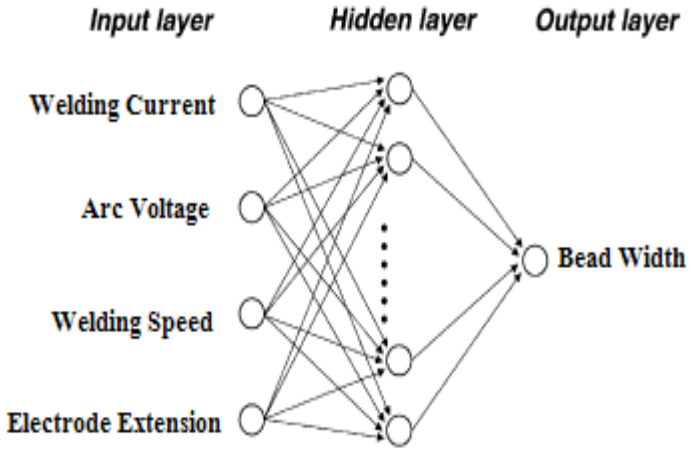

Figure 2: Architecture for the developed NNBPA model.

3.2 Development of NNPSO model

The scheme developed to predict weld quality in SAW process using NNPSO technique is shown in Figure 3. It is built using Matlab functions. The input weld parameters considered in the model are welding current, welding speed, arc voltage and electrode sickout with weld bead width, bead reinforcement, depth of penetration and weld bead hardness as outputs. The data required for training and testing the NNPSO model is taken from the experimental data in Table 1 supported with data from regression analysis. In this model, back propagation algorithm of neural network is replaced by PSO algorithm. Here the randomly

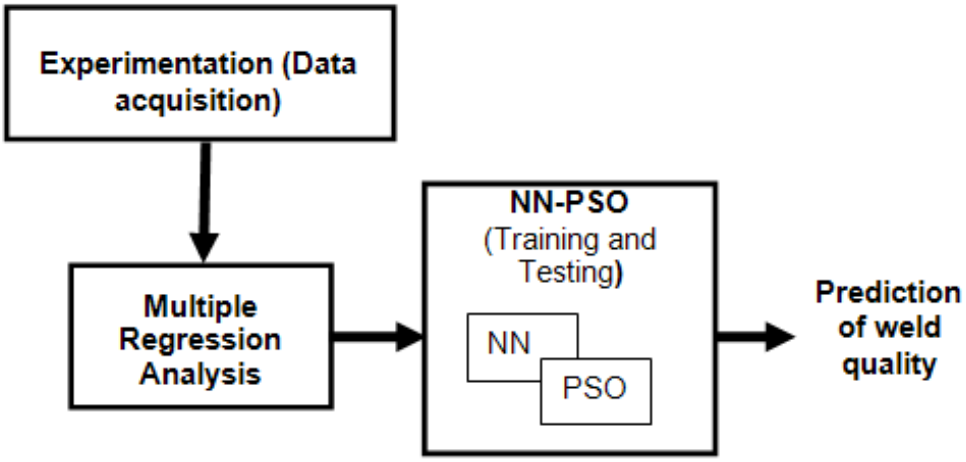

Figure 3: Proposed NN-PSO model for weld quality prediction.

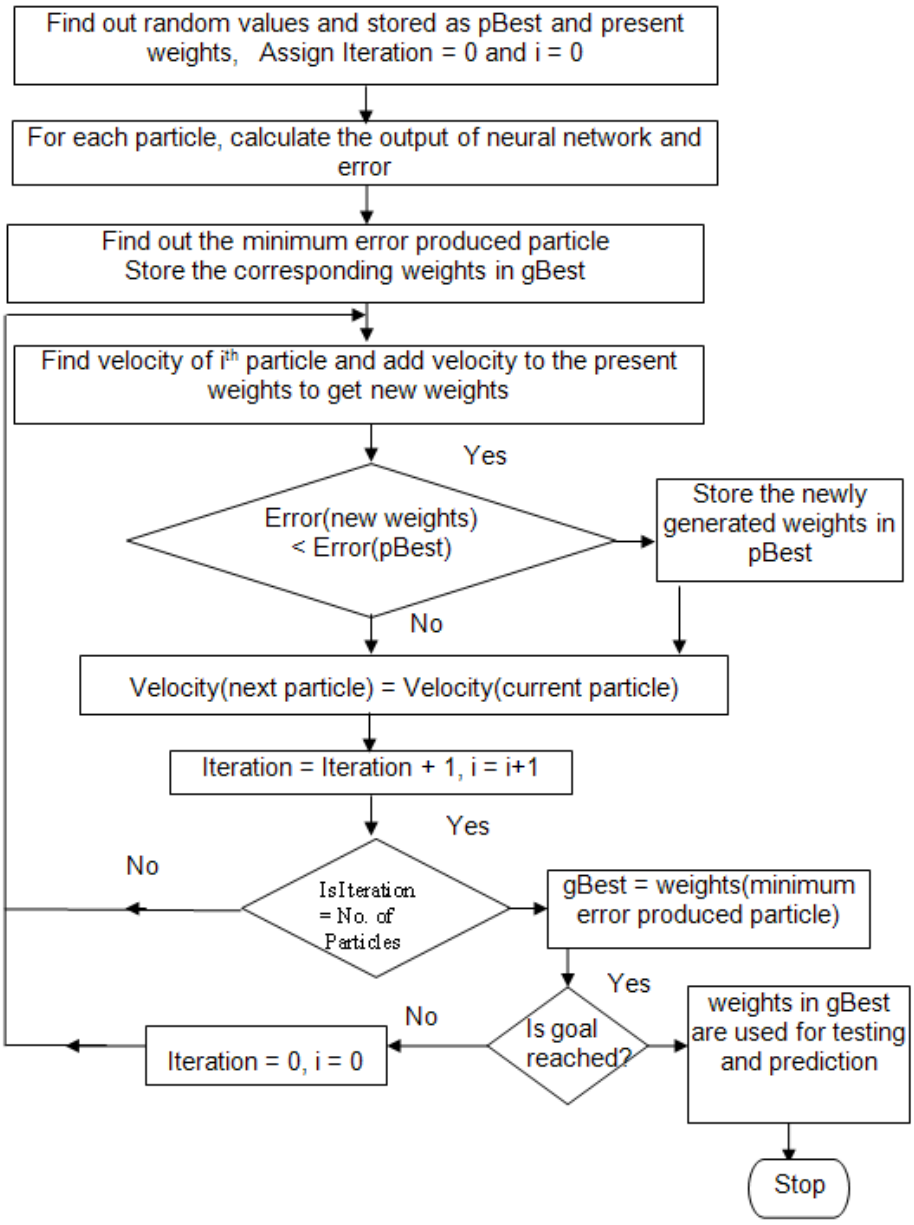

Figure 4: Flowchart for training the neural network using PSO algorithm.

generated weights are assigned in each link of neural network. In particle swarm optimization algorithm, pBest is the location of the best solution of a particle has achieved so far. gBest is the location of the best solution that any neighbour of a particle has achieved so far. Initially random numbers are generated for each particle and these random values are considered as pBest and present weights. Velocity is calculated using the equation 2 and added with the present weight in each link of neural network. For each particle, the newly calculated weights are compared with the pBest weights and the minimum error produced weights are stored in pBest. Initial velocity V is assumed to be 1 and gBest is the weights of minimum error produced particle. New weight is calculated as in equation 3.

$$V1 = W \times V + C1 \times Rand1 \times (pBest[w1]\text{-}present[w1]) + C2 \times Rand2 \times (gBest[w1] - present[w1]) \quad (2)$$

$$\text{New weight } wi = \text{current weight } w + \text{new } V1 \quad (3)$$

where C1 and C2 are two positive constants named learning factors (usually Cl= C2 = 2). Rand1 and Rand2 are two random functions in the range [0, 1]. W is an inertia weight to control the impact of the previous history of velocities on the current velocity. The operator W plays the role of balancing the global search and the local search; and was proposed to decrease linearly with time from a value of 1.4 to 0.5. As such, global search starts with a large weight and then decreases with time to favour local search over global search. When the number of iterations is equal to the total number of particles, goal is compared with the error produced by the gBest weights. If the error produced by the gBest weights are less than or equal to the goal, weights in the gBest are used for testing and prediction. Otherwise weights of minimum error are stored in gBest and the iterations are repeated until goal reached. The flow chart of the proposed NN-PSO model is shown in Figure 4.

4. RESULTS AND DISCUSSION

Interaction of weld parameters with the weld bead width has a complicated correlation and the results of analyzing the correlations are high. Since the width of the weld bead shows a linear pattern, in the regression analysis the input parameter is expressed in terms of linear equation as given in equation (1). The performance analysis of the developed ANN models to predict weld bead width in terms accuracy and speed are evaluated and compared. The comparison of measured values of weld quality with predicted values obtained from NNBPA and NN-PSO model is shown in Figure 5. The graph shows that the weld quality predicted by NNPSO are closer to the measured value and hence are found to be accurate than the predicted valued from NNBPA. Among the developed models, computational time needed for training the network using NNPSO is less compared with NNBPA. Hence the NNPSO model is found to be superior in computational efficiency than the other. The reason is that PSO stores the gbest as well as pbest solutions in memory. Each individual in the population tries to emulate the gbest and pbest solutions in the memory by updating the PSO equation. Results from Figure 6 shows that NNPSO needs only minimum number of epochs and hence computational time required is less. This is due to that in this proposed method, the random weights used for training the initial network was selected only based on the fitness function that generates the minimum error. So the number of epochs required for training the neural network is greatly reduced.

5. CONCLUSIONS

Prediction and determination weld quality is important for the process and product design of welded structures. The existing prediction measurement, techniques and methods are limited in application. Intelligent hybrid systems are being attempted to develop predictive neural networks. This paper proposes the development of a hybrid weld quality prediction system. The proposed predictive network is a Function Replacing Hybrid system build with the neural network trained by PSO technique. Developed NNPSO model will predict the requisite values of weld quality for given set of parameter combinations in real time with out any extensive and expensive computations. It is validated with the experimentation and proposed method is simple, economical, reliable competent, found fast and ease in prediction. With this encouraging result the prediction model can be further improved upon by including weld bead geometry and weld bead hardness as other influencing parameters on weld quality. Further, hardware controls are to be setup for online weld quality monitoring. Similar intelligent systems can be developed for real time monitoring and quality control of other welding process.

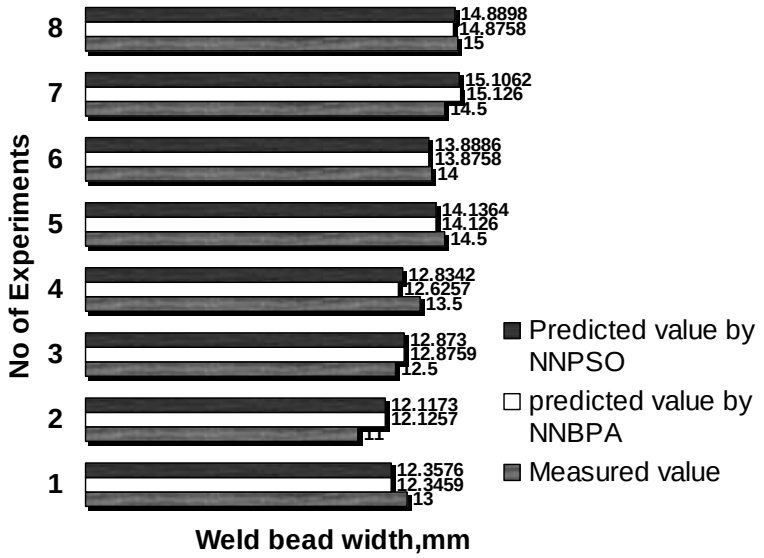

Figure 5: Comparison of weld bead width between measured and predicted values.

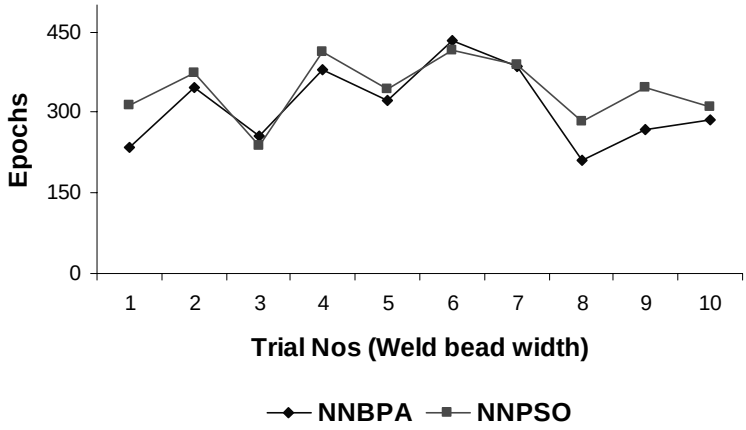

Figure 6: Comparison of performance between NNBPA and NNPSO model.

6. ACKNOWLEDGEMENT

The authors express their sincere thanks to the Ministry of Human Resource Development [MHRD], Government of India for the sponsorship under its Research and Development program.

REFERENCES

[1] Apps, R.L; Gourd, L.M ; Lelson, K.A. (1963). Effect of welding variables upon bead shape and size in submerged-arc welding, Weld Metal Fabrication, Vol.31, 453–457.

[2] Revaandra, J; Parmar, R.S. (1987). Mathematical model to predict weld bead Geometry for flux cored welding, Metal Construction, Vol.19, 31R – 35R.

[3] Kim, I.S; Kwon, W.H; Park, C. E. (1996). The effects of welding process parameters on weld bead width in GMAW processes, The Korea Weld Society,Vol.14, 204-213.

[4] Gupta, V.K; Parmar, R.S. (1986). Fractional factorial techniques to predict dimensions of the weld bead in automatic submerged arc welding, Journal of Institution of Engineers (India),Vol.70, 67–71.

[5] Tarng, Y.S; Yang, W.H. (1998). Optimization of the weld bead geometry in gas tungsten arc welding by the Taguchi method, International Journal of Advanced Manufacturing Technology,Vol.14, 549–554.

[6] Lee, J.L; Rhee, S. (2000). Prediction of process parameters for gas metal arc welding by multiple regression analysis, Proceedings of Institution of Mechanical Engineers – B, Vol.214, 443-449.

[7] Yang, L.J; Bibby, M.J; Chandel, R.S. (2003). Linear regression equations for modeling the submerged-arc welding process, Journal of Materials Processing and Technology, Vol. 39, 33 - 42.

[8] Zeng, X.M; Lucas, J; Fang, M.T.C. (1993). Use of neural networks for parameter prediction and quality inspection in tungsten inert gas welding, Transactions of the Institution of Measurement and Control, Vol. 15, 87–95.

[9] Huang, T.H; Zhang, H.C. (1994). Artificial Neural Networks in Manufacturing: Concepts, Applications and Perspectives, IEEE Transactions on Components, Packaging and Manufacturing Technology-part-A , Vol. 17, 212-228.

[10] Nenad Ivezic ; John D Allen Jr ; Thomas Zacharia. (1999). Neural Network-Based Resistance Spot Welding Control and Quality Prediction, IEEE, 989-984.

[11] Lee, J.I ; Um, K.W. (2000). A prediction of welding process parameters by prediction of back - bead geometry, Journal of Materials Processing and Technology, Vol. 108 , 106- 113.

[12] Li, X; Simpson, S.W ; Rados, M. (2000). Neural networks for online prediction of quality in gas metal arc welding, Science and Technology of Welding and Joining, Vol. 5, 71- 79.

[13] Nagesh, D.S ; Datta, G.L. (2002). Prediction of weld bead geometry and penetration in shielded metal-arc welding using artificial neural networks, Journal of Materials Processing and Technology, Vol. 123, 303–312.

[14] Kim, I.S ; Son, J.S; Park, C.E ; Lee, C.W; Yarlagadda Prasad K.D.V. (2002). A study on prediction of bead height in robotic arc welding using a neural network, Journal of Materials Processing and Technology, Vol. 131, 229–234.

[15] Klein, R; Mucin, V.H ; Klinckhachorn, P. (2002). Predicting the Elasto-Plastic Response of an Arc – Weld Process Using Artificial Neural Networks, IEEE , 440-444.

[16] Edwin Raja Dhas, J; Kumanan, S. (2007).Prediction of weld bead width using artificial neural networks, Proceedings of Factory Automation, Robotics and Soft computing, National Institute of Technology, Warangal, India, 382-385.

[17] Jeongick Lee ; Kiwoan Um. (2000). A comparison in a back-bead prediction of gas metal arc welding using multiple regression analysis and artificial neural network, Optics and Lasers in Engineering, Vol. 34, 149-158.

[18] Eskandari, H; Rezaee, M.R; Mohammadnia, M. (2004). Application of multiple regression and artificial neural networks techniques to predict shear wave velocity from wireline log data for a carbonate reservoir, south west Iran, CSEG recorder, Vol. 42, 40-48.

[19] Mok, S.L; Kwong, C. K; Lau, W.S. (2001). A hybrid neural network and genetic algorithm approach to the determination of initial process parameters for injection moulding, International Journal of Advanced Manufacturing Technology,Vol.18,404-409.

[20] Nariman-Zadeh, N ; Darvizeh, A ; Ahmad-Zadeh, G.R. (2003). Modelling of explosive welding process using GMDH-type neural networks and genetic algorithms, International Multi - Conference, Vol. 21,115-120.

[21] Chao-Ton Su; Tai-Lin Chiang. (2002). Optimal Design for a Ball Grid Array Wire Bonding Process Using a Neuro-Genetic Approach, IEEE transactions on Electronics Packaging Manufacturing, Vol. 25, 13-18.

[22] Su, J.C; Kao, J.Y; Tarng, Y.S. (2004). Optimisation of the electrical discharge machining process using a GA-based neural network, International Journal of Advanced Manufacturing Technology,Vol. 24,81 –90.

[23] Hsien-Yu Tseng. (2006). Welding parameters optimization for economic design using neural approximation and genetic algorithm, International Journal of Advanced Manufacturing Technology,Vol. 27, 897-901.

[24] Kumanan, S; Nannae Sahib, S.K; Jesuthanam, C.P. (2006). Prediction of Machining Forces using neural networks trained by a genetic algorithm, Journal of Institution of Engineers (India),Vol. 87,1-15.

[25] Natarajan, U; Saravanan, R; Periasamy, V.M. (2007). Application of particle swarm optimization in artificial neural network for the prediction of tool life, International Journal of Advanced Manufacturing Technology,Vol.31; 871-876.

[26] Montgomery, D.C ; Peck, E.A. (1992) .Introduction to Linear Regression Analysis, John Wiley &, Sons New York, N.Y.

APEM journal ISSN 1854-6250 *Advances in Production Engineering & Management* 5 (2010) 1, 13 - 24 Scientific paper

EXPERIMENTAL SELECTION OF SPECIAL GEOMETRY CUTTING TOOL FOR MINIMAL TOOL WEAR

Srikant, R., R.*; Subrahmanyam, S., M.**; Krishna, V., P.**
*Corresponding author, Dept. of Mechanical Eng., GIT, GITAM University, Visakhapatnam-530045, India, srikant_revuru@yahoo.com
** Dept of IPE, GIT, GITAM University, Visakhapatnam-530045, India

Abstract:
A major problem in achieving high production rates in metal cutting industry is Tool Wear. Prolonged tool life has gained significance with the discovery of materials like hard steels, and the urge to maintain tighter geometric tolerances and improved surface finish. Strengthening of the edge and prevention of its deterioration is achieved by the several edge geometries that have been proposed; the most prominent being chamfered tools and honed tools. But, the investigation of the effect of different chamfer angles and honed radii on the machining parameters and tool life is not much done. The present work is an attempt to study the influence of these variables on tool wear. EN-8 steel with sharp tool and different chamfered and honed tools has been machined and experimental investigations have been carried out. Variations in cutting forces, tool wear, and thus tool life, have been observed for all the cases. Inferences drawn are validated and the performance of the tools for workpieces with different hardness is assessed by machining EN-9 under similar cutting conditions using similar tools as in the previous case. Results obtained in both the cases are analogous, thus validating the conclusions made. The work can be extended by considering more values chamfer angle and honing radii.

Key Words: Chamfered Tool, Honed Tool, Metal Cutting, Tool Wear

1. INTRODUCTION

The present day cutthroat competition prompts towards developing processes and materials that perform satisfactorily, in prolonged usage. Production costs and times need to be minimized to achieve the goals. Undesirable effects such as tool wear and tool breakages not only result in deterioration in surface finish and dimensional accuracy of the finished parts, possible damage to the workpiece and machine, but also increase production times. For modern machine tools, a major portion of downtime is attributed to tool failure. Hence new strategies to reduce tool wear, thus improve tool life, are under research and are being developed.

Understanding tool wear mechanism/phenomenon is essential to devise new methodologies for enhancing tool life. Various mechanisms simultaneously contribute to tool wear. Due to the constant rupture of the cutting tool with hard particles in the workpiece, the cutting edge of the tool deforms. This mechanism is known as Abrasion wear and is a major cause of tool failure. Due to the high temperatures and pressures prevalent at the cutting tool-workpiece junction, the tip of the cutting tool gets adhered to the workpiece. The process is similar to welding and this mechanism is known as Adhesion wear. Diffusion wear occurs due to the high temperatures at the cutting edge of cutting tool; as material transfer takes place from the tool tip to the chip, tool cutting edge loses hardness. Due to the combination of aforementioned different mechanisms, tool wear occurs in various forms that include Flank wear, Crater wear, Notch wear and Nose wear.

Tool wear rarely occurs in an isolated form and is a combination of different mechanisms. It is relatively rare to find pure adhesive wear, as the material transferred during adhesive wear often causes abrasive wear. Abrasive wear involves loss of material by formation of

chips as in abrasive machining. A convenient way of studying abrasive wear is in terms of specific energy, required to remove a unit volume of material [1].

During continuous machining, a wear land develops at tool flank, known as Flank wear. Flank wear is caused by constant rupture of cutting tool against just-machined surface due to adhesive and abrasive wear mechanisms. It is measured by the width of wear land and results in changes in the mechanics of the cutting process. Flank wear increases with progress in machining time and results in increased tendency for chatter and changes in the dimensions of the product.

Crater wear results from a combined evolution of high cutting temperatures and high shear stresses creating a crater on the rake face some distance away from the tool edges, quantified by depth and cross-sectional area of the crater. Crater wear arises due to combination of different wear mechanisms: adhesion, diffusion or thermal softening and plastic deformation. Crater wear changes the effective rake angle and the chip-tool contact length and also reduces the amount of force that the tool can withstand. Normally, limiting value of flank wear is reached before that of crater wear and hence the study of flank wear is more critical.

One of the challenges posed lies in devising methods for the classification/estimation of cutting tool wear. This seemingly simple task has proved to be rather difficult probably due to the fact that tool wear introduces small changes in a process with a very wide dynamic range. The task can be subdivided into a number of stages, generation of a feature or set of features indicative of tool condition, corresponding sensor selection and deployment and finally analysis of the collected and processed information so as to determine tool wear.

1.1 Tool wear monitoring

Conventionally, based on his experience, knowledge and expertise, an operator judges the condition of the cutting tool [1-3]. Sensory information like presence of smoke, smell, etc. is used to arrive at this decision. In many cases, information from a single sensor may not be sufficient and hence more sensors may be employed. The idea pursued in this anticipates learning, pattern recognition and sensor fusion abilities of human operators. With advent of unmanned industries, on-line monitoring systems are used to replace human operators.

Techniques for on-line tool wear monitoring can be grouped into two main categories: direct sensing and indirect sensing techniques [2]. Both the direct and indirect methods of tool wear sensing techniques are reported to be attempted extensively. However, direct methods are less beneficial as the cutting area is largely inaccessible, and hence on-line monitoring of tool condition becomes difficult.

The indirect methods include, touch trigger probes, optical, radioactive, proximity sensors and electrical resistance measurement techniques. These methods involve in recording one of the process variables that can be correlated to tool wear. The usual cutting parameters measured are cutting forces, acoustic emission, temperature, vibration, spindle motor current, torque and strain.

1.2 Chamfered tools and honed tools

As optimizing cutting conditions is little in control of the operator, new strategies are devised to restrict tool wear progression. Application of lubricants, though advantageous, is not of much use in high speed machining operations. Cutting tools with coatings and special edge geometries have emerged as a promising solution. Edge preparation of the tools is critical for acceptable tool life in turning. Due to the brittle nature of the materials used to machine steel, strong edge geometries help to prevent premature tool failure or accelerated tool wear by edge chipping. The problem is magnified by the large cutting load and negative rake angles typically used for hard turning. Thus, tool manufacturers have developed the practice of preparing cutting edges with a honed radius or edge chamfer to strengthen the edge. These tools have shown improved tool life compared to unprepared (or up-sharp) tools.

Single point cutting tools are characterized by the loss of tool tip in the initial stages of wear. Deterioration of the tip weakens the tool and results in the loss of its functionality [4,5]. Research to strengthen the tool tip has engendered tools of special geometry like chamfered and honed tools [4,6]. Ren at al [6] proposed an analytical model based on tool geometry, cutting conditions and steady state temperatures in shear and chip rake face contact zones to estimate influence of chamfer angle on cutting forces and temperatures. applied the minimum energy principle to total energy and calculated the shear angle. Corresponding shear strain and stresses were estimated. Zhou et al [7] studied the effect of chamfer angle on tool wear of PCBN cutting tool in super finishing hard turning. The correlation between cutting force, tool wear and tool life were investigated. The optimized cutting angle of chamfer for PCBN tools is suggested as 15°. Movahhedy et al [8] carried out numerical analysis of metal cutting with chamfered as well as blunt tools. It was concluded that though chip formation process is not much affected, cutting forces have increased with chamfered tools. It is generally agreed that chamfered tools increase tool life but lead to increased cutting forces. Though work is reported in PCBN tools, the behaviour of chamfered HSS tools is not studied.

When the cutting tool is relatively brittle or subjected to a hard workpiece, the very tip of the tool is rounded off to prevent chipping. This has been attracting the researchers of late. A lightly honed edge has a radius of about 0.03mm while a heavily honed tool has a radius of about 0.125mm. Mayer et al [9] measured machining forces in virgin and worn out tool. They proposed a combination of chamfered and honed tools for better tool life. Kountanya [10] studied the tool wear progression with honed tools and concluded that though cut-in wear is more for honed tools, wear growth gets stabilised later on and is less on further rise in machining time compared to sharp tools. They reported an increase in the cutting forces with increase in honed radius. Fang et al [11] studied the effect of chamfered and honed tools in machining three aluminium alloys 7075-76, 6061-T6 and 2024-T351. Cutting forces, thrust force, their ratios and chip thickness were measured. A model was proposed to predict chip formation characteristics. Cemented carbide tools were used in the study.

Majority of the works reported on the subject do not deal with the popular HSS tools and also the proposed models are for chip flow characteristics or cutting forces. Tool wear models are not proposed. Also the performance of chamfered tools and honed tools is not compared; both are dealt with separately. The present work investigates the effect of tool tip geometry on tool wear and cutting forces, considering chamfered and honed HSS tools. Cutting force is chosen as a parameter to estimate tool flank wear. Turning of EN-8 steel using H.S.S tool under constant cutting conditions is carried out. A lathe tool dynamometer is used to find out radial force data. The tool profile has been analyzed under an optical projector to estimate the growth of flank wear under progressive machining [12]. The projected profile of the tool in different stages of machining is compared with that of virgin tool and width of flank wear land is measured. Limiting value of 0.6mm of maximum flank wear width is considered. The performance of both tools is compared. A mathematical model is proposed for tool wear based on regression. To validate the results obtained, another material, typically a harder one; EN-9 is turned with tools of similar geometry.

2. EXPERIMENTAL SET-UP AND PROCEDURE

EN-8 steel is turned under constant cutting conditions. To validate the conclusions drawn and to study the influence of workpiece hardness on the behaviour of the tool, turning of EN-9 (carbon-0.5%) is carried out. Workpieces of diameter 50mm and 915 mm length are machined.

A 3 HP lathe of make Madras Machine Tool Manufacturer's Ltd., Coimbatore, India is used for the experimentation. H.S.S tool is used for machining. The nomenclature of the tool is 0^0-5^0-30^0-15^0-10^0-10^0-0 as per ISO specifications.

Figure 1 shows the chamfered tool. Chamfer angles are varied from 5 to 20^0 in steps of 5^0. Chamfer width is kept constant at 0.9 mm. The remaining geometry is same as the sharp tool. Figure 2 shows the honed tool. Radius of honing is varied as 0.03, 0.05, 0.1, 0.12

mm. Tools are honed using a tool end cutter and are verified with the tool maker's microscope. Cutting forces are measured using a lathe tool dynamometer (Make : Lakshmi Controls and Instrumentation Controls, Measuring range : 0-2000 N, Type : Cantilever type strain gauge dynamometer, Accuracy : ± 2% , Sensitivity : 1 N).

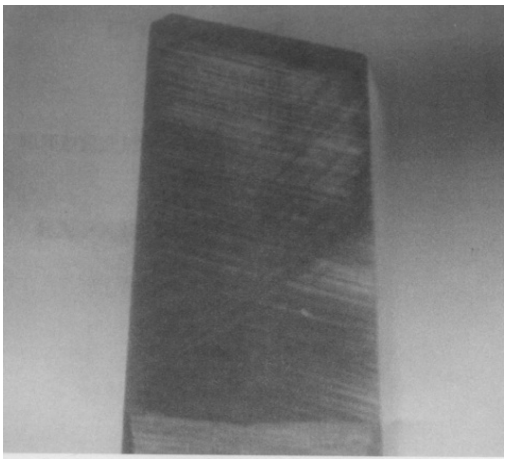

Figure1: Chamfered Tool.

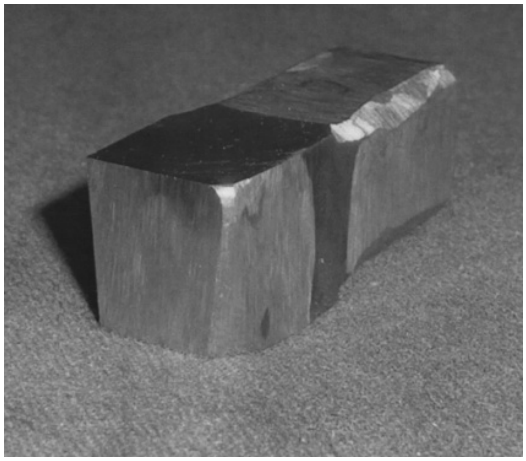

Figure 2: Honed Tool.

At regular intervals of machining, cutting tool is analysed under an optical projector to measure tool flank wear.

A lens of magnification 20 is used to analyse tool profile. Optical projector has provisions for rectangular movement of the table on which tool is placed. To make tool flank parallel to table a wooden rest is prepared.

Machining is performed on a lathe with specifications mentioned above. EN-8 and EN-9 steel are selected as workpiece. A H.S.S cutting tool is used for machining. Constant cutting conditions are maintained. An average Cutting speed of 100 m/min, feed rate of 0.2514 mm/rev and depth of cut of 1 mm is maintained.

Machining is carried out and in intervals (one minute initially up to 3 min and 5 min thereafter, up to 40 min) tool profile is analysed under an optical projector. Tool profiles obtained after machining are compared with initial tool profile and flank wear is determined.

3. RESULTS AND DISCUSSIONS

3.1 Radial cutting force

In the present work radial component of cutting force is chosen as a parameter to estimate tool flank wear. A lathe tool dynamometer is used to measure radial force component of cutting force. Measurements are taken with progress in machining time. Figure 3 shows variation of radial force with machining time for chamfered and sharp tool. Cutting forces are consistently higher for the chamfered tool. The forces increase with the chamfer angle; the obvious reason being the increase in the contact area of the tool and workpiece, resulting in increased friction. In all the cases, for chamfered as well as sharp tool, it can be seen that radial force increases with progress in machining time. Initially, rise in radial force is high and gradually gets slowed down. After sometime, rise in cutting force is low.

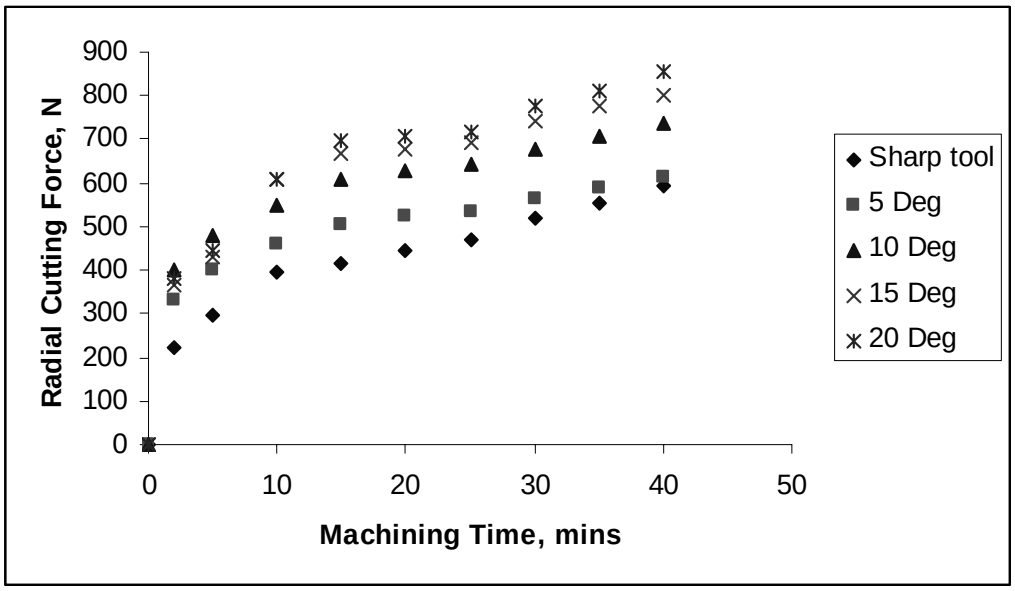

Figure 3: Variation of radial force with machining time for chamfered and sharp tool (EN-8).

Figure 4 shows the variation of cutting force with machining time for honed tools with different honing radius and sharp tool. Cutting forces are consistently higher for honed tools. The forces increase with the honing radius. It can be seen that in both honed and chamfered tools, the cutting forces are much higher compared to sharp tools. However, cutting forces are higher in chamfered tools compared to the honed tools. This may be attributed to the fact that chamfered tools have an area contact with the workpiece, while the rounded honed tool has point, at the maximum a line contact. As the contact is less, the cutting forces are less in honed tools compared to the chamfered tools.

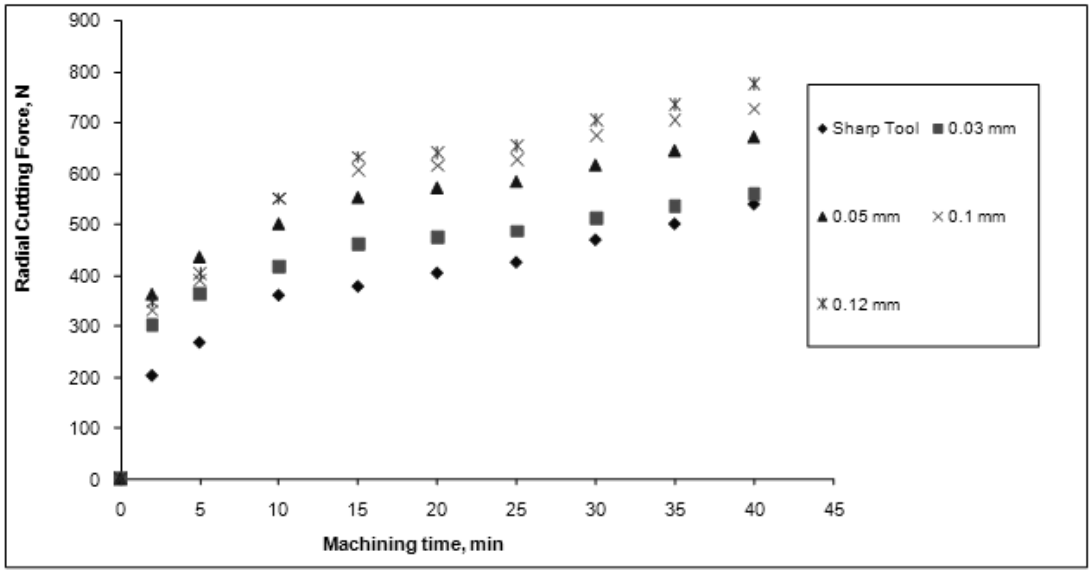

Figure 4: Variation of radial force with machining time for honed and sharp tool (EN-8).

3.2 Tool flank wear

Tool flank wear is measured at different instances of machining with progress in machining time. Figure 5 shows variation of flank wear with progress in machining time for chamfered and sharp tool.

Figure 5 shows that growth of flank wear is initially high and slowly gets constant for some time. On further machining, rise in flank wear is accelerated. Tool wear in case of sharp tool is highest. It is interesting to note that tool wear decreases with chamfer angle up to 15° and then raises. Hence minimum tool wear is observed for 15° chamfer angle. For better understanding of the implication of the chamfer angle, Figure 6 plots tool life (extrapolated values) versus chamfer angle. Chamfer angle of 0° represents a sharp tool. The results clearly demonstrate that tool life tends to increase with chamfer angle up to 150 and then decreases. One possible reason for this could be that while chamfering strengthens the tool tip, excessive chamfering may lead to increased tool-workpiece contact and damage the tool.

Figure 7 shows the growth of flank wear is for honed and sharp tools. It may be observed that the tool wear progression follows a similar trend as in case of chamfered tool. The influence of honing radius is interesting to note. The tool with honing has lesser tool wear compared to the sharp tool. However, honed tools do not show initially high wear. This stage is reached by the honed tools after machining for about 10 min. The possible reason maybe that machining causes the rounded portion of the tool to be lost by sharpening it. The tool then becomes analogous to a sharp tool and then the tool wear takes place just as in a sharp tool. In other words, the tool wear mechanism is postponed for sometime in the honed tools. It may be observed that honed tools have considerably less wear compared to the sharp tool and tool wear decreases with honing radius.

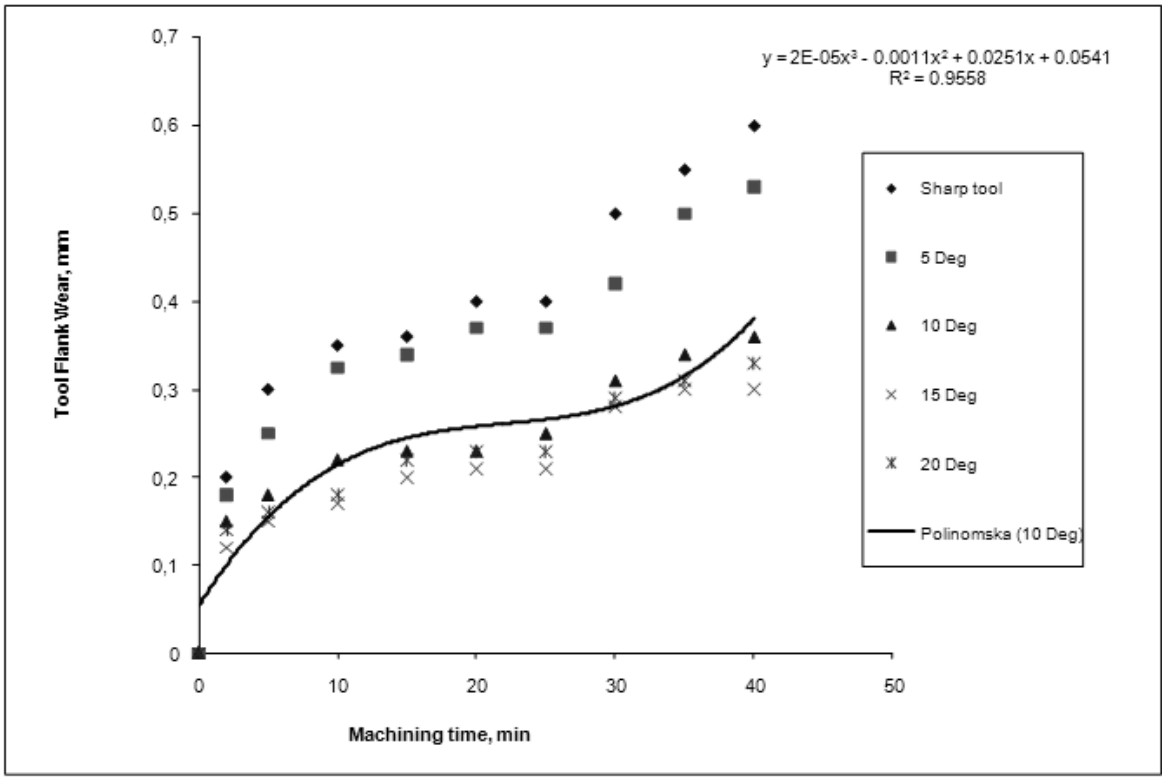

Figure 5: Variation of flank wear with machining time for chamfered and sharp tool (EN-8).

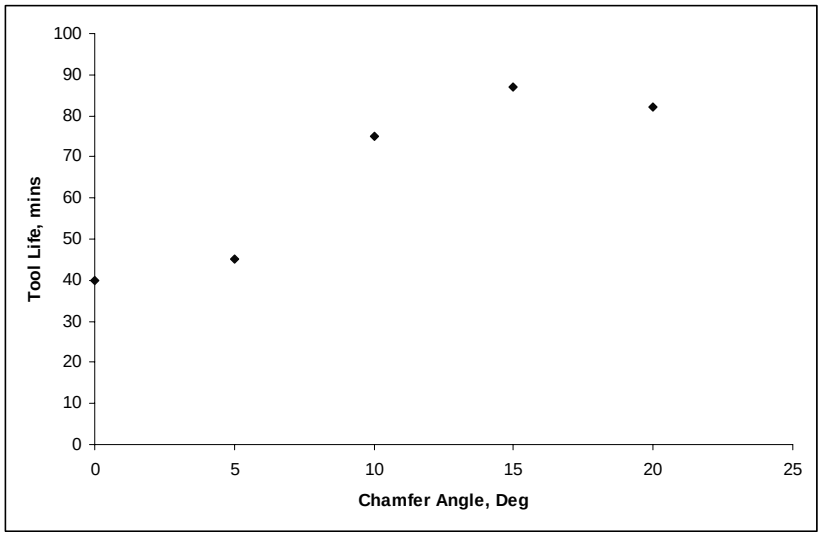

Figure 6: Variation of tool life with chamfer angle (EN-8).

For clarity, tool life is plotted against honing radius in Figure 8. As in the above case, sharp tool is taken as a tool with zero honing radius. It may be inferred from the results that cutting tools with honed edge has lesser tool wear, thus longer tool life, compared to the chamfered tools. Though honed tools with larger honing radius demonstrate higher tool life, providing much honing radius may result in excessive ploughing and may be disastrous to the tool. Results suggest that tool life for honed tools is much longer compared to the chamfered tools.

Cutting tool wear trends in both honed and cutting tools follow a curve of third degree of the form:

$$Y=AX^3 + BX^2+CX+D \quad (1)$$

where, Y represents Tool Flank Wear, X represents machining time and A, B, C, D are constants that depend on the tool, workpiece and other machining parameters. The individual equations are shown in the figures.

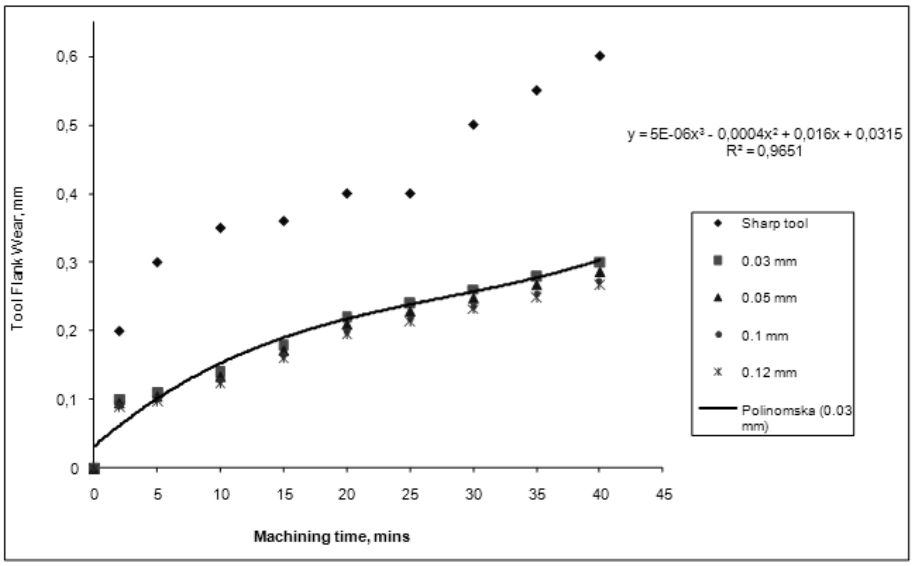

Figure 7: Variation of flank wear with machining time for honed and sharp tool (EN-8).

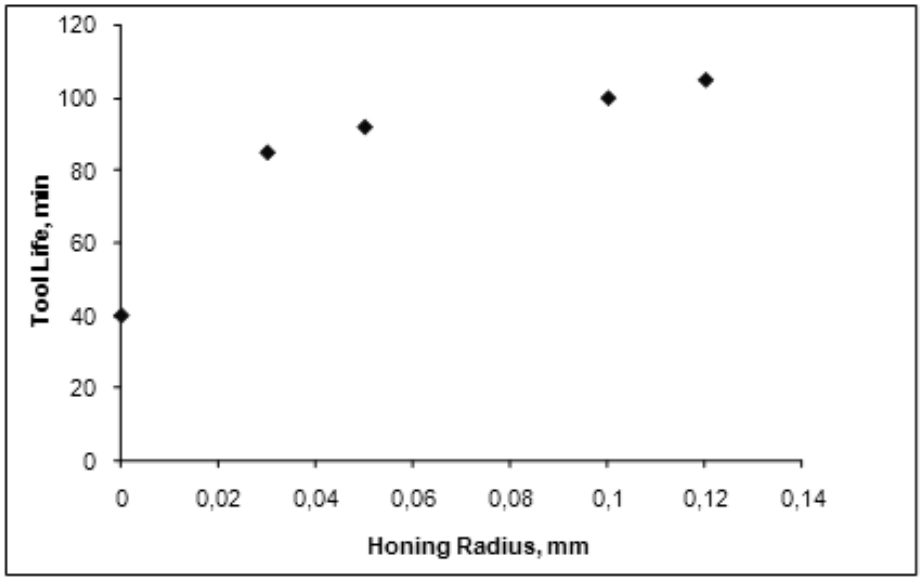

Figure 8: Variation of tool life with honing radius (EN-8).

An average regression above 0.95 is observed in both the cases. To validate the inferences drawn from the above work, another material, EN-9 is taken and is machined using tools of similar geometry.

The results show that the forces obtained in machining EN-9 are considerably higher, due to higher content of carbon that leads to hardness of the material, however, the cutting forces follow the same pattern as in case of machining EN-8 (Figure 9-10). The results are similar to those obtained by machining EN-8. Honed tools produce higher cutting forces compared to the sharp tools. It is interesting to note that in both cases, chamfered tools produce higher cutting forces.

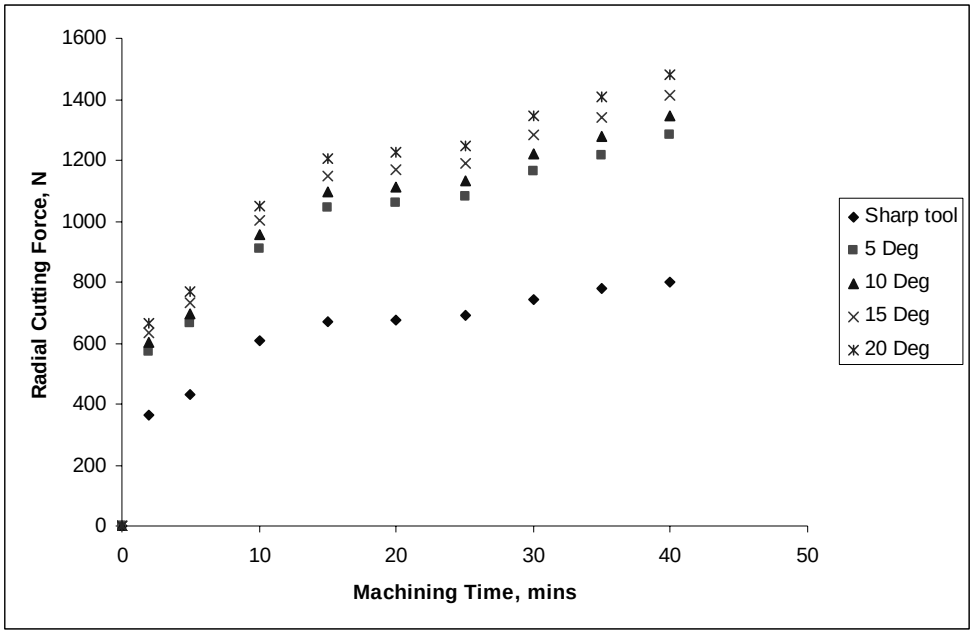

Figure 9: Variation of radial force with machining time for chamfered and sharp tool (EN-9).

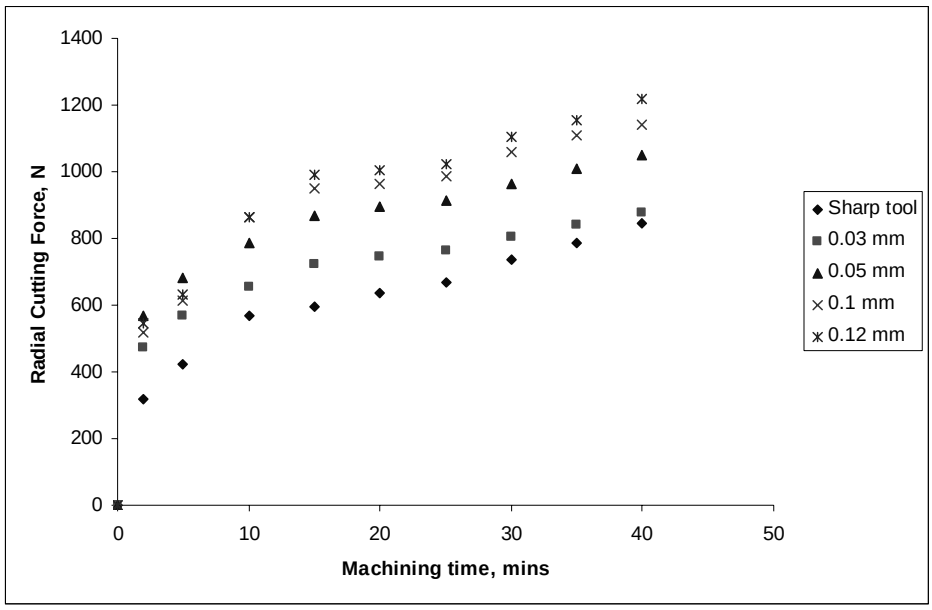

Figure 10: Variation of radial force with machining time for honed and sharp tool (EN-9).

Figure 11 shows the growth of tool flank wear in case of machining EN-9 with chamfered and sharp tools. It can be noted that tool wear is much less in chamfered tools compared to the sharp tool. Also the difference between the sharp tool wear and the chamfered tool wear is very large. This clearly indicates the better suitability of chamfered tools for machining hard materials. Further, even in this case, as in case of machining EN-8 steel, the tool with 15° chamfer angle has minimum tool flank wear.

Figure 12 presents tool flank wear growth in honed and sharp tools while machining EN-9 steel. The presented results show that tool wear is less for honed tools compared to the sharp tool. Also, tool wear is found to decrease with increase in honing radius. Further, it may be noted that difference in tool flank wear for honed tools and sharp tool is much more than in case of machining EN-8. Thus, in both the cases of chamfered and honed tools, it is evident that these tools are best suited for machining harder materials.

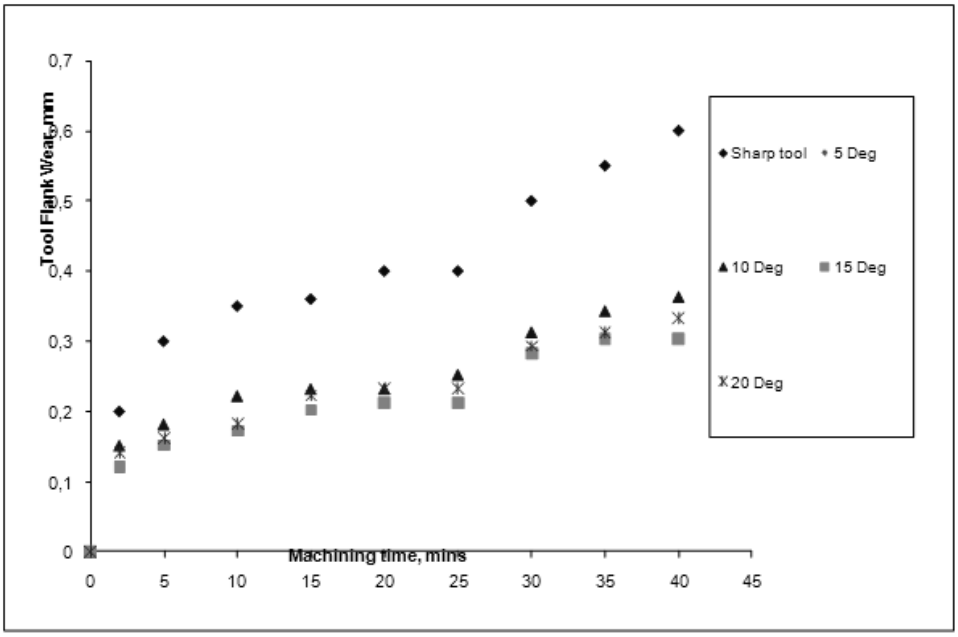

Figure 11: Variation of flank wear with machining time for chamfered and sharp tool (EN-9).

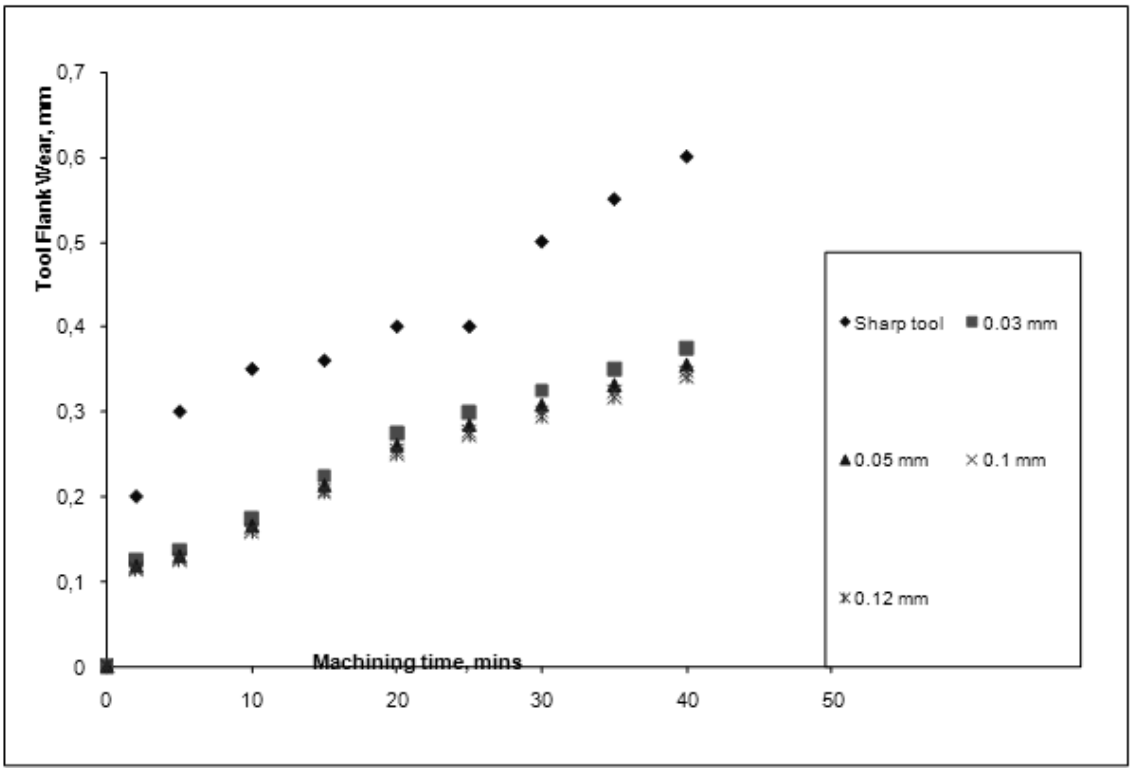

Figure 12: Variation of flank wear with machining time for honed and sharp tool (EN-9).

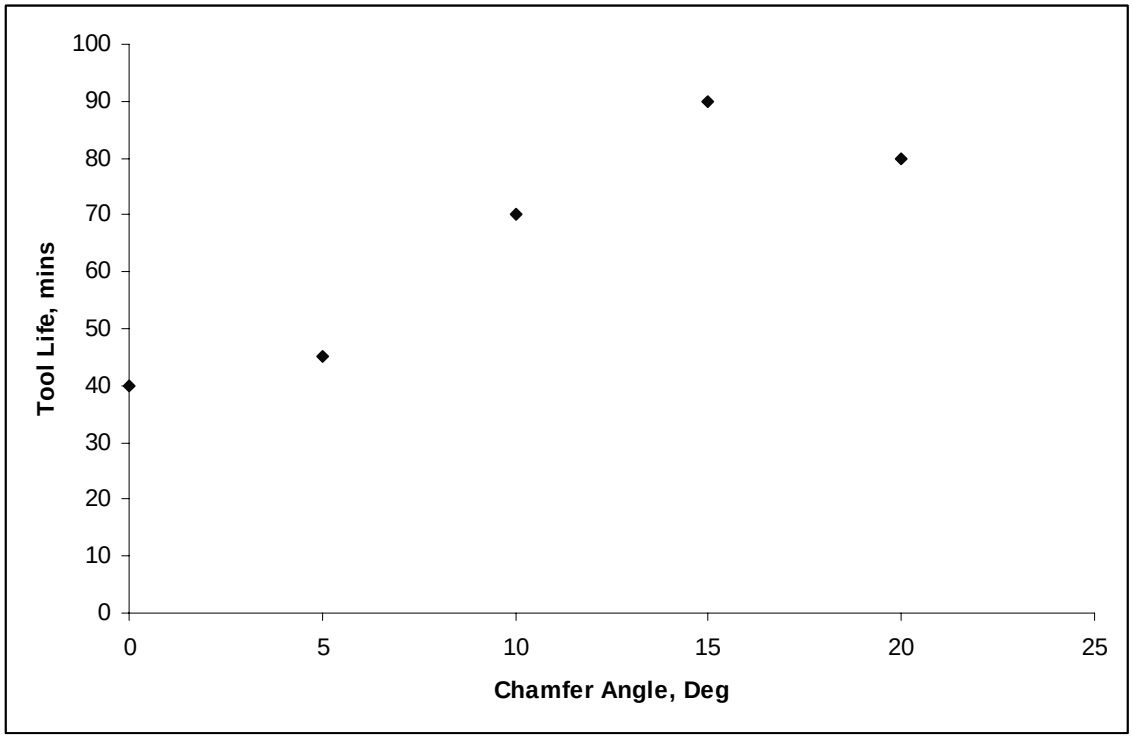

Figure 13: Variation of tool life with chamfer angle (EN-9).

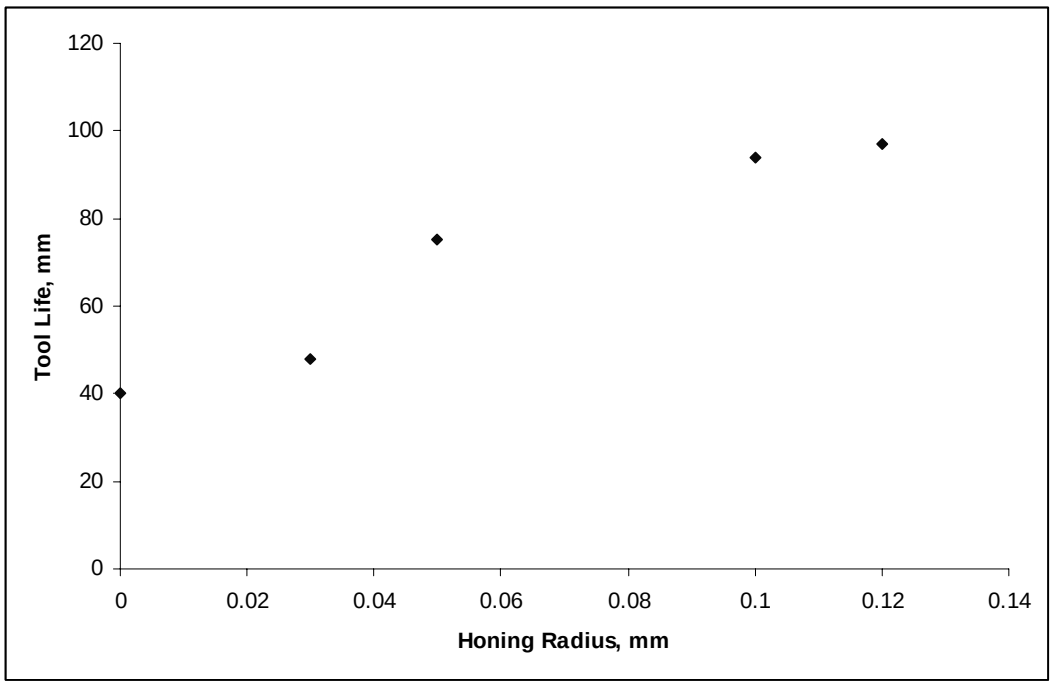

Figure 14: Variation of tool life with honing radius (EN-9).

In case of machining EN-9, it can be noted that in both chamfered and honed tools, tool wear tends to follow a third degree polynomial curve, similar to the machining of EN-8 steel. Regression coefficient is found to be 0.96. As in the previous case, tool life is evaluated for both chamfered and honed tools (Figure 13, Figure 14).

It is noteworthy that results are synonymous is both combinations of tool and workpiece thus validating the findings.

4. CONCLUSIONS

Chamfered tools and honed tools are subjected to lesser tool wear compared to sharp tool, since initial cut phase of tool flank wear is postponed in them. However, cutting forces are higher in chamfered and honed tools compared to sharp tool. Compared to chamfered tools, honed tools showed less tool wear. Chamfered tool with 15° chamfer angle is subjected to minimum tool wear, as this is a break-even between the increased strength and the increased tool-workpiece contact area. However, in honed tools, tool wear is low for higher honing radius. The major limitation of the work is that experimentation is carried out only for a set of chamfer angle and honing radii, in view of the practical difficulties; this can be extended and future work may be carried with finer tunings of the values to identify more optimal chamfer angle and honing radius.

ACKNOWLEDGEMENTS

We are thankful to the technicians of the Machine Shop and Metrology lab of GITAM UNIVERSITY who helped very much for the completion of the project.

REFERENCES

[1] Milton C. Shaw, (2004). "Metal Cutting Principles", 2nd Edition, Oxford University Press, USA.

[2] Du R, Zhang B, Hungerford W and Pryor T (1993), "Tool condition monitoring and compensation in finish turning using optical sensor." ASME Symposium, Mechatronics, 63, 245-251.

[3] Karthik A, Chandra B, Ramamoorthy B and Das S (1997). "3d Tool wear measurement and visualisation using stereo imaging." International journal of machine tools and manufacturing, 37(11), 1573-1581.

[4] Yigit Karpat, Tugrul Ozel, John Sockman, William Shaffer (2007). "Design and Analysis of Variable Micro-Geometry Tooling for Machining Using 3-D Process Simulations", Proceedings of International Conference on Smart Machining Systems, National Institute of Standards and Technology, Gaithersburg, Maryland, USA.

[5] Yigit Karpat and Tugrul Ozel (2007)."3-D FEA of Hard Turning: Investigation of PCBN Cutting Tool Micro- Geometry Effects", Transactions of NAMRI/SME 1 Volume 35.

[6] Ren H, and Altintas Y (2000). "Mechanics of Machining With Chamfered Tools", Journal of Manufacturing Science and Engineering, Volume 122, Issue 4, pp. 650-659.

[7] Zhou, J.M, J.M, Walter,H., Anderson, M., Sathl, J.E (2003). "Effect of chamfer angle on wear of PCBN cutting tool", Int.J.Machine tools and Manufacture, 43, pp.301-305.

[8] Movaheddy, M.R, Altintas, Y, Gadala, M.S (2002). "Numerical analysis of metal cutting with chamfered and blunt tools", J.of Manufacturing science and Engineering, Trans of ASME, Vol.124, pp.179-188.

[9] Zhou J M, Walter H, Andersson M and Stahl J.E (2003). "Effects of tool edge hone and chamfer on wear life", International Journal of Machine Tools and Manufacture, Vol. 43(3), pp.301-305.

[10] Raja K.Kountanya and William J.Endres (2004). "Flank wear of edge-radiused cutting tools under ideal straight-edged orthogonal conditions", J Mfg Science, Trans.ASME, Vol.126, pp.496-505.

[11] Fang, N., Wu, Q. (2005). "The effects of chamfered and honed tool edge geometry in machining of three aluminium alloys", Int.J. of Machine tools and Manufacture, 45, pp.1178-1187.

[12] Venkatesh, V.C and Chandrasekaran, H (1982). "Experimental Methods in Metal Cutting", Prentice-Hall of India Pvt. Ltd.

APEM journal ISSN 1854-6250 *Advances in Production Engineering & Management* 5 (2010) 1, 25 - 32 Scientific paper

SUCCESS FACTORS OF NEW PRODUCT DEVELOPMENT PROCESSES

Schimmoeller, L., J.
Lynchburg College, 1501 Lakeside Drive, Lynchburg, Va 24501
Schimmoeller@lynchburg.edu

Abstract:
Developing new products is difficult but vital for organizations to succeed. This paper examines the critical factors of new product development and the influence of each of these factors on product development outcomes. This investigation involved a literature search and the findings are presented as a matrix of citations that identifies which of the product development components of product performance, speed, and development costs is enhanced by the key success factors of cross-functional teams, upper-management support, and a supportive organizational structure. Findings indicate that all three key success factors are necessary for a successful product development process and may not be used cafeteria style where a firm selects which to apply to projects. This is the first research to suggest that sponsors of project development teams must give each of the process key success factors a high priority to improve the probability of a successful product development effort.

Key Words: Product Development, Project Management

1. INTRODUCTION

Launching new products is an essential attribute of successful businesses as they survive and grow [1][2]. The ability to develop these new products to compete in existing or new markets is a core competency of many successful firms [3]. It is important for the survival of these firms to understand which factors affect the components of successful product development processes.

In early studies of product development, research focused on the product to be developed rather than the process of product development. By the 1970's, the focus expanded to include the study of the process of new product development [4]. Product development efforts are typically organized as projects and managed by the classical triad of project components; product performance, schedule, and cost. In the context of product development, these project components are often termed product performance, speed to market, and development cost. These three components are each influenced by the product development process.

There have been a number of studies to suggest the key success factors used in the process of successful product development include the use of cross-functional teams, support of upper-management, and support of the organizational structure [5][6][7][8]. Lacking from this analysis is the understanding of which key success factors contribute to which of the specific product development components of product performance, speed, and cost. A better understanding of this relationship would aid managers to focus their efforts by supporting product development with the most essential key factors to optimize the product development components that have the highest priority, whether it is product performance, speed to market, or development cost.

2. REVIEW OF THE LITERATURE

The literature review is organized into three sections. The first section examines the measurements that define a successful product development. The second section reviews the literature that analyzes the key success factors that result in a successful product

development process. The third section examines the affect these key success factors have on measurements of product development success.

2.1 Measurements of new product development

Measurement of new product development is not consistent throughout the literature but most variations of measurement focus on product performance, development time, and the cost of development [9]. Successful new products in the service industry can be more difficult to measure than manufacturing products but may use the same measurement categories [10].

Product performance may be defined as the product performing to its specification [9]. Quality may be analyzed as a separate measure [3] but it is common to assume that products meeting specification are quality products and meet the needs of the customer. Product specifications are typically created by marketing and used by the development team to determine the features of the product being offered [9]. Product specifications usually include the features of a product and its target market and cost. Marketing is tasked with determining the product performance requirements and it is the development team's charter to meet those specifications. While determining customers' needs is critical to a successful product development, the scope of this review is limited to the product development team and so will consider the process of developing the product after receiving the specification from marketing.

Speed of development time is important for company survival [6][3]. Firms focus on gaining competitive advantage by developing products in short time periods [11][12]. Rapid product development allows a company to react quickly to changes in the competitive environment and has been identified as an attribute of successful firms [1]. By developing products faster, companies not only bring them to market quicker, but they can launch additional products with the same level of resources [11].

The cost of project teams to develop new products is mission critical to the success of a firm [11]. It does more than affect the bottom line; it can be linked with the number of projects a company can develop with limited resources. A company that spends fewer resources than competitors on new product development may choose to do additional development or use the saved money for other competitive advantages. The results of reduced development cost on the firm may only marginally improve the bottom line; it is the ability to seize market opportunities that presents the biggest opportunity.

2.2 Key success factors of new product development

Researchers have concluded there are many critical components of new product development but the most common organizational traits found in firms with a successful new product introduction process are the use of cross-functional teams, management support, and a supportive organizational structure. Each of these facets will be examined in greater detail.

The multi-functional co-operative approach using cross-functional teams has been reported as the most important factor in improving development processes [5]. Cross-functional teams are widely used throughout industry to resolve complex issues such as the challenges of new product development [13][9]. These teams are often the only means of developing complex products. Cross-functional teams are more difficult to manage but their combination of differing skills allows them to solve intricate problems [11]. Communication both within the cross-functional team and between the team and the outside organization is a critical issue that must be resolved to enable superior team performance [14].

Senior management commitment has also been identified as an important ingredient to a successful new product development [4][7][14]. Further research determined management support improves project team performance reducing the duration to make key decisions while the team receives key political, emotional, and financial support [12]. Management planning and reviews ensure that human and financial resources are available and set the

criteria to evaluate the product or service [8]. Progress is tracked and resources are available as defined in the project plan.

Multiple studies report that a proper organizational structure must be in place to support successful new product development [4][6][7]. Additional research found support by top executives is important to a successful project, but the organizational structure may be more important because it has a continuous, daily influence on the team and mediates the environmental factors in which the team operates [15]. Communication is a key factor both within the team and between the team and the others, including management, suppliers and the customers and is aided greatly by an appropriate organizational structure [16].

Research has been shifting from the products under development to the processes that develop products and formalizing those processes to improve product development [16]. The proper supportive organizational structure may lead to a formal product development process defined as having a well-documented process where managers are able to reference and furnish documentation that they are following the process [11]. Progress is documented as project teams proceed through the development process. Attention to process characteristics and the influence of these factors on successful launches of new products is increasing [16].

2.3 Effects of development components on process measurements

Successful introduction of new products is important to company survival but the failure rate of new products may be as high as 50 percent [2]. With the stakes very high and failure common, it is important to determine the relationship between the components of successful new product development and their relationship to the key success factors used to measure the success of the process. These relationships are illustrated in Figure 1.

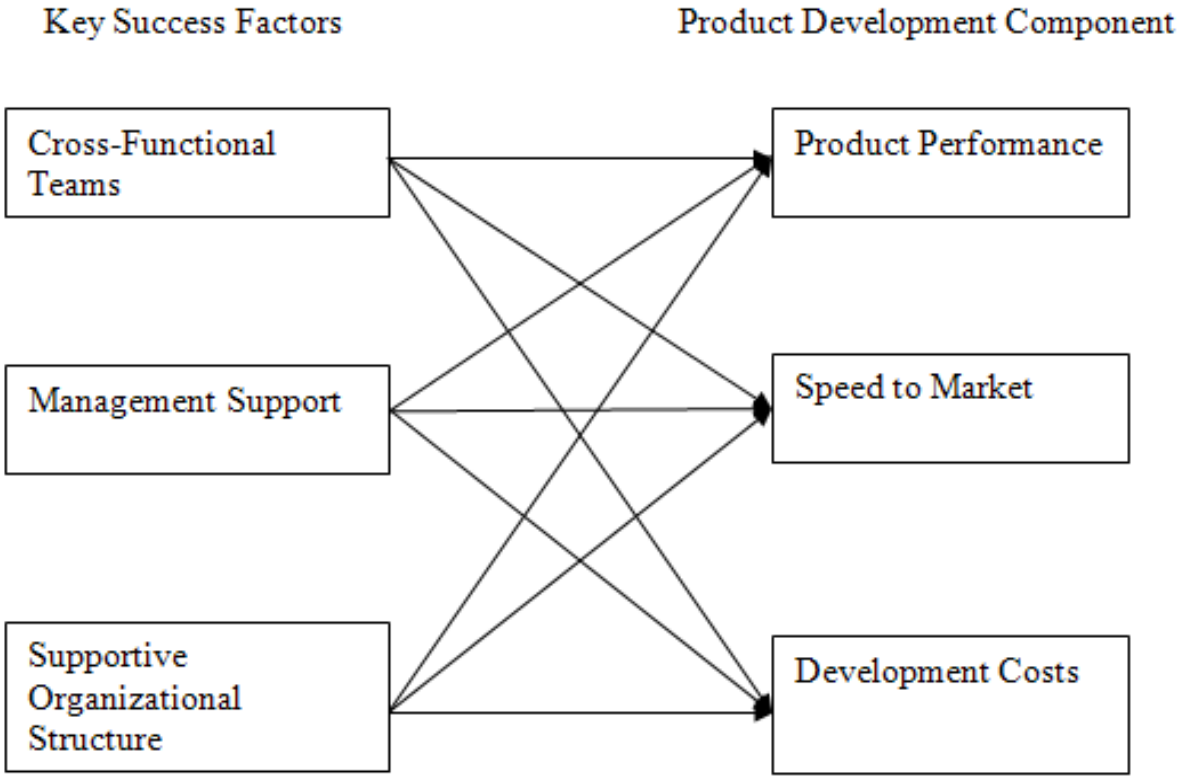

Figure 1: Relationship of key success factors to product development components.

The concept tested was that a new product development process may be broken down to its specific components of product performance, speed to market and development cost and these components are individually affected by the key success factors of cross-functional teams, management support, and supportive organizational structure. The current literature of product development was reviewed for evidence of these relationships.

3. RESULTS

The results of the literature review are compiled in Table I. Articles supporting the link of specific key success factors to individual product development components are listed. Each of the individual product development components; product performance, speed, and development cost, is examined to determine if there is evidence that each of the key success factors of cross-functional teams, management support, and a supportive organizational structure are important to its success.

3.1 Product performance

Researchers identified that cross-functional teams improve the performance of a product due to enhanced problem solving skills [17][11]. Many problems are too complex for one discipline to resolve. By the application of various skills, these teams were able to significantly improve product performance. The combination of differing skills of cross-functional teams has been demonstrated to yield better products with reduced resources [9].

Investigators determined management support communicated a clear vision of team objectives while simultaneously giving team members the freedom to pursue that vision resulting in improved product team performance [18]. Senior managers may use control through the project leader or with direct influence. These managers help project leaders gain resources while increasing the respect the leader receives from the team. The product vision from senior managers aids in problem solving for the team. Research found this vision and direction for the team is especially critical in the development of high-tech products [17]. Close monitoring of project status by senior managers demonstrates the importance of a product under development to both team members and others in the organization [13]. This close monitoring also helps the team gain cooperation from others in their organization while increasing risk-taking and innovation.

Supportive organizational structure for product development has a number of influences that have a positive effect on team success [13]. Organizational structure, particularly a deliberate development process, is vital to the success of product development. This purposeful, formalized development process increases project planning and success. An organizational structure that improves communication both internal and external to the team is critical [18]. Furthermore, an organizational structure based on the concepts of Just-In-Time may significantly improve product performance, including 61% better quality [3].

Table I: Results of literature review.

Product Development Component	Key Success Factor	Article
Product Performance	Cross-Functional Teams	Griffin (1997) Lynn & Akgun (2003) Ulrich & Eppinger (2000)
	Management Support	Hayes, Clark & Lorenz (1985) Lynn & Akgun (2003) Sethi, Smith & Park (2001)
	Supportive Organizational Structure	Hayes, Clark & Lorenz (1985) Meybodi (2003) Sethi, Smith & Park (2001)
Speed	Cross-Functional Teams	Griffin (1997) Lynn & Akgun (2003) Ulrich & Eppinger (2000) Zahra & Ellor (1993)
	Management Support	Cooper & Kleinschmidt (1995) Cooper & Slagmulder (1997) Hart & Service (1993) Hayes, Clark & Lorenz (1985) Lynn & Akgun (2003) Sethi, Smith & Park (2001) Zahra & Ellor (1993)
	Supportive Organizational Structure	Griffin (1997) Hayes, Clark & Lorenz (1985) Lynn & Akgun (2003)
Development Costs	Cross-Functional Teams	Likert (1975) Ulrich & Eppinger (2000)
	Management Support	Cooper & Kleinschmidt (1995)
	Supportive Organizational Structure	Hayes, Clark & Lorenz (1985) Meybodi (2003)

3.2 Speed to market

The link between cross-functional product development teams and the speed of product development has been repeatedly demonstrated [11][17][12]. These diverse teams act concurrently and require less time than the previous development method of functional groups operating in a linear approach. By project teams working simultaneously, product design is shorted by reducing project errors and rework [9]. Empirical evidence supports using cross-functional teams to reduce product development time and the more unique or complex the product, the bigger the savings from using cross-functional teams [11].

Management support has been empirically demonstrated to improve the performance of cross-functional teams and therefore improving speed to market in addition to improving co-operation from other resources within the organization [5][13][12]. Additionally, this support reduces the time to make decisions to keep teams on schedule [12]. A clearly defined management vision for a project improves the focus of the project team toward their goals [17].

Top management support is important to secure resources, both personnel and financial, for the prompt completion of a development effort [20]. Executive champions help to acquire human and capital resources. Furthermore, they stimulate communication and cooperation between different functional groups which helps reduce cycle time [18][19].

Internal organization structure is critical to supporting cross-functional teams, making it important in minimizing speed to market. Speed depends on the internal organization, including carefully planned predevelopment activities [18][11]. Additionally, the increased communication of a proper organizational structure improves project speed [17]. Empirical evidence indicates that formal product development processes improve an organization's ability to manage interactions and interfaces and increases the probability of on-time project completion. As products grow more complex, organizational interfaces become exponentially more complex and the need for a formal process significantly increases [11].

3.3 Development costs

Cost to develop new products is referenced far less in the literature than product performance or speed of development. The rewards for getting to market with the first and best product overshadow excessive cost. High development cost may be passed on to customers in high technology markets if the product has enough superior performance to warrant the additional price [21].

There is more literature studying the cost of the products developed than the development costs. Measurements indicate that 89% of product costs are designed into the product during development [19]. Additionally, the use of JIT principles during product development resulted in 38% less manufacturing cost [3]. The manufacturing costs of most products outweigh the development cost resulting in less study of those development costs. However, a productive process yields lower project costs [18]. Therefore, it may be inferred that a supportive organizational structure, particularly an efficient formal product development process, will yield lower development costs. Furthermore, teams with management support have more productive product development efforts [20]. Studies of cross-functional teams tend to focus on speed and product performance but other research has found the use of cross-functional teams also resulted in lower development costs [22][9].

4. CONCLUSIONS

This paper investigated linking the key success factors of the product development process, such as cross-functional teams, management support, and a supportive organizational structure, to the product development components of new product development such as product performance, speed and development costs. Much of the research on product development processes focuses on determining the key success factors of successful new product development processes and not the specific individual project metrics, such as performance, speed, and costs. However, the author was able to find evidence in the literature that the three key success factors each had a part in improving the individual components of product development. These findings indicate that all three key success factors are necessary for a successful product development process and may not be used cafeteria style where a firm may select which to apply to projects. Sponsors of project development teams must give this a high priority to improve their probability of a successful product development effort.

The primary key success factor of the development process that has been reviewed in previous literature is the use of cross-functional teams. This review has shown there is

limited research into the influence of cross-functional teams on product performance or the cost of product development but there has been extensive study into the speed of product development which has been demonstrated as aiding competitive advantage and is critical to the success to many companies. As a measure of successful product development, cost of development is viewed as much less significant as the advantage gained by rapid product development.

The study of firm level variables such as a supportive organization provides only limited explanation of project outcomes [13]. The same organizational structure may be used on all product development efforts with widely varying results but different projects have varying levels of senior management support and that has a consequence on team member performance and innovativeness, which is reflected in the level of success of the project.

4.1 Future research

There is an opportunity for future study to examine these relationships. These relationships may seem obvious but industry is still coupled with product development processes that are vital for company success but fail nearly 50 percent of the attempts. Researchers note a better understanding of the linkages within the product development model would be useful [18]. An opportunity to learn more about the components of new product development and their influence on several of the measures of new product success may improve our understanding of the vital process of new product development.

Other researchers support the need to improve our understanding of how the influence of senior managers affects product development results [18]. This research demonstrates management support as a vital factor in all components of the development process indicating a better understand of senior management support might improve the performance of future product development efforts.

REFERENCES

[1] Axarloglou, K. (2003), The Cyclicality of New Product Introductions, The Journal of Business, Vol. 76, No. 1, 29-48.

[2] Lee, Y.; O'Connor G. (2003), New Product Launch Strategy for Network Effects Products, Academy of Marketing Science, Vol. 31, No. 3, 241-255.

[3] Meybodi, M. (2003), Using principles of just-in-time to improve new product development process, Advances of Competitiveness Research, Vol. 11, No. 1, 116-125.

[4] Cooper, R. (1979), The Dimensions of Industrial New Product Success and Failure, Journal of Marketing, Vol. 43, No. 3, 93-103.

[5] Hart, S.; Service L. (1993), Cross-functional Integration in the New Product Introduction Process: An Application of Action Science in Services, International Journal of Service Industry Management, Vol. 4, No. 3, 50-66.

[6] Hwand, A. (2004), Integrating Technology, Marketing and Management Innovation, Research Technology Management, Vol. 47, No. 4, 27-31.

[7] Lester, D. (1998), Critical Success Factors for New Product Development, Research Technology Management, Vol. 41, No. 1, 36-43.

[8] Raymond, M.; Ellis B. (1993), Customers, Management, and Resources: Keys to new consumer product and service success, The Journal of Product and Brand Management, Vol. 2, No. 4, 33-45.

[9] Ulrich, K. T.; Eppinger, S. D. (2000). Product design and development. McGraw-Hill, New York.

[10] Edgett, S.; Snow K. (1997), Benchmarking measures of customer satisfaction, quality and performance for new financial service products, The Journal of Product and Brand Management, Vol. 6, No. 4, 250-257.

[11] Griffin, A. (1997), The Effect of Project and Process Characteristics on Product Development Cycle Time, Journal of Marketing Research, Vol. 34, No. 2, 24-35.

[12] Zahra, S.; Ellor D. (1993), Accelerating New Product Development and Successful Market Introduction, S. A. M. Advanced Management Journal, Vol. 58, No. 1, 9-15.

[13] Sethi, R. Smith, D.; Park C.W. (2001), Cross-Functional Product Development Teams, Creativity, and the Innovativeness of New Consumer Products, Journal of Marketing Research, Vol. 38, No. 1, 73-85.
[14] Connell, J., Edgar, G., Olex, B., Scholl, R., Shulman, T.; Tietjen, R. (2001), Troubling Successes and Good Failures, Engineering Management Journal, Vol. 13, No. 4, 35-39.
[15] Papadakis, V.; Burantas D. (1998), The Chief Executive Officer as Corporate Champion of Technological Innovation: An empirical investigation, Technology Analysis & Strategic Management, Vol. 10, No. 1, 89-110.
[16] Wotruba, T.; Rochford L. (1995), The Impact of New Product Introduction on Sales Management Strategy, The Journal of Personal Selling & Sales Management, Vol. 15, No. 1, 35-51.
[17] Lynn, G.; Akgun A. (2003), Launch Your New Products/Services Better, Faster, Research Technology Management, Vol. 46, No. 3, 21-26.
[18] Hayes, R. H.; Clark,K.; Lorenz C. (1985). The uneasy alliance: Managing the productivity-technology dilemma: 337-375. Harvard Business School Press, Boston.
[19] Cooper, R.; Slagmulder, R. (1997). Target Costing and Value Engineering, Productivity Press, Portland OR.
[20] Cooper, R.; Kleinschmidt, E. (1995). Benchmarking the Firm's Critical Success Factors in New Product Development. Journal of Product Innovation Management, Vol. 11, No.5, 374-391.
[21] Davila, A.; Wouters, M. (2004). Designing Cost Competitive Technology Products through Cost Management. Accounting Horizons, Vol. 18, No. 1, 13-26.
[22] Likert, R. (1975). Improving cost performance with cross-functional teams. Management Review, Vol. 65, No. 3, 36-43.

APEM journal ISSN 1854-6250 *Advances in Production Engineering & Management* 5 (2010) 1, 33 - 44 Scientific paper

WORKABILITY STUDIES ON Al-20%SiC POWDER METALLURGY COMPOSITE DURING COLD UPSETTING

Ramesh,T. *; Prabhakar, M* & Narayanasamy, R**
* Department of Mechanical Engineering, National Institute of Technology, Tiruchirappalli, India.
** Department of Production Engineering, National Institute of Technology, Tiruchirappalli, India.
E-mail: tramesh@nitt.edu, mprabha2000@rediffmail.com

Abstract:
The application fields of bulk metals have been limited because of their lack of workability criteria. Powder metallurgy composites have superior mechanical properties such as high strength, elastic strain limit and fracture toughness and workability behaviour. In order to improve the workability criteria, conducting experiments under cold conditions so as to investigate the super plastic behaviour of the materials, has been investigated during cold upsetting. The present study has been performed to evaluate the effect of the workability behaviour of pure Aluminium and Al -20% SiC powder metallurgy composites introducing various sizes of the second phase particles, namely, 120 μm, 65 μm and 50 μm and for the aspect ratios of 0.9 and 1.2. The effect of second phase particle size on the workability of the material composites proposed has been investigated over this work. The experimental results were analyzed under triaxial stress state condition. The formability stress index, various stress ratio parameters were obtained for each particle size additions and aspect ratios. The relationship between various stresses against the axial strain has been studied.

Key Words: Metal Matrix Composite, Aluminium, Silicon Carbide, Plastic Behaviour

1. INTRODUCTION

Metal forming is an important plasticity working technique, which is used in many types of applications especially in the industrial products of light weight and high strength. Many authors have found that the composite materials are stronger than conventional alloys [1, 2]. Particle reinforced Aluminium alloy matrix composite is one of the best material to replace the conventional structural alloys. However, the demand for such materials has been limited to high cost applications due to their complex processing. Powder metallurgical technique is one the most excellent route of low cost processing to produce high quality products of near net shape.

The ductile failure of the Al matrix has been studied for the nucleation, growth and coalescence of voids [3]. Studies have revealed that the Al-SIC composite gives better tensile fatigue performance compared to monolithic alloy [4]. Compression deformation test on Al-5%SiC composite has been carried out at elevated temperature and it has been found that the SiC added Al P/M composite gives better formability compared to pure Al and proved thro FEM technique [5].

Workability is concerned with the extent to which a material can be deformed in a specific metal working process without the initiation of cracks [6]. The cold forging process has major limitation on crack formation. So the ductile fracture prediction is very important for the cold forging operations. The prediction of ductile fracture in metalworking operations has therefore attracted the attention of many researchers for more than five decades. The prediction of powder metallurgical composite's fracture initiation increases the composite usages in a safe environment without failure. This will be useful to produce near net shape products to improve the quality of P/M products.

Shima and Oyane [7] studied the frictionless closed-die compression. The stresses in the direction of compression have been evaluated in relation to the relative density. A new yield function for compressible powder metallurgy materials was proposed by Doraivelu et al. [8]. The yield function has been derived based upon a yield criterion and this function was experimentally verified for the uniaxial state of compressive stress using the P/M Aluminium alloy. But this function has not been verified with other state of stresses.

Workability criterion of P/M compacts have been discussed by Abdel-Rahman et al., [9], investigating the effect of relative density on the forming limit of P/M compacts during upsetting. These authors also have proposed the criteria called formability stress index (β) for describing the effect of the mean stress and the effective stress with the help of two theories, proposed by Kuhn-Downey and Whang-Kobayashi. Further, authors have extended their investigations on the effect of relative density on the formability stress index (β) and concluded that the workability has quantitative relationship with the density. The effect of relative density can be measured by the simple experiments.

A new generalized yield criterion of porous sintered P/M metals was proposed by Narayanasamy and Ponalagusamy [10], considering an anisotropic parameter. In addition, a new flow rule with anisotropic parameter for porous metal was also proposed. Satsangi et al. [11] studied the forging behaviour and densification of porous powder metal both theoretically and experimentally. They presented incremental and piecewise linear elastic plastic finite element method for analysis of forging. Narayanasamy et al. [12] presented some of the important criteria generally used for the prediction of workability.

In this paper, a complete investigation on the workability criteria of Al and Al-20% SiC powder preforms was made during cold upsetting. Powder metallurgy preforms with various particle size and aspect ratios were discussed for studying the behaviour of workability during cold upsetting under triaxial stress state condition.

2. EXPERIMENTAL DETAILS

2.1 Compacts preparation

Atomized Aluminium powder of -100 μm was procured and analyzed for its purity. The same was found to be 99.7 percent and 0.3% insoluble impurities. The characterization of Al powder was studied by determining the flow rate, apparent density and particle size distribution and the details are listed in Table I. To investigate the particle size distribution, Metallographic studies were made with Scanning Electron Microscope and the image is provided in Figure 1. A sieve analysis was performed to determine the particle size distribution and the same is referred in Table 1. Powder mix corresponding to Al-20% SiC was blended on a pot mill to obtain a homogeneous powder blend. The size of Silicon carbide powder mixed was 50, 65 and 120 micrometers. Green compacts of the powder blend was prepared on a 1.0 MN capacity hydraulic press using suitable punch and die assembly as shown in Figure 2. The compacting pressure applied was 517.566 MPa, which was maintained for all composition of SiC composites.

The free surfaces of the compacts were coated with an indigenously developed ceramic mixture [13] and dried under room-temperature conditions for a period of 9 hours. A second coating was applied at a direction of 90° to the direction of first coating and was allowed to dry for a further period of 9 hours under the same conditions as stated above.

2.2 Sintering

Sintering of powder sequentially involves the establishment and growth of bonds between the particles of powder at their areas of contact and migration of the grain boundaries formed at the bonds. Bonds form between the particles during sintering, and the number of particle bonds increases as the temperature increases.

X-ray diffraction (XRD) patterns of the specimen reinforced with 10 wt% SiC is shown in Figure 3. Al peaks and SiC peaks were indexed using JCPDS files (file number 040787 and

49-1431 respectively). The XRD pattern confirmed the presence of Al matrix and SiC particulate in the composite.

Table I: Characteristics of aluminium.

	Sieve number (μm)	**wt.% retained**
Aluminium	+106	00.26
	+90	02.54
	+75	14.73
	+63	17.58
	+53	24.86
	+45	12.33
	+38	06.27
	-38	21.42
Apparent density (g. cm^{-3})		1.030
Flow rate, (by Hall flow meter) (50 g^{-1})		32.00

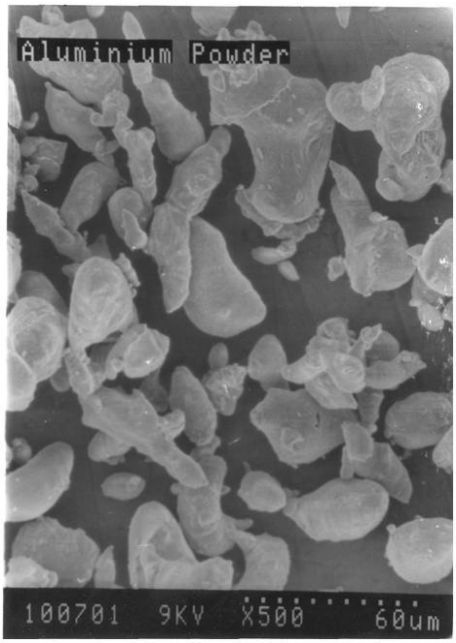

Figure 1: The SEM photograph of aluminium powder.

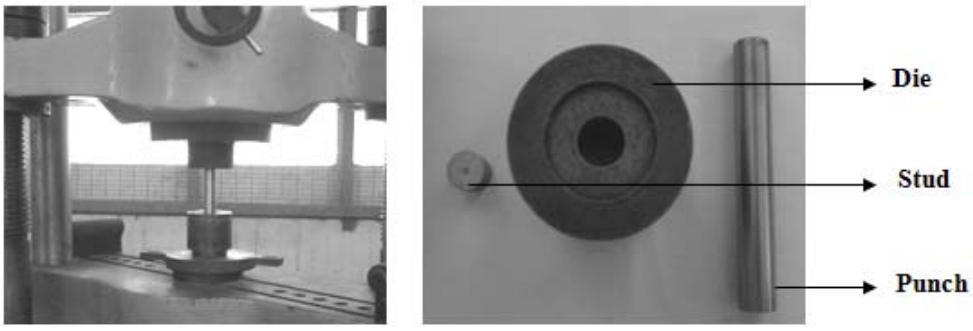

Hydraulic press Die set parts

Figure 2: Photographs of hydraulic press and parts of compacting Die.

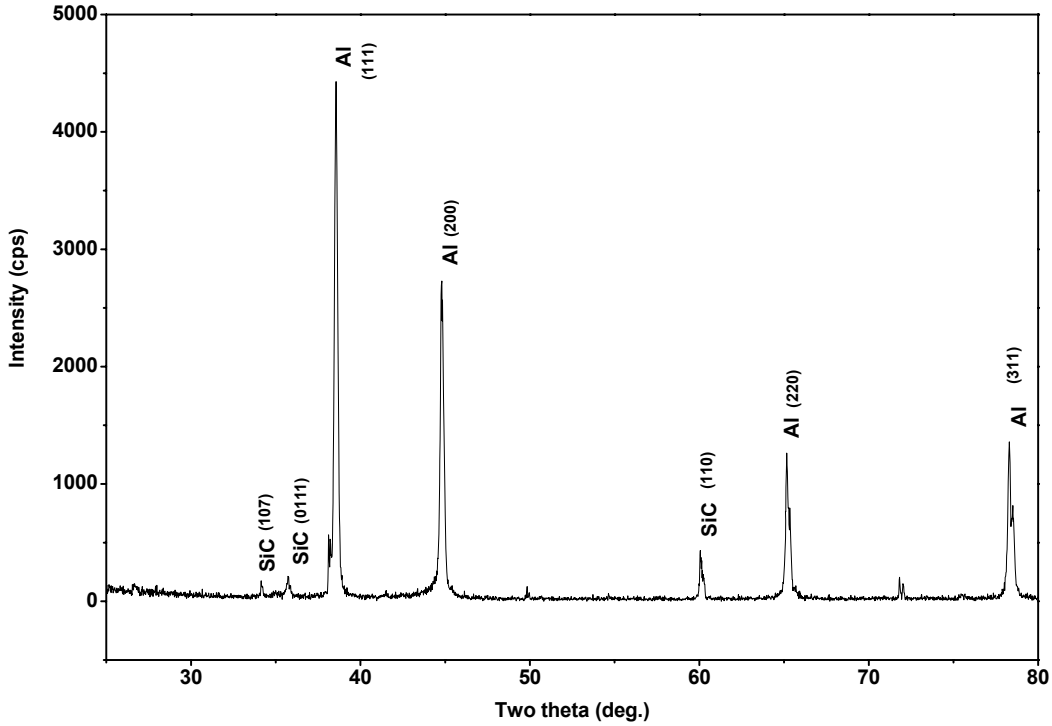

Figure 3: XRD results for the preform of Al-10% SiC composite.

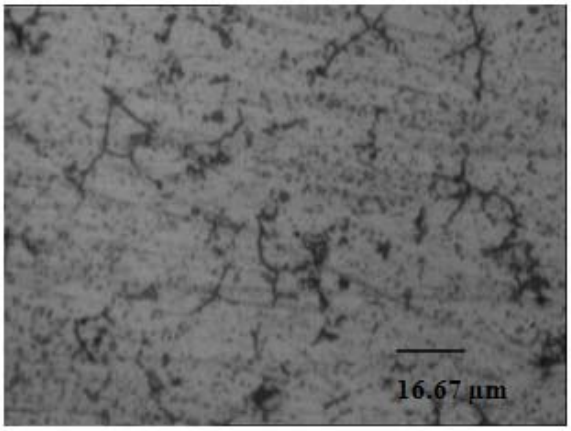

Figure 4(a): Microstructure of as sintered Al-0% SiC P/M perform.

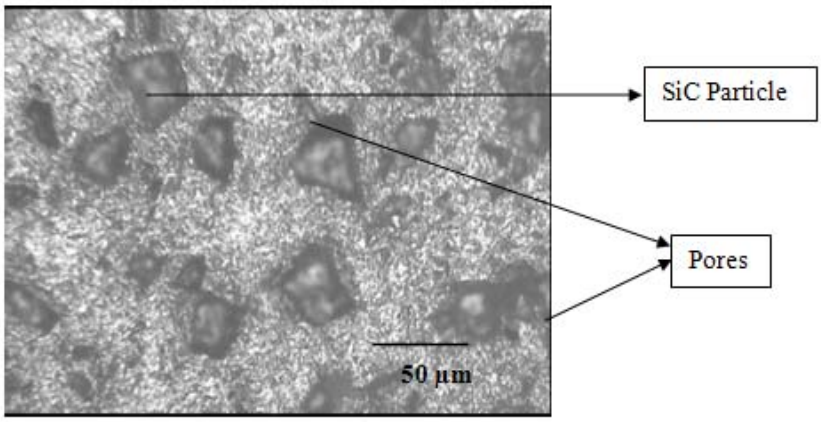

Figure 4(b): Microstructure of as sintered Al-20% SiC P/M perform – 50 microns.

Figures 4(a)-(d) show microphotographs of sintered preforms of Al with various particle sizes of SiC. In the case of sintering apart from bonding, the main factor affecting the properties of a sintered Al part is the amount of combined SiC formed in the Al. The maximum combined SiC content is achieved at 605°C, while additional strengthening at higher temperature is caused by increased sintering as is evident by the elimination of grain boundaries and spheroidization of pores. Time of sintering also affects the amount of combined SiC formed. The sintering time above 120 minutes leads to almost complete absence of grain boundaries and substantial spheroidization of pores. Accounting the aforementioned characteristics of sintered powder metallurgy Al-SiC, the ceramic-coated compacts were sintered in an electric muffle furnace in the temperature range of (605 ± 10)°C for a sintering time of 120 minutes and allowed to get cooled to room temperature in the furnace itself. The microstructure of sintered Al and 50 μm SiC added Al is shown as black color pores and white Al regions in Figures 4(a)-(b). Addition of 65 and 120 μm of SiC has resulted in reduced pores and more amount of Al with white background are shown in Figures 4(c)-(d). The ceramic coatings over the specimen were machined off and further machining was carried out to such dimensions, so that to obtain preforms with initial aspect ratios 0.9 and 1.2.

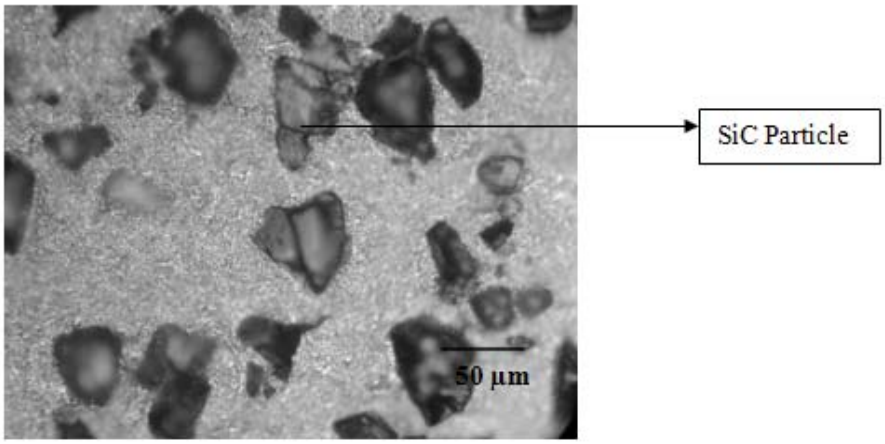

Figure 4(c): Microstructure of as sintered Al-20% SiC P/M perform – 65 Microns.

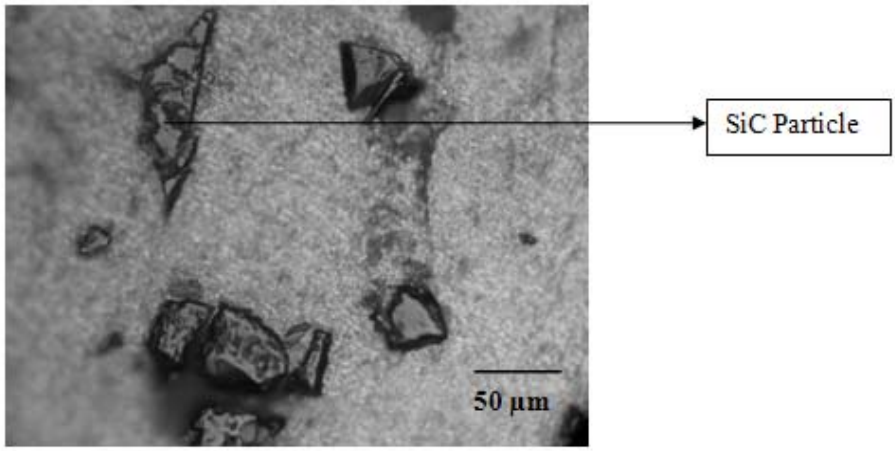

Figure 4(d): Microstructure of as sintered Al-20% SiC P/M perform – 120 Microns.

2.3 Deformation test

Initial diameter (D_0), initial height (h_0) and the initial preform relative density (ρ_0) of the specimen were measured and recorded. Each compact was subjected to the incremental compressive loads of 0.01 MN and the upsetting was carried between two flat, mirror finished

open dies on a hydraulic press of 1.0 MN capacity. The deformation was carried out until the appearance of first visible crack on the free surface. After each interval of loading, dimensional changes in the specimen such as height after deformation (h_f), top contact diameter (D_{TC}), bottom contact diameter (D_{BC}), bulged diameter (D_B) and density of the preform (ρ_f) were measured. The schematic diagram showing the various parameters measured before and after deformation is provided in Figure 5.

Using the Archimedes principle, the density of upset preforms was also determined after every loading interval. The deformation tests are continued until the fracture occurs at outer surface of the specimen as shown in Figure 6.

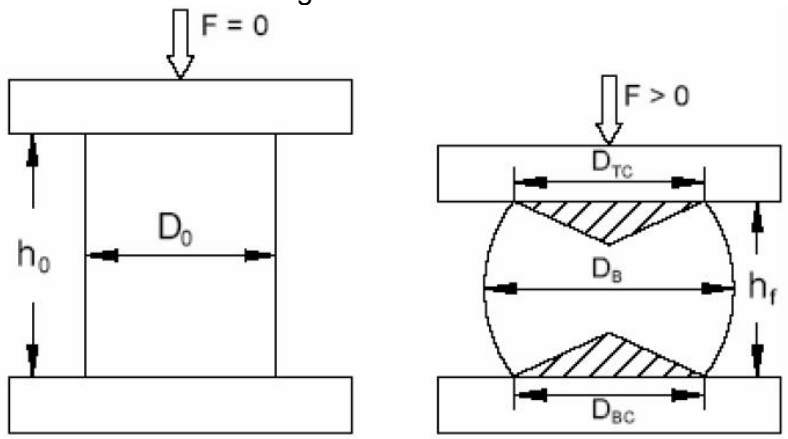

Figure 5: Upset test preform before and after deformation.

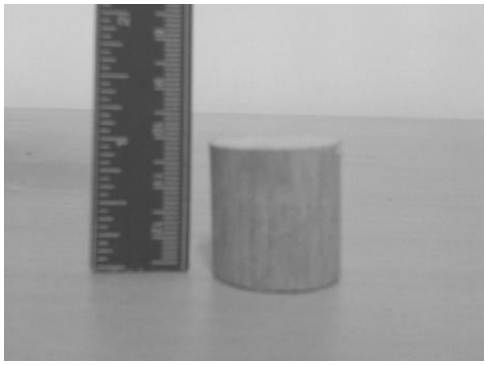

Before deformation

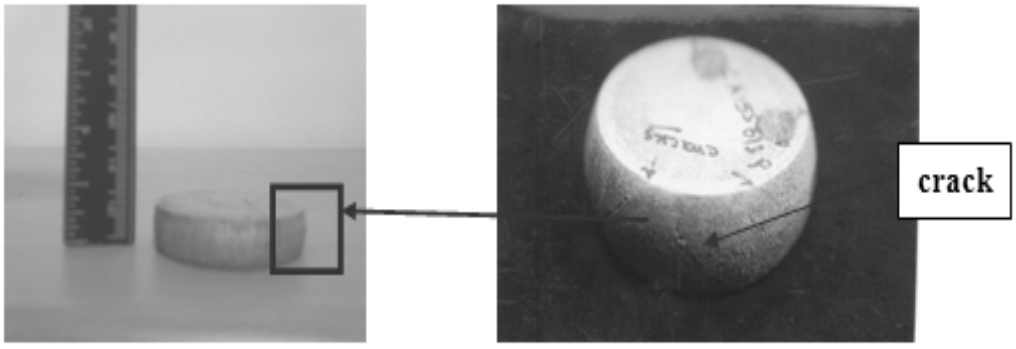

After Deformation

Figure 6: Photographs showing preform of before and after deformation test.

3. THEORETICAL INVESTIGATIONS

The various upsetting parameters under triaxial stress state condition are determined with the application of the following expressions.

3.1 Stress

The state of stress in a triaxial stress condition is given by Narayanasamy et al., [17] as follows:

$$\alpha = \frac{(2+R^2)\sigma_\theta - R^2(\sigma_Z + 2\sigma_\theta)}{(2+R^2)\sigma_Z - R^2(\sigma_Z + 2\sigma_\theta)} \quad (1)$$

From the Equation (1) for the known values of Poisson ratio (α), Relative density (R) and true axial stress (σ_z), the true hoop stress component (σ_θ) can be determined as follows:

$$\sigma_\theta = \left(\frac{2\alpha + R^2}{2 - R^2 + 2R^2\alpha}\right)\sigma_Z \quad (2)$$

At triaxial stress state condition, the relative density (R) of the compacts plays a vital role in the determination of the true hoop stress component (σ_θ).
The true hydrostatic stress is given by,

$$\sigma_m = \left(\frac{\sigma_r + \sigma_\theta + \sigma_z}{3}\right) \quad (3)$$

Since $\sigma_r = \sigma_\theta$ in the case of axisymmetric triaxial stress condition, the above equation becomes as follows:

$$\sigma_m = \left(\frac{\sigma_Z + 2\sigma_\theta}{3}\right) \quad (4)$$

The true effective stress can be determined from the following expression in terms of cylindrical coordinates as explained elsewhere [17]

$$\sigma_{eff}^2 = \frac{\sigma_z^2 + \sigma_\theta^2 + \sigma_r^2 - R^2\left(\sigma_z\sigma_\theta + \sigma_\theta\sigma_r + \sigma_z\sigma_r\right)}{\left(2R^2 - 1\right)} \quad (5)$$

Since $\sigma_r = \sigma_\theta$ for cylindrical axisymmetric upsetting operation, the true effective stress is determined as follows:

$$\sigma_{eff}^2 = \frac{\sigma_z^2 + 2\sigma_\theta^2 - R^2\left(\sigma_z\sigma_\theta + \sigma_\theta^2 + \sigma_z\sigma_\theta\right)}{\left(2R^2 - 1\right)} \quad (6)$$

The Equation 6 can be rewritten as

$$\sigma_{eff} = \left(\frac{\sigma_z^2 + 2\sigma_\theta^2 - R^2\left(\sigma_z\sigma_\theta + \sigma_\theta^2 + \sigma_z\sigma_\theta\right)}{\left(2R^2 - 1\right)}\right)^{1/2} \quad (7)$$

3.2 Formability stress index

As an evidence of experimental investigation implying the importance of the spherical component of the stress state on fracture, a parameter called a Formability Stress Index 'β' is given by,

$$\beta = \frac{3\sigma_m}{\sigma_{eff}} \tag{8}$$

This index determines the fracture limit as explained in the reference [9].

3.3 Strain

The true axial strain (ε_z) is expressed as given below:

$$\varepsilon_Z = \ln\left(\frac{h_0}{h_f}\right) \tag{9}$$

The true hoop strain (ε_θ) can be determined by the following expression as described elsewhere [17].

$$\varepsilon_\theta = \ln\left(\frac{2D_b^2 + D_c^2}{3D_o^2}\right) \tag{10}$$

The stress formability index (β) provided in the Equation 7 can be derived for the triaxial stress state condition.

4. RESULTS AND DISCUSSIONS

Figures 7 (a)-(b) have been plotted between various triaxial stresses namely the true hoop stress (σ_θ), the true effective stress (σ_{eff}) and the true mean stress (σ_m) and the true axial strain (ε_z) for Al containing three different SiC particle sizes namely 50, 65 and 120 μm and for two aspect ratios. For any given composition of composite, as the particle size of SiC increases, the true hoop stress (σ_θ), the true effective stress (σ_{eff}) and the true mean stress (σ_m) decreases. From these figures it is understood that the true hoop stress (σ_θ), the true effective stress (σ_{eff}) and the true mean stress (σ_m) are affected by the aspect ratios and its particle size. As a SiC particle size decreases the porosity level decreases and the relative density increases for the same compacting pressure. This may be one of the reasons for the increasing stresses for lower particle sizes of SiC added composite.

Figure 8 has been plotted between the formability stress index (β) and the relative density for Al containing three different SiC particle sizes and for two different aspect ratios namely 0.9 and 1.2. The slope value between the formability index (β) and the relative density increase with increasing of SiC content. The SiC particle occupies the pores between Al particles. Since the pore size is very small, formability stress index value increases during plastic deformation. Pure Al makes bigger pores, and hence the formability index (β) value also reduces. It is further observed that the pore size becomes smaller and smaller for the lower sizes of SiC content and hence the formability stress index value also increases. As the aspect ratio increases the formability stress index decreases because of more porous bed height. This indicates that the aspect ratio value 0.9 (smaller value) shows better densification compared to other aspect ratio.

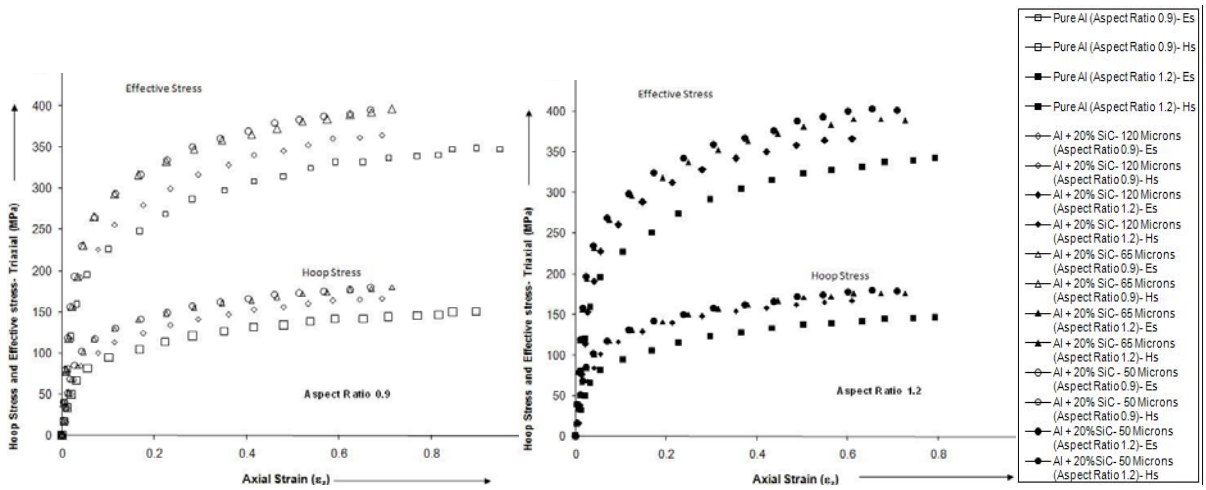

Figure 7(a): The variation of true Hoop stress (σ_θ) and true effective stress (σ_{eff}) with respect to the True Axial strain (ε_z) under triaxial stress state condition.

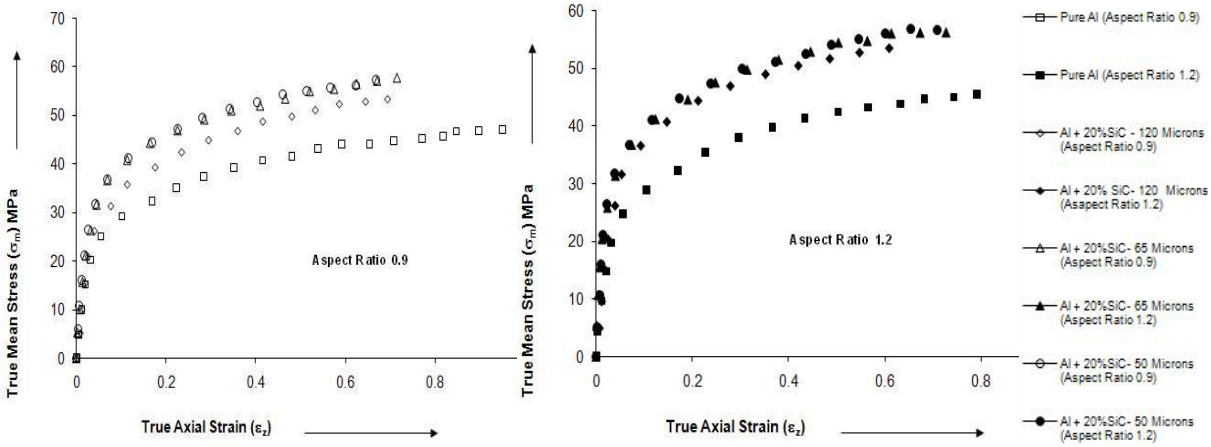

Figure 7(b): The variation of true mean or hydrostatic stress (σ_m) with respect to the true axial strain (ε_z) under triaxial stress state condition.

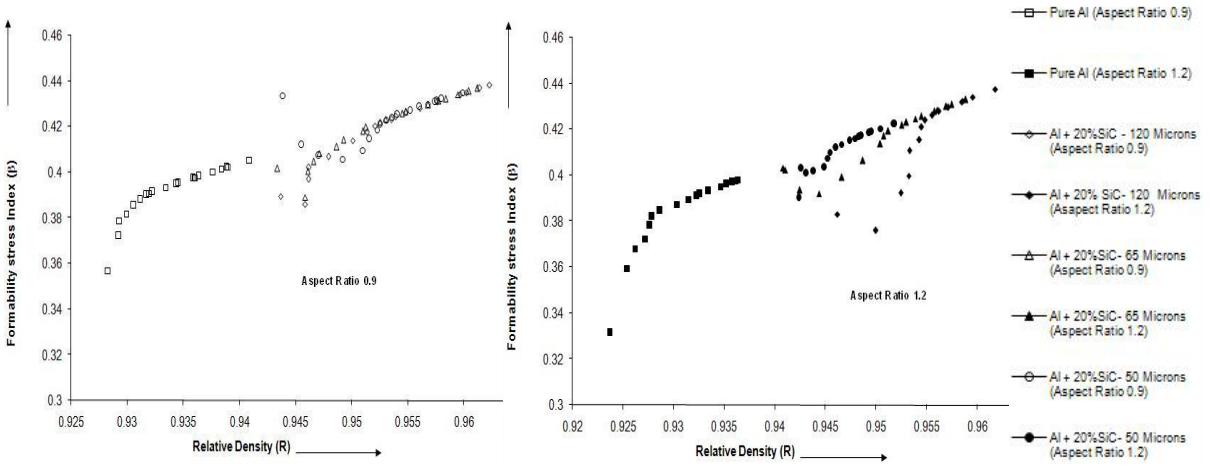

Figure 8: The variation of formability stress index (β) with respect to the relative density (R) for Al-20% SiC composite.

Figure 9 has been plotted between the stress ratio parameter ($\sigma_\theta / \sigma_{eff}$) and the Relative density (R) for Al containing three different SiC particle sizes and for two different aspect ratios namely 0.9 and 1.2. As the Relative density increases, the stress ratio parameter ($\sigma_\theta / \sigma_{eff}$) also increases because the true hoop stress (σ_θ) continues to increase rapidly during deformation. As the SiC particle size increases the stress ratio parameter ($\sigma_\theta / \sigma_{eff}$) is found to be higher compared to pure Al. In the case of pure Al the pore size is larger compared to Al-SiC composites and these results in lower stress ratio parameter ($\sigma_\theta / \sigma_{eff}$) value. The stress ratio parameter decreases with an increasing aspect ratio.

Figure 10 has been plotted between the stress ratio parameter (σ_z / σ_m) and the relative density (R) for Aluminium containing three different SiC particle sizes and for two different aspect ratios namely 0.9 and 1.2. As the SiC particle size increases, the stress ratio parameter decreases because Al-SiC composite exhibits fine pores compared to pure Al. In the case of fine pores, higher SiC particle size added composite increases the true mean stress (σ_m) value required for deformation and therefore the stress ratio parameter (σ_z / σ_m) decreases with increase in SiC particle size. As the aspect ratio increases to 1.2, the true mean stress (σ_m) value further increases and the true strain required for plastic deformation also increases before fracture. Here it is possible to conclude that the true mean stress (σ_m) value is well associated with the pore size.

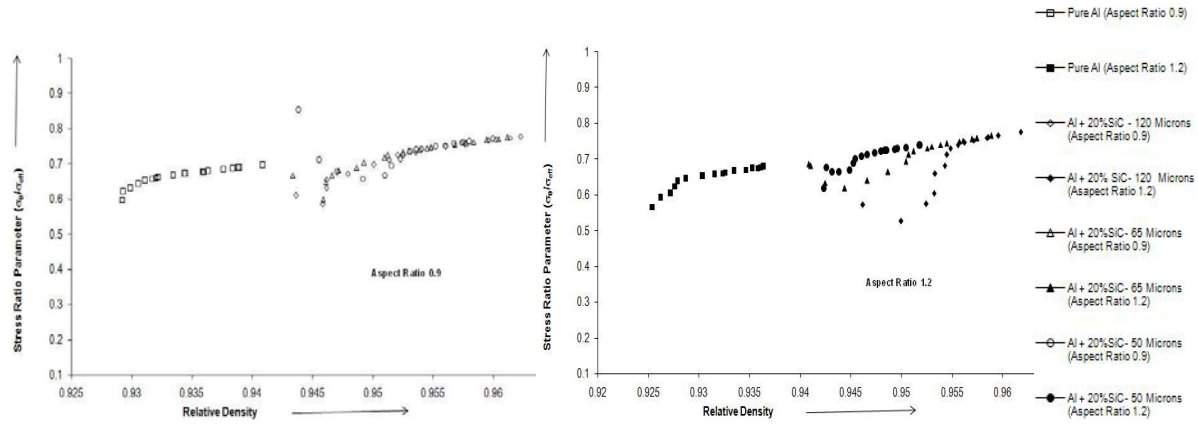

Figure 9: The variation of stress ratio parameter ($\sigma_\theta/\sigma_{eff}$) with respect to the relative density (R) for Al-20% SiC composite.

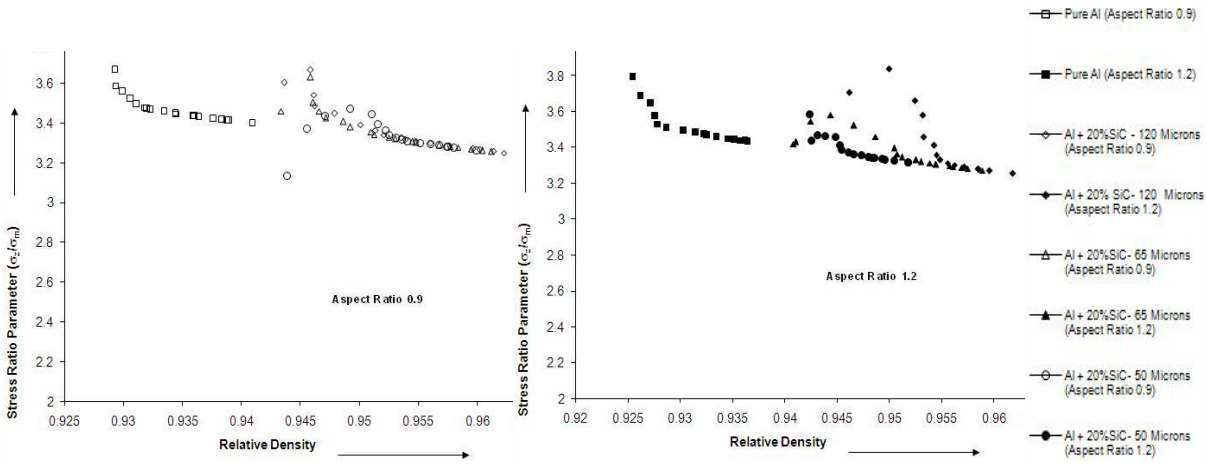

Figure 10: The variation of stress ratio parameter (σ_z / σ_m) with respect to the relative density (R) for Al-20% SiC composite.

Figures 11 (a)-(b) have been plotted between the fracture strain (ε_f) and the formability stress index (β) for the upsetting of Al, Al–SiC powder compacts of three different particle size

addition of SiC and for two different aspect ratios under triaxial stress state condition. It is observed that the fracture strain of the preform depends on the percentage addition of SiC. From this figure, it is further noted that for preforms with higher particle size of the SiC, the initiation of crack appears at a lower fracture strain value. However, it exhibited higher formability stress index (β). As the aspect ratio increases to 1.2, the fracture strain (ε_f) and the formability stress index (β) value decreases.

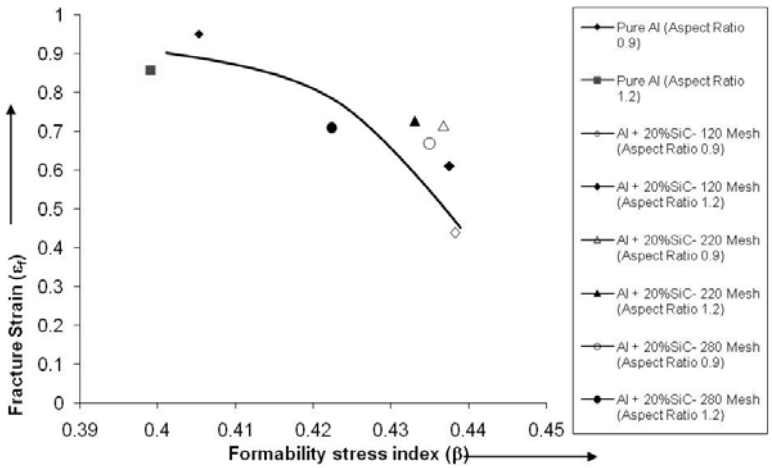

Figure 11: The variation of fracture strain (ε_f) with respect to formability stress Index (β).

5. CONCLUSIONS

The following conclusions can be drawn from the above results and discussions.

- As the Silicon carbide particle size increases the pore size becomes smaller.
- As the pore size becomes smaller, the formability stress value increases.
- Aspect ratio 0.9 shows higher formability stress value compared to aspect ratio 1.2 because of better densification.
- The stress ratio parameters ($\sigma_\theta / \sigma_{eff}$) is found to be higher for Al-SiC composites compared to pure Aluminium because of better densification.
- The stress ratio parameters (σ_z / σ_m) decreases in the case of Al-SiC composites compared to pure Aluminium because of fine pore size associated with high hydrostatic stress (σ_m).
- For preforms with higher particle size addition of SiC, the initiation of crack exhibits at lower fracture strain.
- For the higher aspect ratio, the relative density decreases.

NOMENCLATURE

F	Force applied on the cylindrical preform for deformation
h_0	Initial height of the cylindrical preform
h_f	Height of the barreled cylinder after deformation
D_0	Initial diameter of the preform
D_B	Bulged diameter of the preform after deformation
D_{TC}	Top contact diameter of the preform after deformation
D_{BC}	Bottom contact diameter of the preform after deformation
α	Poisson's ratio
σ_z	True stress in the axial direction
σ_θ	True stress in the hoop direction
σ_r	True stress in the radial direction

σ_{eff} Effective stress
σ_m Hydrostatic stress
σ True stress
ε True strain
ε_z True strain in the axial direction
ε_θ True strain in the hoop direction
ε_r True strain in the radial direction
β Formability Stress Index
ρ_o Initial preform density of the preform
ρ_f Density of the preform after deformation
ρ_{th} Theoretical density of the fully dense material
$R(or)\frac{\rho_f}{\rho_{th}}$ Relative density

REFERENCES

[1] Yulong Li , K.T. Ramesh, E.S.C. Chin, (2004). The mechanical response of an A359/SiCp MMC and the A359 aluminum matrix to dynamic shearing deformations, Material Science and Engineering A, Vol. 382, 162–170.

[2] Yulong Li , K.T. Ramesh, E.S.C. Chin, (2004). Comparison of the plastic deformation and failure of A359/SiC and 6061-T6/Al2O3 metal matrix composites under dynamic tension, Material Science and Engineering A, Vol. 371, 359–370.

[3] Y.X. Lu, X.M. Meng, C.S. Lee, R.K.Y. Li, C.G. Huang, J.K.L. Lai, (1999). Microstructure and mechanical behaviour of a sic particles Reinforced Al-5cu composite under dynamic loading, Journal of materials processing technology, Vol. 94, 175-178.

[4] Ze wen huang, Ian R. Mccoll, Samuel J. Harris, (1996). Notched behaviour of a silicon carbide particulate reinforced Aluminium alloy matrix composite, Materials science and engineering A Vol. 215, 67-72

[5] S.Szczepanik, W. Lohnert, (1996). The formability of the Ai-5%SiC composite obtained using p/m method, Journal of materials processing technology, Vol. 60, 703-709

[6] Edited by George.E. Dieter, ASM publications, USA, 2000, Hand book on workability analysis and applications.

[7] Shima, S., Oyane, M, (1976). Plasticity theory for porous metals, International Journal of Mechanical Sciences, Vol. 18, 285–291.

[8] Doraivelu, S.M., Gegel, H.L., Gunasekaran, J.S., Malas, J.C., Morugan, J.T., (1984). A new yield function for compressible P/M materials, International Journal of Mechanical Sciences, Vol. 26,No. (9/10), 527–535.

[9] M.Abdel-Rahman, M.N.El-Sheikh, (1995). Workability in forging of powder metallurgy compacts, Journal of materials processing technology, Vol. 54, 97-102.

[10] R. Narayanasamy, R. Ponalagusamy, (2000) A mathematical theory of plasticity for the upsetting of compressible P/M materials, Journal of materials processing technology, Vol. 97, 107-109.

[11] P.S.Satsangi, P.C.Sharma, R.Prakash, (2003) An elastic-plastic finite element method for the analysis of powder metal forging, Journal of materials processing technology, Vol. 136, 80-87.

[12] R. Narayanasamy, R. Ponalagusamy, K.R. Subramanian, (2001) Generalised yield criteria of porous sintered powder metallurgy metals, Journal of materials processing technology, Vol. 110, 182-185.

[13] R. Narayanasamy, T. Ramesh, K.S. Pandey, (2005). Some aspects on workability of aluminium–iron powder metallurgy composite during cold upsetting, Material Science and Engineering A, Vol. 391, 418–426.

[14] ASM International; 2002, Production Sintering Practices. In: Powder Metal Technologies and Applications, ASM Handbook, Vol.07, pp. 468- 503.

[15] R. Narayanasamy, T. Ramesh, K.S. Pandey, S.K. Pandey, (2008). Effect of particle size on new constitutive relationship of aluminium–iron powder metallurgy composite during cold upsetting, Matererials and Design, Vol. 29, 1011–1026.

APEM journal ISSN 1854-6250 *Advances in Production Engineering & Management* 5 (2010) 1, 45 - 58 Scientific paper

A FRAMEWORK FOR SIMULTANEOUS RECOGNITION OF PART FAMILIES AND OPERATION GROUPS FOR DRIVING A RECONFIGURABLE MANUFACTURING SYSTEM

Rakesh K., Jain P.K., Mehta N.K.
Department of Mechanical & Industrial Engineering,
Indian Institute of Technology (I.I.T.), Roorkee (India)
E-Mail: rax16dme@iitr.ernet.in, pjainfme@iitr.ernet.in

Abstract:
With markets becoming increasingly competitive and customers demanding new product types/styles with ever-shortening life cycles, the conventional manufacturing systems have been rendered unfit in fulfilling the new manufacturing objectives of flexibility and responsiveness. Reconfigurable Manufacturing Systems (RMS) has been envisaged to have the capability to face these challenges by providing the exact functionality and capacity that is needed, exactly when it is needed. In RMS, products/parts are grouped into families, each of which requires a particular manufacturing system configuration in terms of the Reconfigurable Machine Tools (RMTs), their layouts etc. The system is reconfigured to produce the next family, once the production of the current family is finished, and so forth. The foundation for the success of an RMS, therefore, lies in the issue of 'recognition of appropriate sets of part families'. In the present work, a methodology based on adaptation of hierarchical clustering procedure is proposed so as to simultaneously yield sets of part families at different similarity levels and the corresponding operation groups.

Key Words: Reconfigurable Manufacturing System, Part Family Recognition, Hierarchical Clustering

1. INTRODUCTION

Reconfigurable manufacturing systems have been identified as manufacturing systems which provide the exact functionality and capacity that is needed, exactly when it is needed by rapidly rearranging or changing their constituent components [1, 2, 3, 4]. In RMS, each part may require a particular system configuration depending on the operations required for its manufacturing. However, RMS is made economically more attractive by recognizing part families having similar operations so that the whole family requires a single system configuration to manufacture all its member parts [5]. One part family is manufactured at a time by a system configuration having suitably configured RMTs catering to its operational requirements. The production of next family starts only when the system is reconfigured as per the operations required for the next family [5]. Therefore, the issue of finding appropriate part families and corresponding operation groups is central to the problem of designing a reconfigurable manufacturing system. These tasks are accomplished by applying the philosophy of group technology (GT) that takes advantage of the similarities between design characteristics and/or manufacturing attributes and/or functions of the given set of parts to group together similar parts for a common purpose.

The objective of this work is to propose a systematic procedure for simultaneous recognition of part families and corresponding operation groups for an effective and economic working of an RMS. The proposed procedure is an adaptation of agglomerative hierarchical clustering algorithm founded on two postulations. First, each part is manufactured using alternative operation sequences, all equally weighted. Second, a higher value of similarity measure implies a higher commonality of operations leading to less machine idleness. Therefore, an operation sequence that associates with a part family at the highest value of the similarity measure will be selected and the remaining will be discarded.

The paper has been structured as follows. Section 2, casts a glance on application of GT in the design of manufacturing systems, comparing RMS with cellular manufacturing systems (CMS). Section 3 presents the details of RMS model considered in this study. There is a whole gamut of literature available on methods for obtaining families of parts and groups of machines, especially in the context of CMS. As reconfigurable manufacturing paradigm has its own distinct characteristics, these methods cannot be directly adopted. In section 4, methodologies of cell formation in CMS are reviewed with the objective of identifying one that can be conveniently modified and adapted for the RMS model considered in this study. A discussion is presented on the attributes to be considered for formation of RMS part families, similarity coefficient and alternative operation sequences with reference to the considered RMS model. Building upon this foundation, a procedure for simultaneous recognition of parts families and the formation of corresponding operation groups has been proposed in section 5 and a numerical demonstration of the same has been presented in section 6. Finally, section 7 gives the conclusions and indicates the scope for future work.

2. GT APPLICATION IN DESIGN OF MANUFACTURING SYSTEMS: A GLANCE

Between the extremes of few part types produced in high volumes on dedicated manufacturing systems and a large variety of parts produced in few numbers in a job shop, there is an important category of batch manufacturing, which constitutes approximately 75% of total discrete part manufacturing activities [6]. The traditional process layouts have high material handling and tooling costs, complex scheduling and loading, lengthy setup times and high quality control costs associated to them, which significantly affect manufacturing cost, quality and delivery lead times. However, to compete in the increasingly challenging global environment characterised by demand for high flexibility and responsiveness, it is essential to improve productivity in manufacturing to increase market share and profitability. Application of GT in the design of manufacturing systems is an approach directed at these objectives. GT adoption in batch manufacturing allows the manufacturing system to gain economic advantages similar to those of dedicated manufacturing systems and at the same time helps in gaining the flexibility of job shops. Design of manufacturing systems such as flexible manufacturing systems (FMS), CMS etc. has been founded on the concepts of GT.

In CMS productivity is improved by exploiting similarities in manufacturing requirements such as machining operations, tooling, setups, material handling etc. Parts having similar manufacturing requirements are grouped into part families and processed together by dedicated machine cells. Therefore, GT implementation decomposes a large manufacturing system into smaller subsystems (cells), each specialized in the production of a part family. But, the highly unpredictable market environment and ever-shortening product life cycles have rendered these permanent cells inefficient [4]. Fortunately, the growing research and development in modular machines, RMTs and other supporting technologies has paved the way for the new manufacturing paradigm of RMS that promises customised flexibility with high responsiveness [1, 2, 4, 7]. In RMS, each part requires a specific system configuration. System can be reconfigured every time a new/next part order is to be executed. However, each reconfiguration incurs cost in rearranging the resources. Application of GT in RMS design can help in reducing the number of such reconfigurations required by dividing the large number of part types into a smaller number of families having similar manufacturing requirements. Therefore, GT application in RMS may enable it to execute a large part mix in fewer reconfigurations of the system.

3. THE PROPOSED RMS MODEL

The RMS model considered for study is assumed to be exposed to a complex environment, characterized by fierce competition, highly variable demand, compulsion to adopt new processes, frequent changes of the product mix and frequent introduction of new products. It possesses the features described below.

1. Manufacturer receives orders for Q different part types for manufacturing in the next reconfiguration cycle. The order receipt is closed at a certain pre-defined time limit before the completion of running reconfiguration cycle to provide sufficient time for the reconfiguration exercise. Out of the Q part types, only those P (≤Q) part types are accepted which satisfy two conditions as per company policy: (i) the total order di of all the customers for a particular part type pi must exceed a pre-decided minimum quantity, $D_{min(i)}$ (i.e. $di \geq D_{min(i)}$) and (ii) the anticipated execution time of all the orders must not exceed a predefined maximum allowable reconfiguration cycle span.

2. Each part, p_i is manufactured in ordered quantity, d_i using various machining operations by one of the various alternative operation sequences.

3. These part types are divided into F part families so that $1 \leq F \leq P$. Therefore, in extreme cases, either all the part types will fall in the same family or each family will be consisting of only one part type. The key attribute of a part family is that all the part types within a family require same operations and hence same production resources.

4. At any time the cell is constituted of suitably configured RMTs to cater to operational requirements of one part family only. The production of next family starts only when the cell is reconfigured as per the operations of this new family after the completion of the present family. Reconfiguration of the cell is achieved by relocation and reconfiguration of RMTs to enable them to perform operations required for the new family. RMTs are reconfigured using various combinations of basic modules (BMs) and auxiliary modules (AMs) [1-7]. The reconfiguration of the system that enables it to cater to a new family is defined as Primary Reconfiguration (PR). The sequence, in which the various part families are considered for production is termed as Primary Reconfiguration Sequence (PRS).

5. All the parts belonging to a family require common RMTs but they may have different routes through these RMTs. Therefore while switching over the production from one part to another within a family; the relocation of RMTs may be required. The reconfiguration of the cell that enables it to cater to next part within the same family is defined as Secondary Reconfiguration (SR). The sequence, in which the parts belonging to a family are considered for production is termed as Secondary Reconfiguration Sequence (SRS).

6. A Reconfiguration Cycle (RC) is completed when all the parts are manufactured as per the planned PRS and SRSs. Reconfiguration Cycle Span or simply the Cycle Span (CS) of an RMS is the time taken to execute the whole RC.

4. LITERATURE REVIEW, DISCUSSION AND APPOSITE DEDUCTIONS

4.1 Attributes

The operations dictate the type of machine tools needed and the sequence of operations impacts the flow of the material. Therefore, the operations and their sequences are among the most relevant attributes for the design of a CMS, where the aim is to configure permanent cells [6]. In the proposed RMS model, it has been assumed that all the parts belonging to a family are manufactured on a system configuration that provides all the resources required for their manufacturing. If the parts of a family follow different routes, the cell may undergo secondary reconfigurations to accommodate it. It implies that for a part to be a member of a family, commonality of operations is a sufficient condition and therefore the exact route need not be considered. Further, in CMS demand data has a direct influence on cell formation. For evenly distributing the work load amongst the cells, it is necessary either to include the part type(s) with heavy demand in smaller families or provide duplicate copies of machines. In the proposed RMS all the parts are manufactured sequentially (one after the other) on the same system and orders are accepted as per a predefined policy which ensures that the manufacturing time of all the parts does not exceed the cycle span of the cell. Therefore, demand data will also not influence the decision of part family formation. Thus, the operations required to manufacture a part are the most relevant attributes for the considered RMS model, consistent with the objective of minimising the number and hence,

cost of reconfigurations. Therefore, binary part-operation incidence matrix (POIM) that ignores the information on exact routes is sufficient input for this problem.

4.2 GT Methods

GT application in CMS cell formation (CF) problem incorporates two sub-problems: the identification of 'part families' and formation of 'machine groups'. In a RMS design problem also 'Part Family' recognition and 'Operation Groups' formation are preliminary requirements. A broad literature review of cell formation techniques in CMS was conducted to identify a suitable technique to fulfil the requirements of RMS model in hand.

It has been observed that the descriptive procedures available in the literature are not highly sophisticated or accurate, whereas, mathematical programming approaches are incompletely formulated and computationally complex [8]. Random search algorithms such as simulated annealing, genetic algorithms and neural networks provide solutions, which do not depend on the initial solution and have an objective value closer to the global optimal. However, the gain in applying these general algorithms may be undone by the computational effort, since these procedures are slower than other procedures [9]. Non-hierarchical clustering methods such as ISNC [10], ZODIAC [11] and GRAFICS [12], require the information on the number of groups to be formed in advance. But this is undesirable in RMSs. In addition, the arbitrariness of the initial partition of the data set could lead to unsatisfactory results.

For the RMS model under consideration in which only binary POIM is required as initial input, the use of either array based clustering methods or the hierarchical clustering methods seem to be justifiable. Array based clustering methods also called matrix manipulation methods attempt simultaneous grouping of parts and machines through block diagonalisation by reordering rows and columns of the binary incidence matrix. Some of the main matrix manipulation methods are Bond Energy Algorithm [13, 14], Rank Order Clustering [15, 16], Modified Rank Order Clustering [17], Direct Clustering Analysis [18] and Cluster Identification Algorithm [19]. Though these methods achieve acceptable results with low computational cost, they have the disadvantage that results obtained have a dependency on the configuration of initial incidence matrix [15, 17, 19]. Also, it has been observed that in many cases disjoint part families are not identified even with a well structured matrix [9].

The hierarchical clustering procedure groups together similar objects on the basis of the similarities in their attributes. Hierarchical algorithms, which can be agglomerative ('bottom-up') or divisive ('top-down'), find successive clusters using previously established clusters. Agglomerative algorithms begin with each object as a separate cluster and merge them into successively larger clusters based on commonality in attributes measured by a similarity coefficient. On the other hand divisive algorithms begin with the whole set as one cluster and proceed to divide it into successively smaller clusters. It has been observed that in the context of part family formation or machine group recognition, only agglomerative procedure has been used [20].

The traditional representation of this hierarchy is a tree called a dendogram, with individual elements at the top end and a single cluster containing every element at the bottom. Agglomerative algorithms begin at the top of the tree, whereas divisive algorithms begin at the bottom. Cutting the dendogram at a given precision level (similarity level expressed in %) gives a set of families at selected precision. As the precision decreases, a coarser clustering occurs that is distinguished by a smaller number of large size clusters.

In addition to the fact that hierarchical clustering is a well-proven and most broadly implemented method in almost all the fields of Engineering and Science, following are other relevant reasons to adopt this method for part family formation in the present problem:

- it can be easily adapted as per the specific requirements of different problems by suitably defining logically and/or probabilistically justifiable similarity coefficients,

- in CMS cell formation problems, the selection of a set of families are generally made from the dendogram by restricting either precision level or the number of groups. In the presented RMS model it has been proposed that families corresponding to that level of the dendogram have to be selected which minimises the sum of primary reconfiguration costs, secondary reconfiguration costs, material handling costs, machine idle costs etc.

In the light of these facts, agglomerative hierarchical clustering has been selected to use in the present study with appropriate modifications and adaptations for simultaneous formation of part families at various precision levels and operation groups.

The three most widely used hierarchical clustering methods are single linkage clustering (SLC) [21], average linkage clustering (ALC) [22] and complete linkage clustering (CLC) [23, 24]. In SLC, two groups are merged together merely because two parts, one from each group have high similarity to each other. If this process continues, it results into a string effect known as chaining. Since CLC is the antithesis of SLC, it is least likely to cause chaining. ALC produces reasonable results between these two extremes [9] and therefore it is considered as most appropriate for this study.

4.3 Similarity Coefficient

The coefficient that measures the similarity between two objects (parts in our case) on the basis of commonalities between attributes (operations in our case) is called a similarity co-efficient. Selection of an appropriate similarity coefficient is most important for the success of any clustering method. This will influence the shape of the clusters, as some objects (parts) may be close to one another according to one similarity coefficient and further away according to another. Therefore, while choosing a similarity coefficient for a clustering problem, all its specific characteristics, requirements and objectives must be taken into consideration. The similarity coefficient chosen must have a logical and/or probabilistic justification.

The most common similarity coefficient used in GT applications using 'binary object attribute incidence matrix' (POIM in our case) is Jaccard similarity coefficient. The Jaccard coefficient is defined as the size of the intersection divided by the size of the union of the attribute (operation) sets of the corresponding objects (parts). The Jaccard similarity coefficient (S_{mn}) between a pair of objects (m, n) is calculated by equation (1).

$$S_{mn} = \frac{a}{a+b+c}, 0 \le S_{mn} \le 1 \tag{1}$$

where, a number of common operations between two parts,
b number of operations that are required only for part m and
c number of operations that are required only for part n.

In the present study also, the Jaccard similarity coefficient has been used.

4.4 Alternative Operation Sequences

The operations required to manufacture a part and their sequences are stated on a process plan. Process planning is not only a science; it is an art too, involving creativity, innovation, independent thinking, personal preferences and experience. Therefore, a process plan for manufacturing of a part cannot be unique. Further, the fact that each part can have more than one process plan provides more added flexibility in the design of a manufacturing system. Therefore, in the proposed RMS, it has been postulated that a part can have more than one alternative operation sequences. In their CMS models, authors of references [25] and [26] proposed the distribution of the demand of a part among all alternative process plans in the proportion of their usage factors, which indicate the preference given to a process plan. However, reference [26] pointed it out that it would not be preferable to execute all process plans due to enhanced complexity of production planning and associated

additional costs. Therefore, it was proposed to assign equal priority to all process plans and then the best among all alternative plans were selected based on least intercellular movement [26]. The plan so selected would be used for the manufacturing of full demand volume of the concerned part type.

In the proposed RMS model also, it has been proposed to give equal priority to all alternative operation sequences and to select only one operation sequence from the set of alternatives for the manufacturing of full demand volume of the concerned part. If a part is manufactured with more operation sequences in any proportions, it results into more reconfigurations and obviously more associated costs.

A part is associated to a family based on the number of common operations that it shares with other members of the family. An RMT has to remain idle when a member of the family does not require an operation. A higher value of similarity coefficient implies a higher number of operations are common and therefore less machine idleness. Therefore, it is proposed to choose best among all alternative operation sequences based on the highest similarity coefficient. It implies that all the operation sequences will be used in the clustering procedure and an operation sequence that associates itself with a part family at the highest similarity level will be selected and rest will be discarded straightaway.

5. MODIFIED HIERARCHICAL CLUSTERING PROCEDURE FOR RMS

In Figure 1, the basic steps of hierarchical clustering algorithm have been described. Even though, the basic steps are common, researchers have evolved and used a wide spectrum of similarity coefficient definitions and applied a wide choice of adaptations of this basic clustering procedure [9] conforming to the distinct features of the specific problems. The modified agglomerative average linkage hierarchical clustering algorithm proposed in this work uses a special naming scheme as given below.

(a) A part type pi and its jth operation sequence are represented by an object named as a decimal numeral ‘i.j’. The integer part (i) and fractional part (j) respectively represent the part type number and the operation sequences considered. For example, if a part type p2 has three alternative operation sequences, objects named as 2.1, 2.2 and 2.3 will represent three combinations.

(b) If the part type p_i has only one operation sequence, then its representation will be object i.0. The objects so named (as in a & b) are called single part objects as each represents a part family consisting of only one part type (as on the top of the dendogram). Therefore, if as_i is the number of operation sequences for a part type p_i, the total number of objects, M in POIM will be: $\sum_{i=1}^{P} as_i$.

(c) A new family formed by grouping together two existing families is represented by an object named as k.0, where k=h+1. h is the highest integer used to represent an object among all existing objects. The object so created is called a multipart object as it represents a cluster of more than one parts grouped as a family.

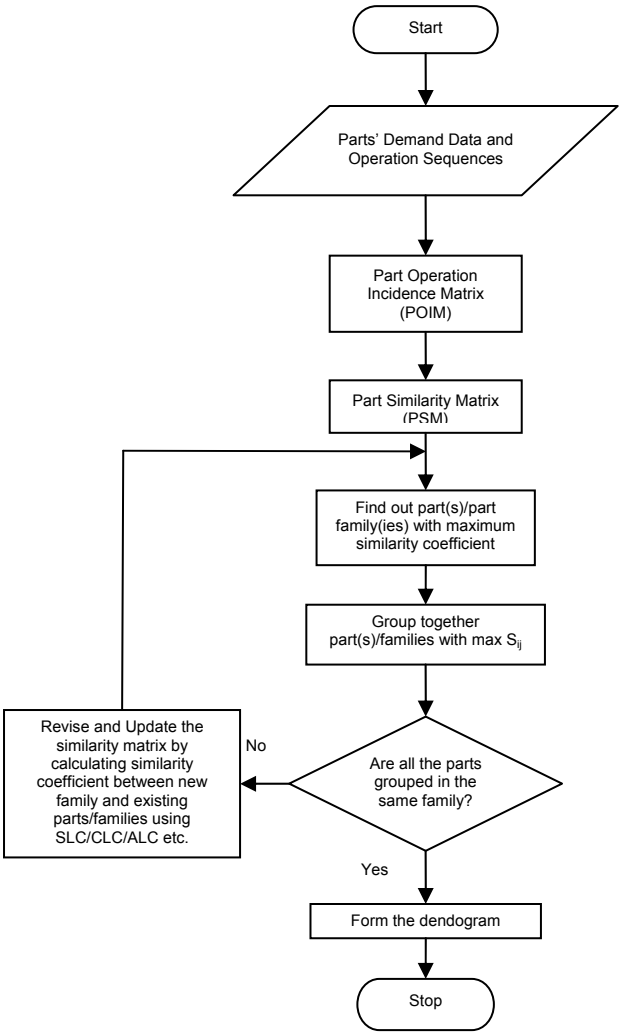

Figure 1: Hierarchical clustering algorithm.

The proposed procedure is as given below.

Step 1: Obtain the information of total demand orders (d_i) of all the Q part types for next reconfiguration cycle and all their alternative operation sequences (Table I). Accept a part type pi for manufacturing as per company's policy.

Step 2: Construct POIM (Table II) progressively by adding the information corresponding to each operation sequence of each part type accepted for manufacturing. If O_p is the total number of operations, POIM is an M x O_p matrix. An entry of 1 in the matrix indicate that the part represented by object in the corresponding row require the operation in the corresponding column and vice versa for a 0 entry.

Step 3: Compute the value of similarity coefficient S_{mn} for each pair of objects (m,n) to form the part similarity matrix (PSM) (Table III). If the pair of objects under consideration represents the same part, S_{mn} is taken as zero. As it has been assumed that only one operation sequence is selected for manufacturing a part, these objects can not be paired. For all other pairs of objects, S_{mn} is calculated using a predefined relationship e.g. Jaccard coefficient. PSM so obtained is an M x M matrix. First three steps of the algorithm are depicted in a flow chart in Figure 2.

Step4: Find the pair(s) of objects having highest value in similarity matrix. If there is only one pair of such objects, go to step 7, otherwise go to the next step.

Step 5: Find out a pair for which both the objects are either of the following:

i. a multipart object i.e. a family formulated in a previous stage (i.e. k.0).
ii. an object representing a single part and its single operation sequence (i.e. i.0)

iii. an object representing a single part and one of its alternative operation sequences and fulfilling the condition that the objects representing rest of the alternative operation sequences for this part do not pair at this similarity level.

If no such pair exist, go to next the step otherwise skip it.

Step 6: Calculate maximum average linkage value for each pair in tie, with all other objects ignoring objects having the same parts as in objects in the pair considered. Find the pair that exhibits the highest maximum average linkage value.

Step 7: Check whether any object in the pair selected has only one part. If not, go to step 10.

Step 8: Check whether the part in each single part object have alternative operation sequences. If not, go to step 10.

Step 9: Update similarity matrix by deleting all rows and columns corresponding to objects representing alternative operation sequences.

Step 10: Join the two objects in the selected pair to form a new object (representing a part family) containing all the parts of two joining objects and name it as per the naming scheme described earlier.

Step 11: Go to step 13, if all the parts are grouped in one family.

Step 12: Go to step 4 after updating the similarity matrix by computing the similarity coefficient between the new object and older objects which were unaltered in the last step.

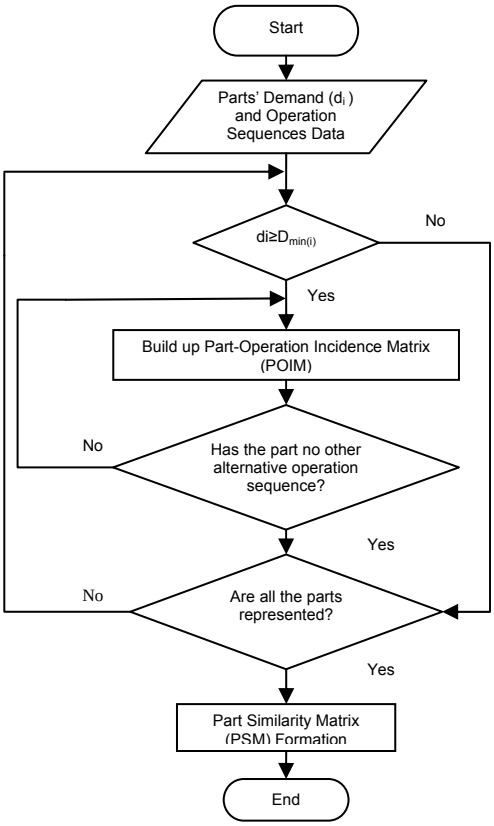

Figure 2: Procedure for POIM & PSM Formation (Steps 1 to 3).

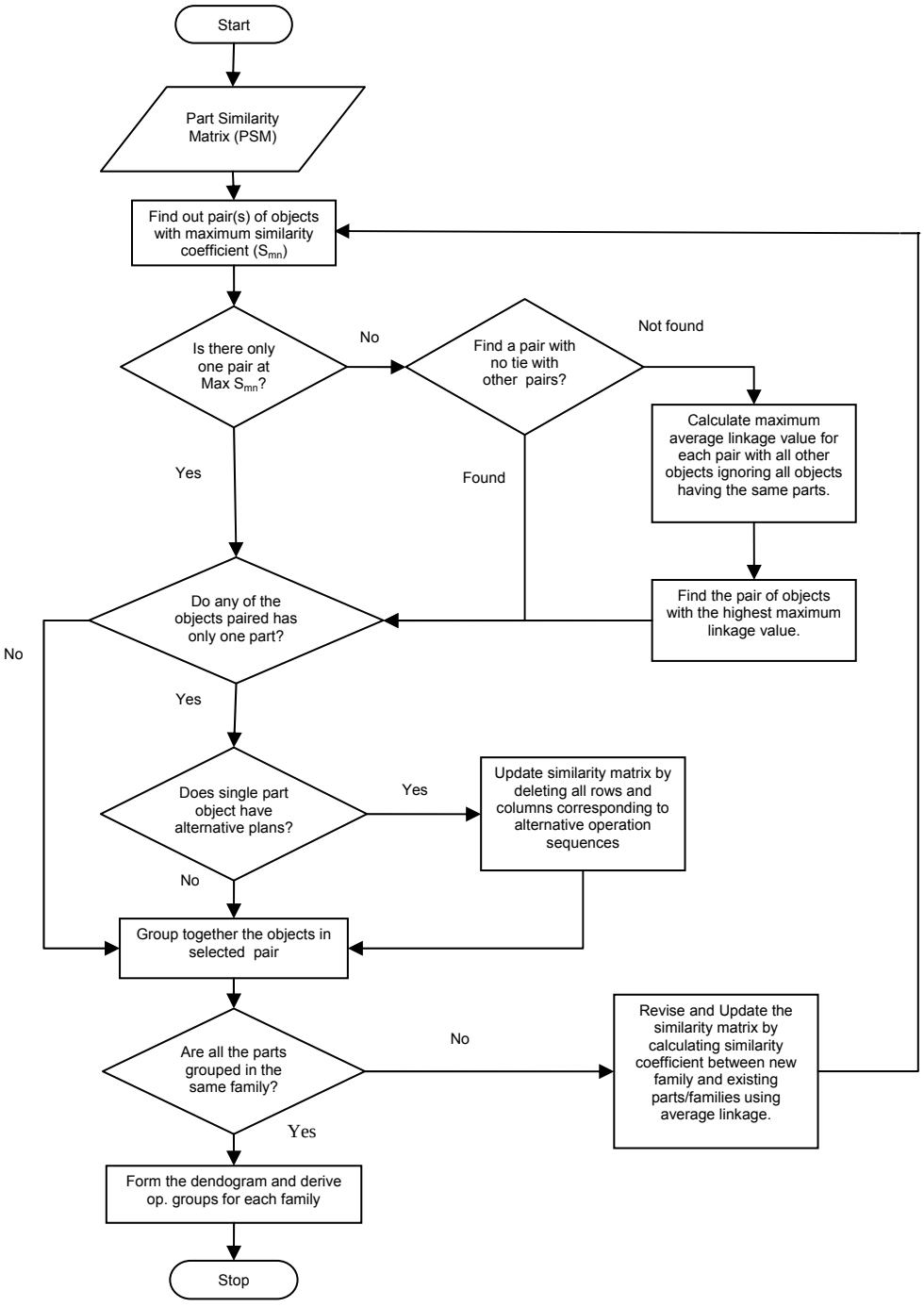

Figure 3: Adaptation of hierarchical clustering algorithm for RMS (Steps 4-14).

In the ALC method the similarity coefficient for a pair of objects is calculated as the average similarity between all the parts in them and is given by the formula

$$S_{uv} = \frac{\sum\sum S_{mn}}{p_u p_v} \qquad (2)$$

Where:

u,v Part families (objects)

m,n Parts belonging to family u and v respectively

p_u and p_v Number of parts in families u and v respectively.

Step13: Construct a dendogram (Figure 5) showing part families identified corresponding to different similarity levels and the selected operation sequences. Table IV depicts the information on the dendogram i.e. the part families and the operation sequence selected for each part. The information on Tables I and IV is translated into operation groups corresponding to each part family (Table V).

6. DEMONSTRATION THROUGH EXAMPLE

To demonstrate the use of the proposed procedure, consider a hypothetical situation where six operations are required for manufacturing of parts in next reconfiguration cycle. Table I shows the alternative operation sequences, the total demand, d_i and the minimum acceptable demand size $D_{min(i)}$ for each part type. POIM is constructed as shown in Table II. Any order $d_i<D_{min(i)}$ is not considered. The POIM (Table II) has total 13 objects and 6 operations.

Table I: Parts demand data and operations sequences.

Part No.	$D_{min(i)}$	Demand (d_i)	Operation Sequence(s)
1	40	60	1-3-6, 2-3-5
2	100	350	3-1-6
3	100	550	2-4-5, 1-3, 2-3-6
4	50	80	2-4, 1-2-3
5	50	100	1-2-4, 2-3-4, 5-4-3
6	100	150	1-6, 1-5
7	100	70	2-3-5, 2-3-6

Table II: Part operation incidence matrix (POIM).

Operation No.→ Object No.↓	1	2	3	4	5	6
1.1	1	0	1	0	0	1
1.2	0	1	1	0	1	0
2.0	1	0	1	0	0	1
3.1	0	1	0	1	1	0
3.2	1	0	1	0	0	0
3.3	0	1	1	0	0	1
4.1	0	1	0	1	0	0
4.2	1	1	1	0	0	0
5.1	1	1	0	1	0	0
5.2	0	1	1	1	0	0
5.3	0	0	1	1	1	0
6.1	1	0	0	0	0	1
6.2	1	0	0	0	1	0

PSM, as shown in Table III is formed by calculating the value of similarity coefficient S_{mn} for each pair of objects in POIM. $S_{mn} = 0$, if objects in a pair represent the same part (for example objects 3.1 and 3.2). Use Equation 1 for all other pairs. Referring to Table III, it is seen that there is only one pair of objects i.e. (1.1, 2.0) that corresponds to the highest similarity value of 1.

Table III: Part Similarity matrix (PSM).

Objects	1.1	1.2	2.0	3.1	3.2	3.3	4.1	4.2	5.1	5.2	5.3	6.1	6.2
1.1	0.00	0.00	1.00	0.00	0.67	0.50	0.00	0.50	0.20	0.20	0.20	0.67	0.25
1.2		0.00	0.20	0.50	0.25	0.50	0.25	0.50	0.20	0.50	0.50	0.00	0.25
2.0			0.00	0.00	0.67	0.50	0.00	0.50	0.20	0.20	0.20	0.67	0.25
3.1				0.00	0.00	0.00	0.67	0.20	0.50	0.50	0.50	0.00	0.00
3.2					0.00	0.00	0.00	0.67	0.25	0.25	0.25	0.33	0.33
3.3						0.00	0.25	0.50	0.20	0.50	0.20	0.25	0.00
4.1							0.00	0.00	0.67	0.67	0.25	0.00	0.00
4.2								0.00	0.50	0.50	0.20	0.25	0.25
5.1									0.00	0.00	0.00	0.25	0.25
5.2										0.00	0.00	0.00	0.00
5.3											0.00	0.00	0.25
6.1												0.00	0.00
6.2													0.00

Objects	7.0 {1.1,2.0}	3.1	3.2	3.3	4.1	4.2	5.1	5.2	5.3	6.1	6.2
7.0 {1.1,2.0}	0.00	0.00	0.67	0.50	0.00	0.50	0.20	0.20	0.20	0.67	0.25
3.1		0.00	0.00	0.00	0.67	0.20	0.50	0.50	0.50	0.00	0.00
3.2			0.00	0.00	0.00	0.67	0.25	0.25	0.25	0.33	0.33
3.3				0.00	0.25	0.50	0.20	0.50	0.20	0.25	0.00
4.1					0.00	0.00	0.67	0.67	0.25	0.00	0.00
4.2						0.00	0.50	0.50	0.20	0.25	0.25
5.1							0.00	0.00	0.00	0.25	0.25
5.2								0.00	0.00	0.00	0.00
5.3									0.00	0.00	0.25
6.1										0.00	0.00
6.2											0.00

(a)

Objects	8.0 {7.0,6.1} i.e. {1.1,2.0,6.1}	3.1	3.2	3.3	4.1	4.2	5.1	5.2	5.3
8.0 {7.0,6.1}	0.00	0.00	0.56	0.42	0.00	0.42	0.22	0.13	0.13
3.1		0.00	0.00	0.00	0.67	0.20	0.50	0.50	0.50
3.2			0.00	0.00	0.00	0.67	0.25	0.25	0.25
3.3				0.00	0.25	0.50	0.20	0.50	0.20
4.1					0.00	0.00	0.67	0.67	0.25
4.2						0.00	0.50	0.50	0.20
5.1							0.00	0.00	0.00
5.2								0.00	0.00
5.3									0.00

(b)

Objects	8.0 {7.0,6.1} i.e. {1.1,2.0,6.1}	9.0 {3.1,4.1}	5.1	5.2	5.3
8.0 {7.0,6.1}	0.00	0.00	0.22	0.13	0.13
9.0 {3.1,4.1}		0.00	0.59	0.59	0.38
5.1			0.00	0.00	0.00
5.2				0.00	0.00
5.3					0.00

(c)

Objects	8.0{7.0,6.1} i.e. {1.1,2.0,6.1}	010.0 {9.0,5.1} i.e. {3.1,4.1,5.1}
8.0 {7.0,6.1}	0.00	**0.07**
10.0 {9.0,5.1}		**0.00**

(d)

Objects	11.0 {8.0,10.0} i.e. {1.1,2.0,3.1,4.1,5.1,6.1}
11.0 {8.0,10.0}	0.07

(e)

Figure 4: Tables (a-e) showing various stages of procedure for the demonstration problem.

Therefore, skip steps 5 and 6. Now, it is observed that both the objects have only one part each. The first object in the pair (i.e.1.1) has alternative operation sequence but the second object (i.e. 2.0) has no alternative operation sequence. Therefore, the similarity matrix in Table III is updated by deleting all rows and columns corresponding to object 1.2. The objects in the pair under consideration (i.e. 1.1 and 2.0) are joined to form a new family named as object 7.0. The new object is named 7.0, as the highest integer used to represent an object in previous stage of the procedure is 6 (objects 6.1 and 6.2).

Table IV: Part families identified at different precision levels.

Precision (in %)	Part families & operation sequence for each part
7	{11.0} i.e {8.0,10.0} i.e. {1.1,2.0,3.1,4.1,5.1,6.1}
59	{8.0} i.e. {1.1,2.0,6.1}; {10.0} i.e. {9.0,5.1} i.e.{3.1,4.1,5.1}
67	{8.0} i.e. {7.0,6.1} i.e.{1.1,2.0,6.1} ; {9.0} i.e.{3.1,4.1}; {5.1}
100	{7.0} i.e. {1.1,2.0}; {3.1}; {4.1} ;{5.1} ;{6.1}

As all the parts are not grouped in one family yet, the similarity matrix is updated by computing the similarity coefficients between the new object (7.0) and the older objects using Equation 2. Table (a) in Figure 4 gives the updated similarity matrix. The procedure is repeated again beginning with step 4. Referring to table (a) in Figure 4, it is seen that there are six pairs of objects exhibiting the highest similarity value of 0.67. These are (7.0, 3.2), (7.0, 6.1), (3.1, 4.1), (3.2, 4.2), (4.1, 5.1) and (4.1, 5.2). Further, in the pair (7.0, 6.1), the first object 7.0 represents a family formulated in a previous stage and the second object 6.1 represents part 6 having an alternative operation sequence but the object representing that (6.2) do not pair at this similarity level. Therefore, the pair (7.0, 6.1) is selected at this stage. Skip step 6.

Now, It is observed that only object 6.1 has one part and it has an alternative operation sequence (i.e. 6.2).The similarity matrix in table (a) is updated to table (b) after deleting all the rows and columns corresponding to 6.2 and joining 7.0 and 6.1 to form a family namely 8.0.

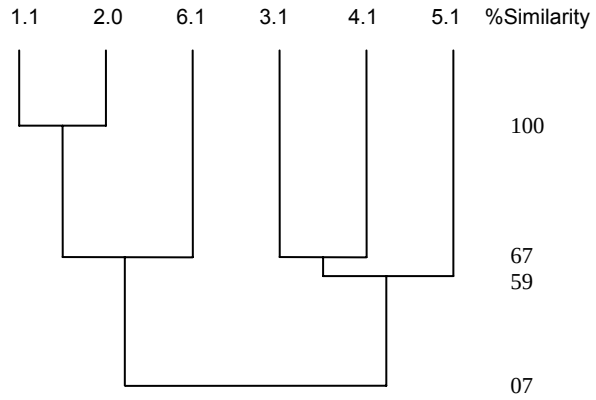

Figure 5: Dendogram.

Referring to table (b), it is seen that that there are four pairs of objects exhibiting the highest similarity value of 0.67. These are (3.1, 4.1), (3.2, 4.2), (4.1, 5.1) and (4.1, 5.2). None of the four pairs fulfil the desired requirement of step 6. Therefore as per step 6, the average linkage value for the first pair (3.1, 4.1) with all other objects in table (b) except 3.2 and 4.2 is determined. Therefore, using equation (2) we find the set of average linkage values for the pair (3.1,4.1) with 8.0, 5.1, 5.2, 5.3 respectively as (0.00 0.59 0.59 0.38). The maximum average linkage value for this pair is 0.59. Similarly, the values for the others pairs are calculated as 0.49, 0.59 and 0.59. As there is a tie on the highest maximum average linkage value, the first pair i.e. (3.1, 4.1) exhibiting this value is selected. It is observed that both the selected objects have one part each and both have an alternative operation sequence (i.e. 3.2 & 4.2 respectively).The similarity matrix in table (b) is updated to table (c) after deleting all the rows and columns corresponding to 3.2 and 4.2 and joining 3.1 and 4.1 to form a family namely 9.0.

Table V: Selected operation groups.

Part Family	Operation Group
{1.1,2.0}	1,3,6
{3.1,4.1}	2,4,5
{1.1,2.0,6.1}	1,3,6
{3.1,4.1,5.1}	1,2,4,5
{1.1,2.0,3.1,4.1,5.1,6.1}	1,2,3,4,5,6

The procedure is repeated until all the parts fall in one family. Tables (d) and (e) depict the subsequent steps for the demonstration problem. The part families identified and the selected operation sequences are compiled as shown in Table IV and depicted in Figure 5 in the form of a dendogram. Operation groups corresponding to each part family are formulated using the information in Tables 1 and 4 as shown in Table V.

7. CONCLUDING REMARKS

In the RMS model considered, the manufacturing system is configured to manufacture a particular family of parts and then reconfigured to manufacture the next one and so on. The significance of selecting an appropriate set of families lies in the fact that the costs incurred on system reconfigurations (both primary and secondary), material handling, machine idleness etc., depend on it. Consequently, the costs of the parts manufactured are directly related to the set of families selected. Therefore, recognition of part families is the foundation stone for the design of a reconfigurable manufacturing system. This research has presented a logical and systematic procedure to group the parts into families and simultaneously an operation sequence is selected from a set of operation sequences for each part. Therefore, an operation group corresponding to each part family is also recognized.

The outcome of the procedure is depicted on a dendogram showing different sets of part families at different similarity levels. The next most important step in RMS design is to choose one of these sets of families to meet the objectives of the company. Presently, the research on identification of parameters that impact the choice of a set of families from the dendogram, selection of RMTs for each operation group, generation of PRS and SRSs etc. is under progress.

REFERENCES

[1] Koren, Y.; Hiesel, U.; Jovane, F.; Moriwaki, T.; Pritschow, G.; Ulsoy, G.; Van Brussel, H. (1999). Reconfigurable Manufacturing Systems, Annals of the CIRP, Vol. 48, No. 2, 527-540.

[2] Mehrabi, M.G.; Ulsoy, A.G.; Koren, Y. (2000). Reconfigurable manufacturing systems: Key to future manufacturing, Journal of Intelligent Manufacturing, Vol. 11, No. 4, 403-419.

[3] Hegui Ye; Ming Liang (2006). Simultaneous Modular Product Scheduling and Manufacturing Cell Reconfiguration Using a Genetic Algorithm, Journal of Manufacturing Science & Engineering , Vol. 128, No. 11, 984-995.

[4] Rakesh, K.; Jain, P.K. (2007). Reconfigurable Manufacturing Systems: an emerging manufacturing paradigm, Proceedings of the Global conference on Production & Industrial Engineering, N.I.T. Jalandhar.

[5] Xiaobo, Z.; Jiancai, W.; Zhenbi, L. (2000). A stochastic model of a reconfigurable manufacturing system, Part 1: A framework, International Journal of Production Research, Vol. 38, No. 10, 2273–2285.

[6] Singh, N. (1996). Systems approach to Computer-Integrated Design and Manufacturing, John Wiley & Sons.

[7] Mehrabi, M.G.; Ulsoy, A.G.; Koren, Y. (2000). Reconfigurable manufacturing systems and their enabling technologies, International Journal of Manufacturing Technology and Management, Vol. 1, Issue 1, 113-130.

[8] Galan, R.; Racero, J.; Eguia, I.; Garcia, J.M. (2007). A systematic approach for product families formation in Reconfigurable Manufacturing Systems, Robotics and Computer-Integrated Manufacturing, Vol. 23, Issue 5, 489-502.

[9] Singh, N.; Rajamani D. (1996). Cellular Manufacturing Systems: design, planning and control, Chapman & Hall.

[10] Chandrasekharan, M.P.; Rajagopalan R. (1986a). An ideal seed non-hierarchical clustering algorithm for cellular manufacturing, International Journal of Production Research, Vol. 24, Issue. 2, 451-464.

[11] Chandrasekharan, M.P.; Rajagopalan R. (1987). ZODIAC-an algorithm for concurrent formation of part-families and machine-cells, International Journal of Production Research, Vol.25, Issue 6, 835-850.

[12] Srinivasan, G.; Narendran, T.T. (1991). GRAFICS: a non-hierarchical clustering algorithm for group technology, International Journal of Production Research, Vol. 29, Issue 3, 463-478.

[13] McCormick, W.T.; Schweitzer, P.J.; White, T.W. (1972). Problem decomposition and data reorganization by a clustering technique, Operations Research, Vol. 20, Issue 5, 993-1009.

[14] King, J.R. (1980a). Machine-component grouping formation in group technology, International Journal of Management Science, Vol. 8, Issue 2, 193-199.

[15] King, J.R. (1980b). Machine-component grouping in production flow analysis: An approach using a rank order clustering algorithm, International Journal of Production Research, Vol. 18, Issue 2, 213-232.

[16] King, J.R.; Nakornchai V. (1982). Machine-component group formation in group technology: review and extension, International Journal of Production Research, Vol.20, Issue 2, 117-133.

[17] Chandrasekharan, M.P.; Rajagopalan, R. (1986b). MODROC: An extension of rank order clustering for group technology. International Journal of Production Research, Vol. 24, Issue 5, 1221-1233.

[18] Chan, H.M.; Milner D.A. (1982). Direct clustering algorithm for group formation in cellular manufacturing, Journal of Manufacturing Systems, Vol. 1, Issue 1, 65-74.

[19] Kusiak, A.; Chow W.S. (1987). Efficient Solving of the Group Technology Problem, Journal of Manufacturing Systems, Vol. 6, Issue 2, 117-124.

[20] Selim, H.M.; Askin, R.G.; Vakharia A.J. (1998). Cell formation in group technology: review, evaluation and directions for future research, Computers & Industrial Engineering, Vol. 34, Issue1, 3-20.

[21] McAuley, J.; 1972, Machine grouping for efficient production, The Production Engineer, Vol. 51, Issue 2, 53-57.

[22] Seifoddini, H.; Wolfe, P. M. (1986). Application of the similarity coefficient method in group technology, IIE transactions, Vol. 18, Issue 3, 271-277.

[23] Gupta, T.; Seifoddini H. (1990). Production data based similarity coefficient for machine-component grouping decisions in the design of a cellular manufacturing systems, International Journal of Production Research, Vol. 28, Issue 7, 1247-1269.

[24] Mosier, C.T. (1989). An experiment investigating the application of clustering procedures and similarity coefficients to the GT machine cell formation problem, International Journal of Production Research, Vol. 27, Issue 10, 1811-1835.

[25] Choobineh, F. (1988). A framework for the design of cellular manufacturing systems, International Journal of Production Research, Vol. 26, Issue 7, 1161-1172.

[26] Patnaik, L.N. (2005). Model of a Cellular Manufacturing System with Reconfigurable Characteristics, Ph. D. Dissertation, MIED, Indian Institute of Technology, Roorkee, India.

APEM journal ISSN 1854-6250 *Advances in Production Engineering & Management* 5 (2010) 1, 59 - 68 Scientific paper

COMPUTER-BASED WORKPIECE DETECTION ON CNC MILLING MACHINE TOOLS USING OPTICAL CAMERA AND NEURAL NETWORKS

Klancnik S. & Senveter J.
University of Maribor, Faculty of Mechanical Engineering,
Smetanova 17, 2000 Maribor, Slovenia
E-Mail: simon.klancnik@uni-mb.si, jernej.senveter@uni-mb.si

Abstract:
In this paper, system for optical determining the workpiece origin on the CNC machine is presented. Similar high sophisticated systems are commercially available but in most cases they are very expensive and so their purchase is economically unjustified. The purpose of our research is to develop an inexpensive system for non-contact determination of the workpiece origin, which is also sufficiently precise for practical use. The system is implemented on a three-axis CNC milling machine Lakos 150 G, which is primarily designed for good machinability materials. Calibration procedure using feed-forward neural networks was developed. With this method the calibration procedure is simplified and the mathematical derivation of camera model is avoided. Learned neural network represents the camera calibration model. After neural network learning is complete, we can begin using the system for determining the workpiece origin. This developed system was through a number of tests proved to be reliable and suitable for use in practice. In the paper, working of system is illustrated with a practical example, which confirms the effectiveness of the implemented system in actual use on machine.

Key Words: Neural Networks, Image Processing, Milling, Workpiece Detection

1. INTRODUCTION

The use of machine vision systems is nowadays more and more present in the automation of industrial processes. These systems can be noticed, in particular, there where it is difficult or even impossible to implement automation through simple or conventional sensors, which are still considered to be more reliable. The machine vision is used for replacing human visual perception, as for example, product quality control, management of technological processes, laboratory analysis of images and similar. Thus, the reproducibility of procedures can be ensured, and the production costs as well as harmful effects of the production process on the environment can be reduced. Such systems help to improve competitiveness of technological processes.

Artificial vision is applicable as a sensor for managing of the system, ever since it imitates the human vision and allows contactless detection of the close vicinity of the industrial system. Since the first researchers in the area of the machine vision systems, describing the use of feedback loop of the artificial vision for the robot position correction and, consequently, the accuracy of the task performance, a considerable development of robot arms, controlled directly on the basis of artificial vision, can be traced. A number of systems of different makers manufacturing systems with fully integrated artificial vision system are available. Those systems are highly sophisticated and their price is high accordingly.

The article presents the development of the system for optical determination of workpiece origin [1] with the use of cheap equipment. The primary objective of our work was to develop a system for automatic determination of workpiece origin on the LAKOS 150G desktop milling machine, which will be less expensive than similar high sophisticated systems available on the market, and its performance will be sufficiently reliable and precise at the

same time. The system was designed in way that it is possible to also use it on other machine tools, where it is necessary to determine the workpiece starting point.

The article is structured in way that first the applied hardware equipment is presented in short. Furthermore, the design of the system and the integration into the LAKOS 150G processing machine is presented in detail, as well as the basic principle of system operation. In order to obtain useful information from the image captured by the camera, it is necessary to process the image with appropriate algorithms for digital image processing. The procedure of image processing is presented in chapter four. The fifth chapter shortly presents the results of the operation of the system for a test example. The article ends with a short conclusion.

2. HARDWARE EQUIPMENT

The optical system for determination of the origin of the workpiece was implemented on the LAKOS 150G desktop milling machine, presented in Figure 1. The LAKOS machine is a desktop 3-axial CNC machine tool developed, in particular, as a teaching aid for educational institutions dealing with mechatronic systems. LAKOS is primarily designed for good machinability materials. It can be used for processing with cutting and operations like coating with adhesives or dyes, application of gaskets, and it can also be used as a robot system for measuring, testing or assembling. Since this is an education machine, its design is simple, thus providing more possibilities for the development of new applications and methods of use. The machine controls are performed by a personal computer equipped with Linux operating system, that is, through EMC2 open source CNC software package.

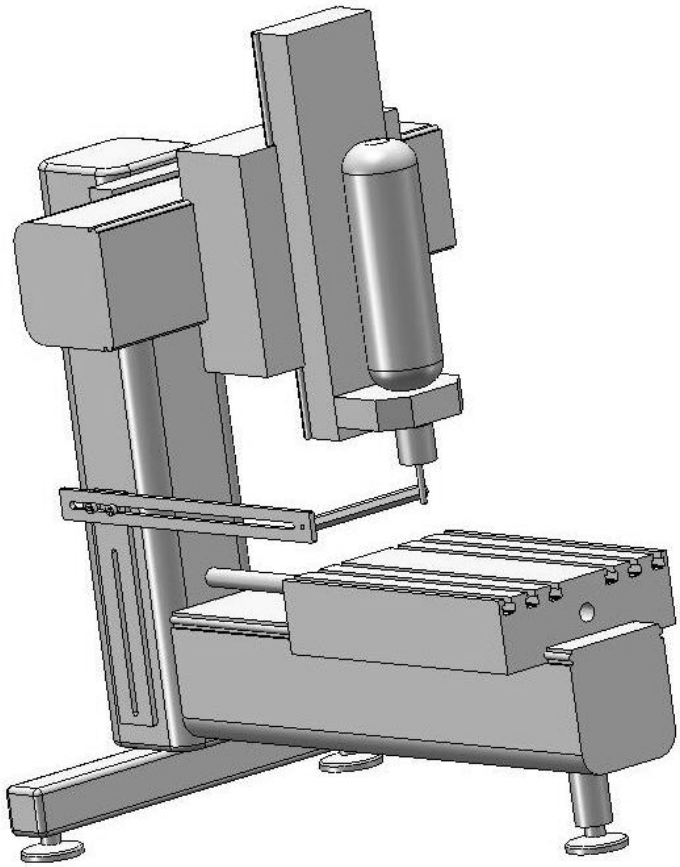

Figure 1: CAD model of LAKOS 150G desktop milling machine.

For the optical determination of the origin of the workpiece, it was necessary to place a camera on the machine. The camera has to be fixed; its position is not to be changed after the calibration of the system. For this purpose, the workshop of the Production Engineering Institute at the Faculty of Mechanical Engineering has manufactured a dedicated stand designed in way that the position of camera can easily be altered according to the requirements of the application using the camera (changing the distance of the camera from the observed object) (Figure 2).

An inexpensive QuickCam camera manufactured by Logitech (Figure 2) was used. This camera can capture up to 30 images per second. The maximum resolution, which can be attained by the direct capturing of the video signal, is 320x240 pixels. The capturing of the video signal on the personal computer is performed via the USB 2.0 interface, whereas the camera focus is regulated manually.

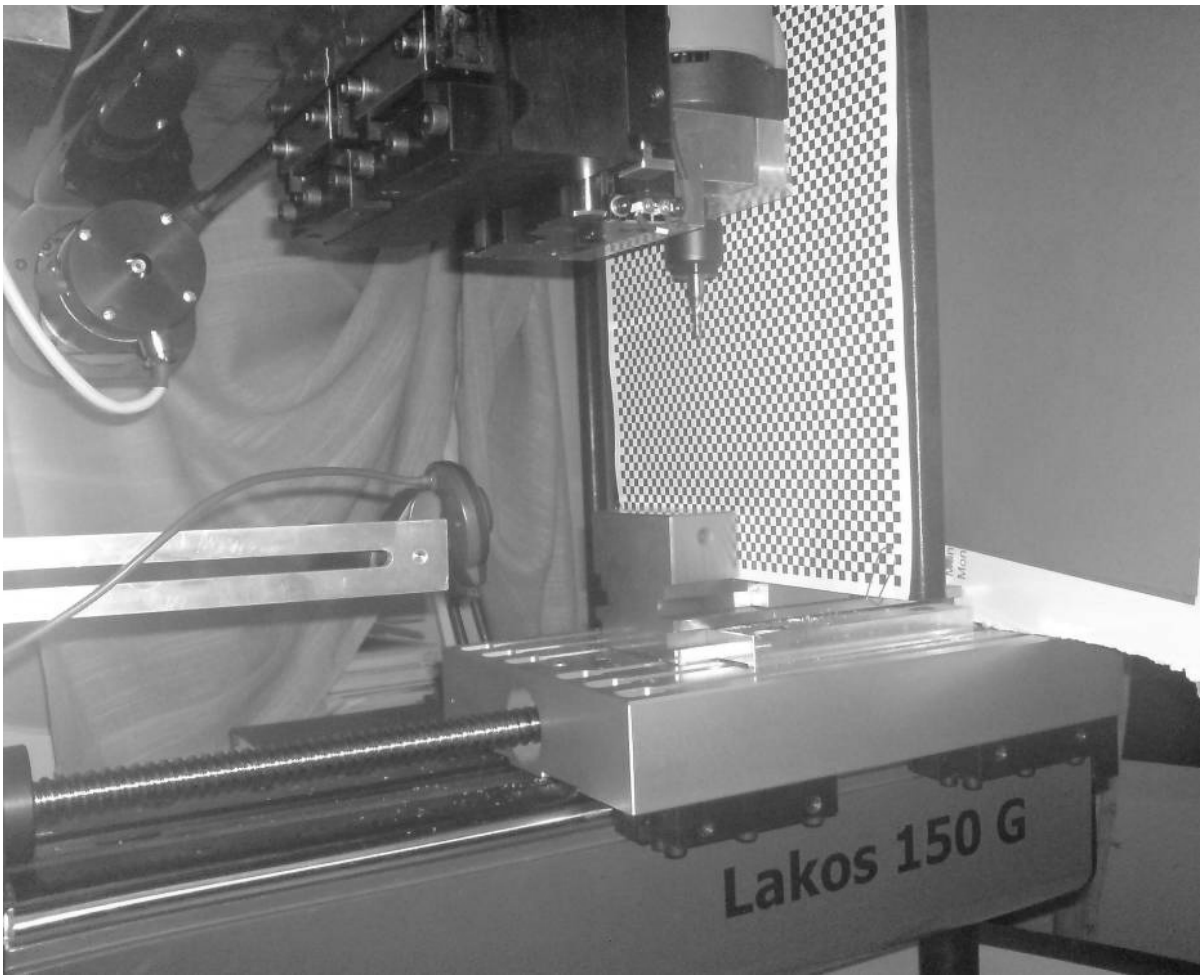

Figure 2: Stand holder for the camera and camera on the LAKOS 150G milling machine.

3. SYSTEM DESIGN

On the basis of the block diagram, the Figure 3 shows the principle of operation of the LAKOS machine, including the integrated optical system. When the workpiece is inserted and fixed, the system for optical determination of the origin [2] is started first. With help of the captured image, coordinates of the zero point of the workpiece are determined individually for each axis within the machine coordinate system. These values are saved in the "stepper.var" file, which is a system file of the EMC2 open source environment and is intended for saving variables, which have to be also preserved at the switch-off of the computer and at the next start-up of the application. When the file with the NC programme is

loaded to the EMC2 environment, the coordinates of the zero point of the raw workpiece are read from the “stepper.var” file. Immediately after that, the processing with the LAKOS 150G can start.

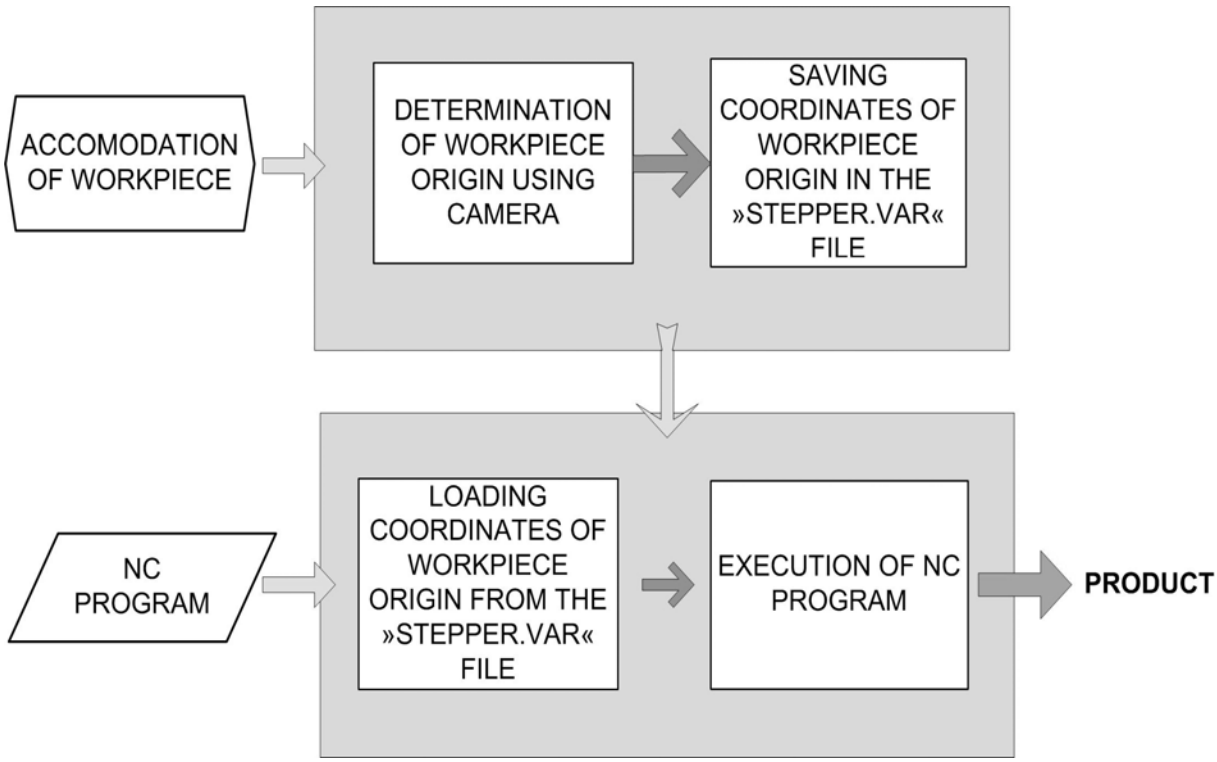

Figure 3: Basic principle of system working.

Figure 4 shows the block diagram of functioning of the module for optical workpiece positioning. Upon fitting the camera to the CNC machine, the system must be first calibrated in order to determine the relations between the coordinates in the captured picture and the robot space coordinates. The calibration process [2] has an especially important role in the machine vision systems aimed to give accurate measurements in real coordinates. Typically, the camera model consists of eleven parameters, namely six so-called external and five internal parameters determining the camera geometrical and optical properties and the camera positions and orientations relative to the outer coordinate system. After the calibration has been performed, it need not be repeated as long as the location of the camera on the robot does not change. In our case the camera calibration was implemented by means of artificial neural network. When learning of the neural network has finished, the use of the workpiece positioning system can start. Through camera the picture of the fixed workpiece is captured. In the next step the captured picture is processed by proper picture processing algorithms [3-9] by extracting from it the information about the position of three zero points of the workpiece in the captured picture. Those coordinates are the input information into the learned neural network having learnt in the stage of system calibration. The output from the neural network is the desired information, i.e., the workpiece position in the robot coordinate system.

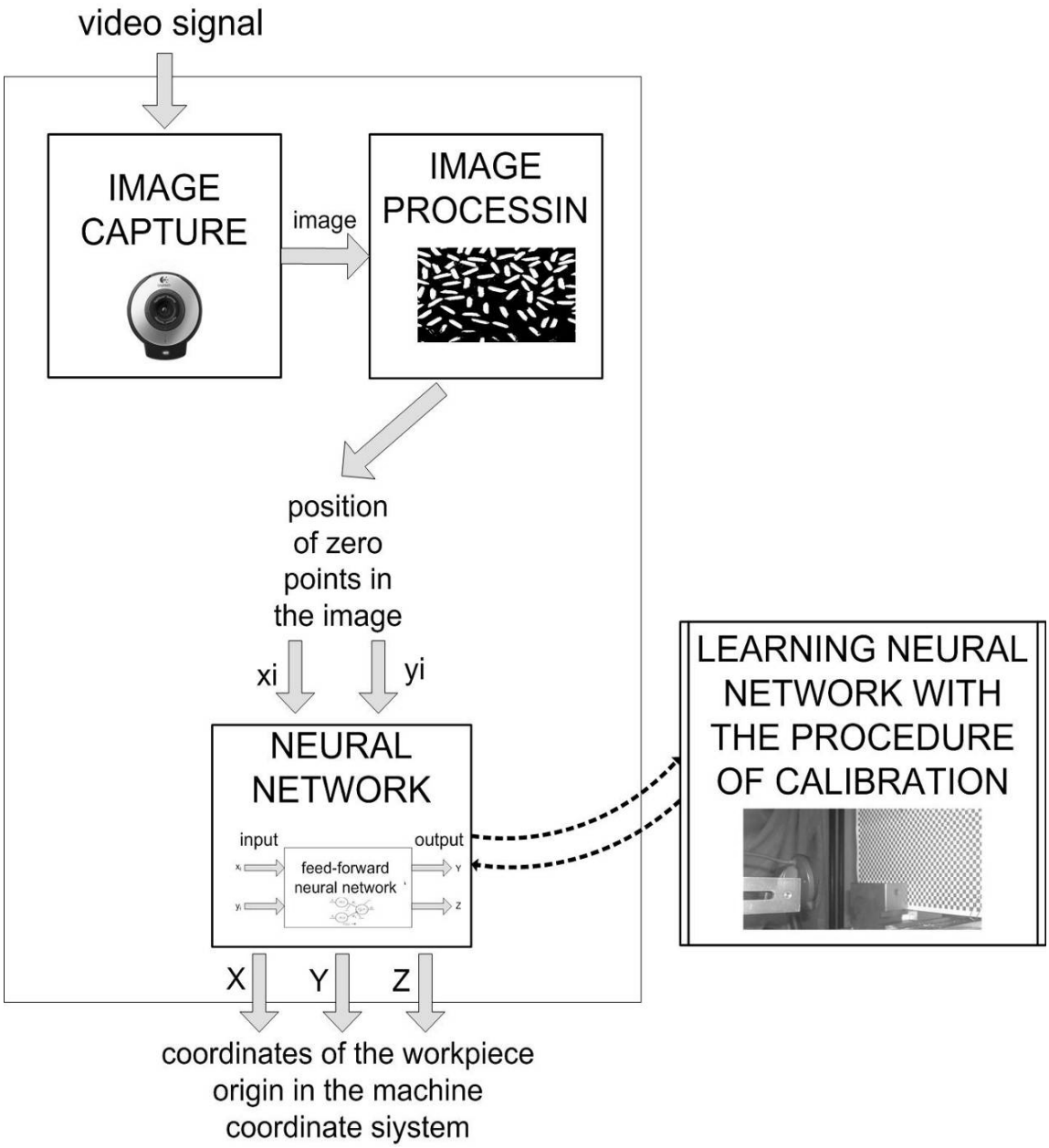

Figure 4: Block diagram of functioning of optical system.

4. IMAGE PROCESSING

By the use of the appropriate algorithms for digital image processing [3-9], the information that we are interested in can be obtained. In our case, the intention is to find an area in the image representing the workpiece origin (edge point of the workpiece). The Figure 5 shows the procedure of image processing.

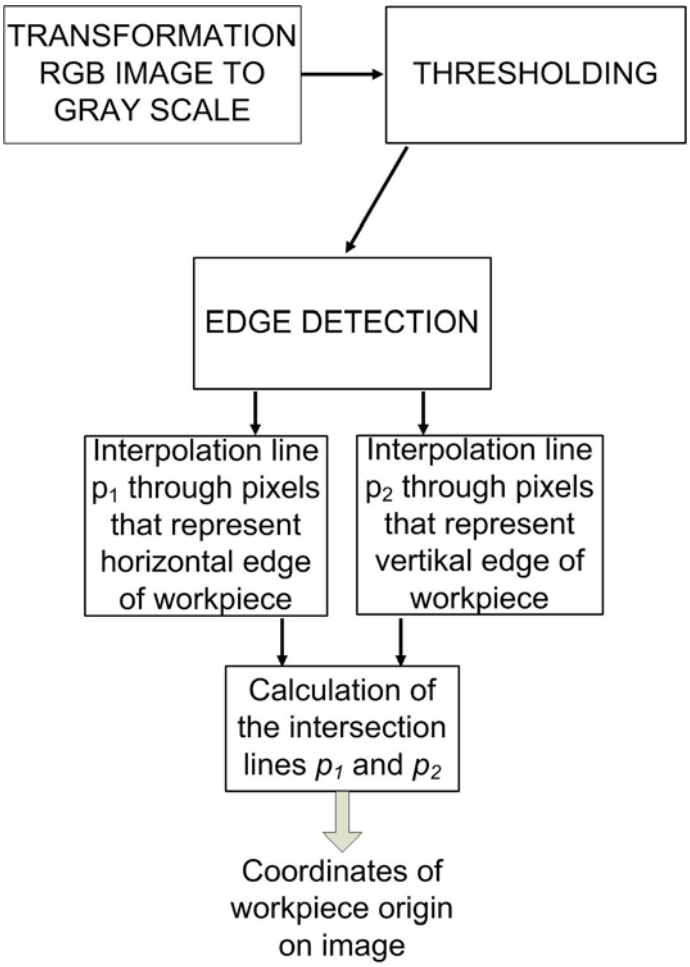

Figure 5: Block scheme of image processing.

Since in the present paper we will limit ourselves to monochromatic images, we have to transform the obtained colour images by using the transformation:

$$Y = 0.299 \cdot R + 0.587 \cdot G + 0.114 \cdot B \tag{1}$$

In the Equation 1 R represents red component, G represents green component and B represents blue component for each individual image element (from now on referred to as pixel), while Y represents the calculated grey scale value. In the next step, the object of interest is separated from the background. This is accomplished by using a threshold method [3]. This method enables us to separate the object of interest (in our case workpiece) from the background. The method is based on a comparison of the gray scale value of each pixel with a certain threshold value. If the gray scale value of the pixel exceeds the value of the threshold, we set the pixel value to 255 while pixels with gray scale value below the threshold value are set to 0. In this way we obtain a binary image with values 255 and 0. The efficiency of this method largely depends on the appropriate selection of the threshold value. We have chosen this value experimentally. Figure 6 represents a flow chart of the image processing employing the threshold method.

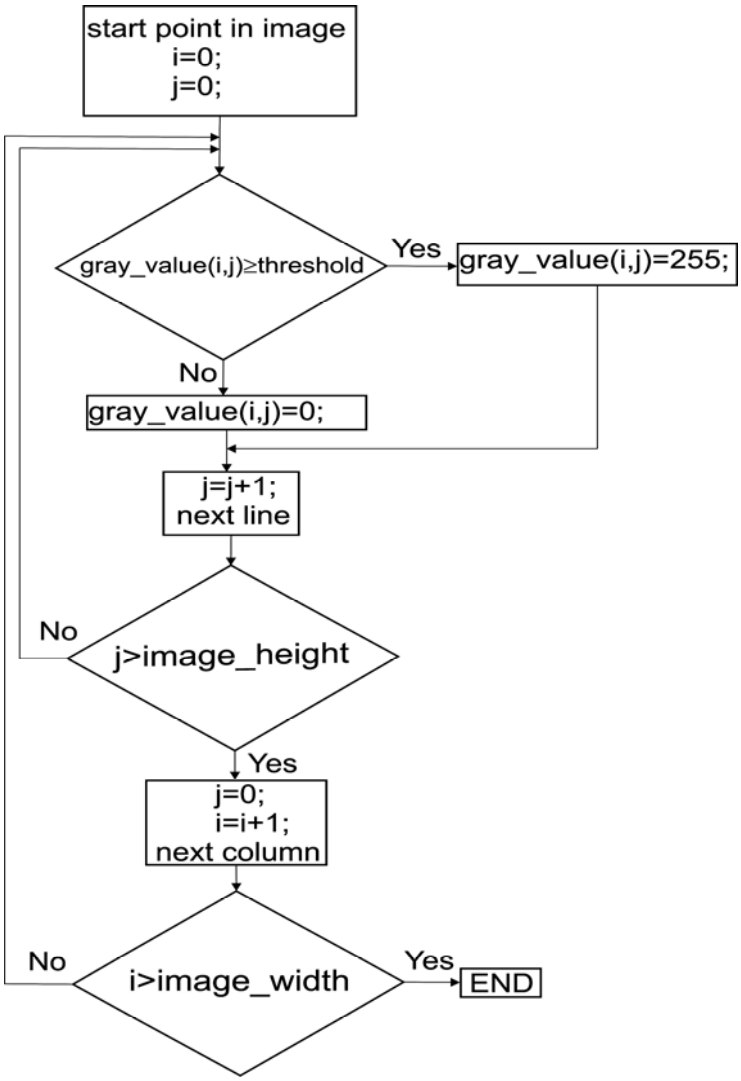

Figure 6: Flow chart of threshold method.

By using edge detection method we can define optical edges in an image. Edge in an image is defined by characteristic alterations of gray scale or colour component values in a specific direction. Our application uses the Sobel algorithm for the detection of edges [3]. This particular algorithm was chosen because our system is set in an environment where the impact of noise is minimal (unchanged scene) and thus making the Sobel detector robust enough for a reliable determination of edges in the image.

5. RESULTS

The system was tested with different workpieces of prismatic shape. In the continuation, the results of the system operation for the test workpiece are represented, with optional insertion of the workpiece in the worktable of the LAKOS milling machine (Figure 6).

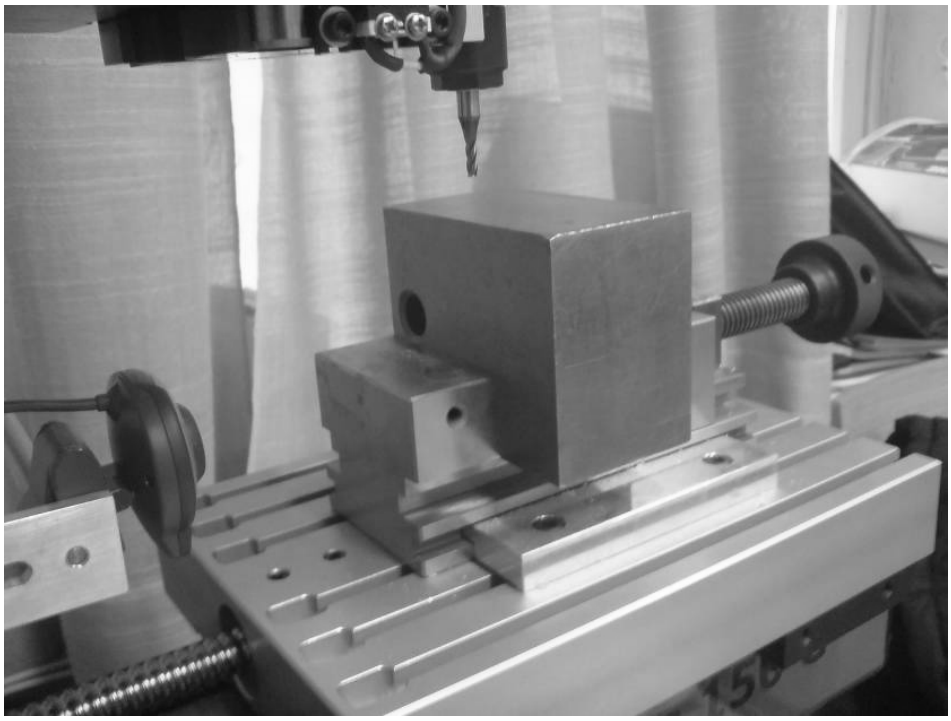

Figure 6: Test workpiece inserted in the LAKOS 150G milling machine.

First, the calibrated camera captures the image of the workpiece. The image is processed with the threshold method. Thus, we separate the searched object from the background. The result of the image processing with the threshold method is presented in Figure 7, where the white colour marks the searched object (workpiece) and the black colour the background.

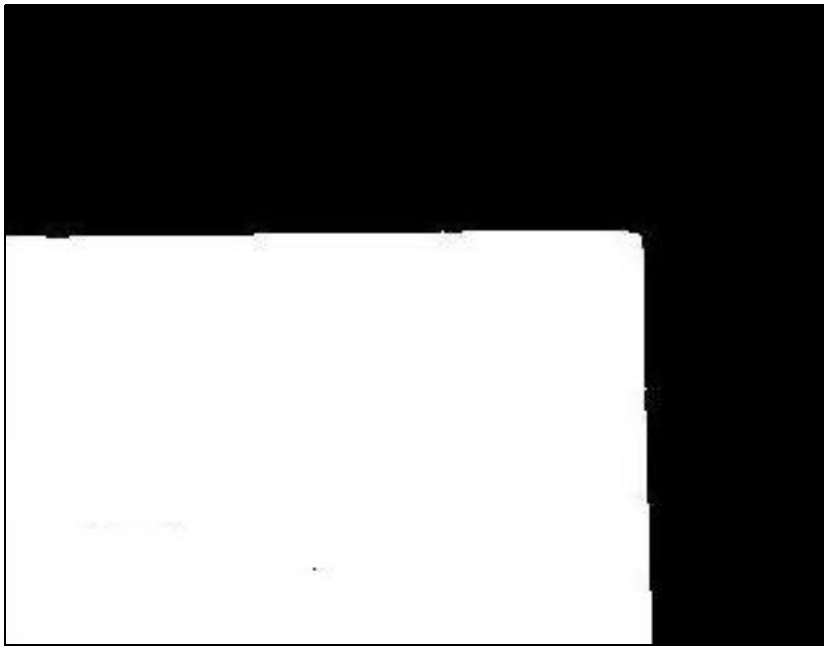

Figure 7: The image is processed with the threshold method.

The Figure 8 shows the results of image processing with Sobel' edge detection algorithm. The detected edges of the workpiece are marked with white colour.

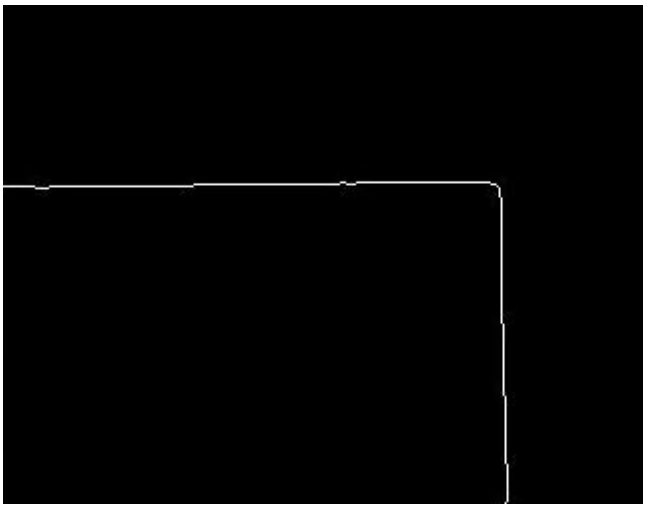

Figure 8: The image is processed with Sobel' edge detector.

The final result of digital processing of the captured image is the determined zero point of the workpiece in the image. The zero point determined by the implemented processing algorithm for the selected test example is shown in Figure 9.

Figure 9: Determined coordinates of the zero point.

It is evident from the Figure 9 that the system determined the coordinates of the zero point (x=249.0 and y=88.2) within the coordinate system where the starting-point is set in the upper left corner of the image. These two values represent the inputs to the neural network, which was taught at the stage of calibration, and its knowledge represents the relation between the coordinates of the image and the coordinates of the machine. The output from the neural network is thus the position of the workpiece zero point within the coordinate system. In the presented test example, the system determined that Y=22.8 mm and Z=92.7 mm. The tools of the machine were moved into that point, where it was established that the system precisely determined the zero point of the workpiece. With the used camera with resolution of 320x240 pixels, it can be theoretically determined the zero point of the workpiece to 0.3 mm precisely at the use of the system on the LAKOS machine (depending on the distance between the installed camera and the observed object). Use of the camera with higher resolution can improve the accuracy of the system.

6. CONCLUSIONS

The developed system for optical workpiece positioning has proved throughout numerous tests to be reliable and adequate for use in practice. The workpiece surroundings remain usually unchanged or single-colour base can be placed in position so that the workpiece is simply distinguished from the background and that the system functioning is reliable and robust. In the future a proper light source will be provided on the machine to illuminate the workpiece and its vicinity uniformly and continuously. Thus, the reliability of functioning of the system in different environments with different illumination of the space (surrounding) will be increased. It can be summarised that the presented system is reliable and effective for the use on the LAKOS 150G milling machine. Likewise, it can be concluded that the system is also appropriate for the use on other processing machines and devices where it is necessary to make a determination of the position of the workpiece.

REFERENCES

[1] Pahole, I., Ficko, M. (2004). Programming of NC machine tools, University of Maribor, Faculty of mechanical engineering, Maribor

[2] Kamnik, M., (2008). Use of the machine vision in adaptable manufacturing systems, master degree, University of Maribor, Faculty of mechanical engineering, Maribor

[3] Gonzalez, R. C.; Woods, R. E. (1993). Digital Image Processing, Addison-Wesley, Boston.

[4] Iglesias, T.; Salmon, A.; Scholtz, J.; Hedegore, R. (2006). Handbook of Machine Vision, Wiley-VCH, Weinheim

[5] Image processing fundamentals, Available from: www.ph.tn.tudelft.nl/Courses/FIP, Accessed on: 14.4.2009

[6] Klancnik, S., Balic, J. & Planincic, P. (2007). Obstacle detection with active laser triangulation, Advances in production engineering & management, Vol. 2, Issue. 2, p. 79-90

[7] Klancnik, S. (2006). Obstacle detection with structured light, Proceedings of the 15th International Electrotechnical and Computer Science Conference ERK'06, Portoroz

[8] Canny Edge Detection Tutorial, Avtor: Bill Green (2002), Available from: http://www.pages.drexel.edu/~weg22/can_tut.html, Accessed on: 14.4.2009

[9] Liang, R. L.; Basallo, E.; Looney, C. G. (2001). Image Edge Detection with Fuzzy Classifier, proceedings of the ISCA 14th international Conference, Las Vegas

NOTES FOR CONTRIBUTORS

APEM seeks to publish articles that identify, extend, or unify the scientific knowledge pertaining to production engineering and management. Articles must meet high standards of originality and rigor. Theoretical, empirical, prescriptive and descriptive contributions are welcome. Unpublished papers (and extended versions of papers presented at conferences) may be submitted for possible publication. Responsibility for the contents of a paper rests upon the authors and not upon the editors or the publisher. **Authors of submitted papers automatically accept a copyright transfer** to PEI, University of Maribor.

Submission
A letter must accompany all submissions, clearly indicating the following: the corresponding author's complete name, affiliation, address, phone and fax numbers, and e-mail address. Short biographies (70-120 words) should be provided that detail the authors' education and work histories as well as their research interests. Small (3.5 x 4.5 cm), black-and-white digitized images of the authors can be included.
All papers for consideration by *Advances in Production Engineering & Management* should be submitted electronically to the Editor-In-Chief. For all documents MS Word text processor should be used (paper size – standard A4, headers and footers – 12.5 mm from edge). Submissions by post are optional (accompanied with a files' CD).
Submissions should be sent to:

Editor-In-Chief: Prof. Dr. Joze Balic
University of Maribor
Faculty of Mechanical Engineering
Production Engineering Institute
Smetanova 17, SI-2000 Maribor, Slovenia - EU
E-Mail: *joze.balic@uni-mb.si*

The review process
Every manuscript that arrives at the editorial office is first reviewed briefly by the editor for general suitability for the journal. Notification of successful submission is sent. After initial screening the manuscript is passed on to at least two referees. A double-blind review process ensures the content's validity and relevance. Referees receive electronic versions of manuscript for review (authors' names and addresses are removed to preserve anonymity). We ask our referees to finish the review within eight weeks.
Based on the comments of the referees, the editor will take a decision about the paper. The following decisions can be made: accepting the paper, reconsidering the paper after changes, and rejecting the paper. Accepted papers may not be offered elsewhere for publication. The editor may, in some circumstances, vary this process at his discretion.
Application of the peer review process indicates journal's standards and overall quality of the research presented.

Length
Papers should be between 8 and 12 pages long including all illustrations and appendices.

Format
Please read the following format instructions carefully. Formatting your paper correctly saves a great deal of editing time, which in turn ensures publication of papers in a timely manner. Papers not formatted correctly will be returned.
The authors must ensure that the paper is complete, grammatically correct and without spelling or typographical errors. Please note that English (U.K.) spelling is adopted. Acronyms are spelled out at first mention but not thereafter unless there is good reason to do so.
It is required to use **Arial font**. **Margins**: 25 mm all around (all pages).

The **structure** of the paper should be as follows: Title of the paper, Authors' names and affiliation, Abstract, Key Words, Introduction, Body of the paper (in sequential headings), Conclusion, (Acknowledgements), References.

The **title** is centred on the page and is **CAPITALIZED AND SET IN BOLDFACE** (font size 16 pt). Please limit the title to a maximum length of 10 words. It should adequately describe the content of the paper.

The **author's name(s)** follows and is also centred on the page (font size 12 pt). A blank line is required between the title and the author's name(s). Last names should be spelled out in full and succeeded by author's initials. The author's affiliation, complete mailing address, and e-mail address (all in font size 11 pt) are provided below. Phone and fax numbers do not appear.

Abstract
A nonmathematical abstract (1000-2000 characters) is required for all papers. It should be an abbreviated, accurate presentation of the contents of the paper. It should contain following information: **purpose** of this paper, **methodology, findings**, **research limitations/implications, practical implications, originality**. Do not cite references in the abstract.

Key Words
The author should provide a list of three to five key words that clearly describe the subject matter of the paper